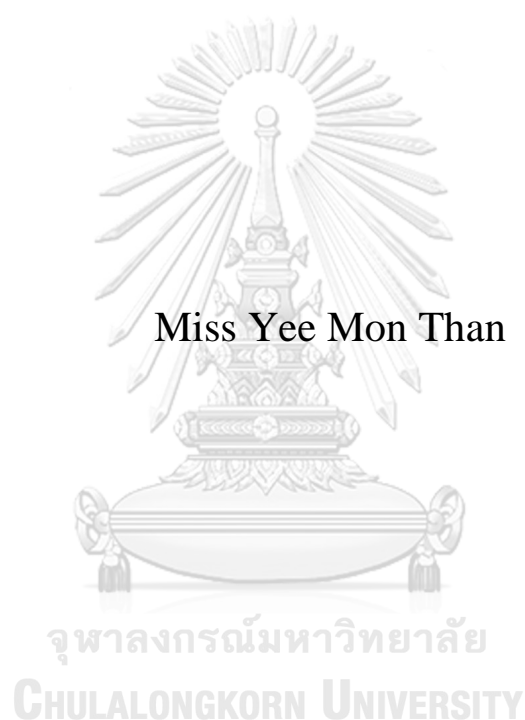


FORMULATION DEVELOPMENT OF EXTENDED AND
IMMEDIATE RELEASE TABLETS USING EXTRUSION-
BASED 3D PRINTING TECHNOLOGY



A Dissertation Submitted in Partial Fulfillment of the Requirements
for the Degree of Doctor of Philosophy in Pharmaceutics
Department of Pharmaceutics and Industrial Pharmacy
FACULTY OF PHARMACEUTICAL SCIENCES
Chulalongkorn University
Academic Year 2020
Copyright of Chulalongkorn University



จุฬาลงกรณ์มหาวิทยาลัย
CHULALONGKORN UNIVERSITY

การพัฒนาสูตรตำรับยาเม็ดชนิดปลดปล่อยแบบทยอยและแบบทันทีด้วย
เทคโนโลยีสามมิติแบบอัดรีด



วิทยานิพนธ์นี้เป็นส่วนหนึ่งของการศึกษาตามหลักสูตรปริญญาเภสัชศา
สตรดุษฎีบัณฑิต
สาขาวิชาเภสัชกรรม
ภาควิชาวิทยาการเภสัชกรรมและเภสัชอุตสาหกรรม
คณะเภสัชศาสตร์ จุฬาลงกรณ์มหาวิทยาลัย
ปีการศึกษา 2563
ลิขสิทธิ์ของจุฬาลงกรณ์มหาวิทยาลัย

Thesis Title	FORMULATION DEVELOPMENT OF EXTENDED AND IMMEDIATE RELEASE TABLETS USING EXTRUSION-BASED 3D PRINTING TECHNOLOGY
By	Miss Yee Mon Than
Field of Study	Pharmaceutics
Thesis Advisor	VARIN TITAPIWATANAKUN, Ph.D.
Thesis Co Advisor	Assistant Professor NARUEPORN SUTANTHAVIBUL, Ph.D. Assistant Professor PHANPHEN WATTANAARSAKIT, Ph.D.

Accepted by the FACULTY OF PHARMACEUTICAL SCIENCES, Chulalongkorn University in Partial Fulfillment of the Requirement for the Doctor of Philosophy

.....
 Dean of the FACULTY OF PHARMACEUTICAL SCIENCES
 (Assistant Professor RUNGPETCH SAKULBUMRUNGSIL, Ph.D.)

DISSERTATION COMMITTEE

..... Chairman
 (Associate Professor ANGKANA TANTITUVANONT, Ph.D.)

..... Thesis Advisor
 (VARIN TITAPIWATANAKUN, Ph.D.)

..... Thesis Co-Advisor
 (Assistant Professor NARUEPORN SUTANTHAVIBUL, Ph.D.)

..... Thesis Co-Advisor
 (Assistant Professor PHANPHEN WATTANAARSAKIT, Ph.D.)

..... Examiner
 (Assistant Professor JITTIMA CHATCHAWALSAISIN, Ph.D.)

..... Examiner
 (WANCHAI CHONGCHAROEN, Ph.D.)

..... External Examiner
 (PRATCHAYA TIPDUANGTA, Ph.D.)

ยี มอน ทานท์ :

การพัฒนาสูตรตำรับยาเม็ดชนิดปลดปล่อยแบบทยอยและแบบทันทีด้วยเทคโนโลยีส

ามมิติแบบอัดรีด . (FORMULATION DEVELOPMENT OF EXTENDED AND IMMEDIATE RELEASE TABLETS USING EXTRUSION-BASED 3D PRINTING TECHNOLOGY) อ.ที่ปรึกษาหลัก : อ. ภาณุ. ดร.วฤณ

จิตาภิวัดนกุล, อ.ที่ปรึกษาร่วม : ศศ. ภาณุ. ดร.นฤพร สุคันธวิบูลย์,ศศ. ภาณุ.

ดร.พรรณเพ็ญ วัฒนาอายุากิจ

เทคโนโลยีการพิมพ์สามมิติด้วยวิธีการฉีดขึ้นรูปสำหรับเภสัชภัณฑ์รูปแบบของแข็งชนิดรับประทาน แสดงผลการผลิตยาเม็ดเฉพาะรายที่แตกต่างเมื่อเทียบกับยาเม็ดที่ผลิตด้วยวิธีดั้งเดิม อย่างไรก็ตามยังมีประเด็นสำคัญด้านคุณภาพของเส้นที่มีตัวยาที่ใช้ผลิตด้วยเทคโนโลยีนี้ซึ่งเกี่ยวกับคุณสมบัติเชิงกล ได้แก่ ความสามารถในการยืดหยุ่น ความแข็งตึง และความเปราะ ในการจัดการปัญหาเหล่านี้จึงมีการผลิตเส้นจากวิธีอัดรีดขึ้นรูปร้อนด้วยการคัดเลือกและบ่งชี้ลักษณะเฉพาะของส่วนผสมทางเภสัชกรรม (พอลิเมอร์ 6 ชนิดและสารช่วยแตกตัว 5 ชนิด) รวมถึงพารามิเตอร์ของกระบวนการสำหรับระบุช่วงของค่าตัวแปรในการออกแบบการทดลอง ดังนั้นจุดประสงค์ของการศึกษานี้คือเพื่อพัฒนาและหาสภาวะที่เหมาะสมที่สุดของยาเม็ดชนิดปลดปล่อยแบบทยอยและแบบทันที โดยทำการบ่งชี้คุณลักษณะสถานะของแข็งของเส้นที่ผ่านการอัดรีดและเม็ดยาที่ผ่านการพิมพ์เพื่อให้เห็นเข้าใจถึงตัวแปรของวัสดุและกระบวนการที่เป็นจุดวิกฤต ผลการทดลองแสดงให้เห็นว่าเส้นที่ผสมด้วยไฮดรอกซีโพรพิลเซลลูโลสสามารถปรับปรุงความสามารถในการยืดหยุ่นอย่างมีนัยสำคัญ พบว่าเส้นและเม็ดที่ผลิตขึ้นมีปัจจัยด้านคุณภาพที่เหมาะสมทั้งด้านเคมีกายภาพ คุณสมบัติเชิงกล การไหล และลักษณะของการปลดปล่อยตัวยาตามต้องการ นอกจากนี้ได้ทำการศึกษาปัจจัยของส่วนประกอบในสูตรตำรับต่อการปลดปล่อยตัวยาและสูตรตำรับที่เหมาะสมที่สุดด้วยการออกแบบการทดลองแบบส่วนผสมคือออปติมัลทางสถิติ พบว่าสูตรตำรับที่เหมาะสมที่สุดของยาเม็ดชนิดปลดปล่อยแบบทยอยประกอบด้วย 10%IMC:49.5%HPC:19.09%PVP/VA:20.94%SLP ที่มีการปลดปล่อยตัวยาตามต้องการเวลา 4, 12 และ 24 ชั่วโมง และพบว่าสูตรตำรับที่เหมาะสมที่สุดของยาเม็ดชนิดปลดปล่อยแบบทันทีประกอบด้วย 30%THY:35%EPO:20%HPC:15%SSG ซึ่งมีการปลดปล่อยตัวยา 85% ภายใน 30 นาที การศึกษานี้ชี้ให้เห็นว่าสามารถพัฒนาสูตรตำรับสำหรับการนำส่งยารับประทานที่มีลักษณะการปลดปล่อยตัวยาตามต้องการด้วยวิธีการออกแบบเชิงคุณภาพ ซึ่งสามารถต่อยอดกับการใช้ประโยชน์ต่างๆของการอัดรีดขึ้นรูปร้อนการพิมพ์สามมิติด้วยวิธีการฉีดขึ้นรูปในทางต่อไป

สาขาวิชา	เภสัชกรรม	ลายมือชื่อนิสิต
ปีการศึกษา	2563 ลายมือชื่อ อ.ที่ปรึกษาหลัก
1	 ลายมือชื่อ อ.ที่ปรึกษาร่วม
	 ลายมือชื่อ อ.ที่ปรึกษาร่วม

6076461933 : MAJOR PHARMACEUTICS

KEYWORD: Controlled release, immediate release, hot melt extrusion, FDM printing, QbD approach

Yee Mon Than : FORMULATION DEVELOPMENT OF EXTENDED AND IMMEDIATE RELEASE TABLETS USING EXTRUSION-BASED 3D PRINTING TECHNOLOGY . Advisor: VARIN TITAPIWATANAKUN, Ph.D. Co-advisor: Asst. Prof. NARUEPORN SUTANTHAVIBUL, Ph.D., Asst. Prof. PHANPHEN WATTANAARSAKIT, Ph.D.

Fused deposition modelling (FDM) based 3D printing technology for oral solid dosage form has shown promising results in the fabrication of individualized tablets compared to conventional method. However, the main concern of this technique is the quality of drug loaded filament including mechanical properties such as flexibility, stiffness and brittleness. To cope with these problems, filaments were produced via hot melt extrusion (HME) by screening and characterizing a series of pharmaceutical mixtures (6 types of polymers and 5 types of disintegrants) and processing parameters for specifying the design space in Design of Experiment (DoE). Therefore, the purposes of the present study were to develop and optimize the extended and immediate release FDM printed tablets using DoE. Solid state characterizations of extruded filaments and printed tablets were performed to understand the critical material and process attributes. The results showed that hydroxy propyl cellulose (HPC)-blended filaments can significantly improve their flexibility. All manufactured filaments and tablets possessed adequate quality attributes such as physicochemical, rheo-mechanical properties and desired drug release profiles. Further, the effect of formulation compositions on drug release and the optimized formulation were investigated by the statistically D-optimal mixture design. The optimized formulation of extended release tablets composed of 10% IMC: 49.5% HPC: 19.09% PVP/VA: 20.94% SLP which resulted in the desired drug release at 4, 12 and 24 h while that of immediate release tablets contained 30% THY: 35% EPO: 20% HPC: 15% SSG with 85% drug release within 30 min. Consequently, this study suggested that the formulation development of oral drug delivery with the required drug release pattern can be achieved by a quality by design approach which could be extended to other HME-FDM applications in pharmaceutical area.

จุฬาลงกรณ์มหาวิทยาลัย
CHULALONGKORN UNIVERSITY

Field of Study: Pharmaceutics
Academic Year: 2020

Student's Signature
Advisor's Signature
Co-advisor's Signature
Co-advisor's Signature

ACKNOWLEDGEMENTS

First of all, I would like to express my deepest gratitude to my advisor, Dr. Varin Titapiwatanakun for her valuable guidance, helpful advices, kindly encouragement throughout the three years of my studies and for the opportunity to study in her international research group.

Special thanks are extended to Assistant Prof. Dr. Narueporn Sutanthavibul and Assistant Prof. Dr. Phanphen Wattanaarsakit for serving as members of my thesis co-advisors.

I also would like to thank all thesis committees Associate Professor Dr. Angkana Tantituvanont, Assistant Professor Dr. Jittima Chatchawalsaisin, Dr. Wanchai Chongcharoen and Dr. Pratchaya Tipduangta for their time, valuable comments and evaluating my thesis.

In addition, my deepest gratitude goes to CU-ASEAN scholarship granted from the Office of Academic Affairs, Chulalongkorn University for the financial supports, tuition fees, stipend in addition to research facilities. I also would like to give my thanks to Graduate School Thesis Grant, Chulalongkorn University; a research fund (Grant number Phar2561-RGI-04 and Phar2562-RGI-01) to V.T.; and T.F., Department of Molecular Pharmaceutics, Meiji Pharmaceutical University. I am especially thankful to Pharmaceutical Research Instrument Center, Faculty of Pharmaceutical Sciences, Chulalongkorn University for permission to utilize the laboratory instrument.

I am grateful to all Minister, Managing Director, General Managers from Ministry of Planning, Finance and Industry (Myanmar) for their permission to attend Ph.D (Pharmaceutics) course in Thailand.

Then, I would like to pay greatly thank to all my colleagues, friends and staffs in Faculty of Pharmaceutical Sciences, Chulalongkorn University for their great support as we have experienced enjoyable times staying in Thailand over the past three years. Finally, I wish my gratitude to my beloved family for their great support, cheerfulness and understanding throughout the study.

Yee Mon Than

TABLE OF CONTENTS

	Page
ABSTRACT (THAI)	iii
ABSTRACT (ENGLISH).....	iv
ACKNOWLEDGEMENTS.....	v
TABLE OF CONTENTS.....	vi
LIST OF TABLES.....	xi
LIST OF FIGURES	xii
LIST OF ABBREVIATIONS.....	1
CHAPTER I.....	2
INTRODUCTION	2
1.1. Introduction.....	2
1.2. Background and rationale	4
1.3. Objectives	7
1.4. Scope of the research.....	8
1.5. Expected benefits	8
REFERENCES	9
CHAPTER II.....	15
LITERATURE REVIEWS	15
2.1. Additive manufacturing	15
2.1.1. Fused deposition modelling (FDM).....	15
2.1.2. Binder jet printing.....	16
2.1.3. Semi-solid extrusion	16
2.1.4. Selective laser sintering (SLS).....	16
2.1.5. Stereolithography (SLA)	17
2.2. Oral solid dosage forms using 3D printing.....	17
2.2.1. Immediate release tablets.....	18

2.2.2. Floating tablets.....	18
2.2.3. Monolithic sustained release tablets	19
2.2.4. Pulsatile drug release tablets.....	19
2.2.5. Enteric release tablets	19
2.2.6. Nano-capsule based formulation	20
2.2.7. Medicines used in 3D printing.....	20
2.3. Strategies for drug dissolution/solubility enhancement.....	22
2.3.1. Solid dispersion	22
2.3.2. Salt formation	25
2.3.3. Co-crystals	26
2.4. Techniques applied for amorphous solid dispersion.....	26
2.4.1. Hot melt extrusion (HME).....	27
2.4.2. Materials used in hot-melt extrusion	28
2.4.3. Spray drying.....	34
2.5. Quality by Design (QbD).....	35
2.5.1. Quality target product profile (QTPP).....	36
2.6. Design of Experiment	37
2.6.1. Screening design	38
2.6.2. Optimizing designs	39
REFERENCES	42
CHAPTER III	51
Statistical Design of Experiment (DoE)-based formulation development and optimization of FDM 3D printed oral controlled release drug delivery with multi target product profile.....	51
3.1. Abstract	52
3.2. Introduction	53
3.3. Materials and methods	55
3.3.1. Materials	55

3.3.2. Optimization study of polymer blends and processing factors	55
3.3.3. Preparation of indomethacin-loaded filaments via hot melt extrusion	57
3.3.4. Fabrication of 3D printed tablets	57
3.3.5. Oscillatory rheology experiment.....	57
3.3.6. Characterization of the filaments and 3D printed objects	58
3.3.7. Statistical Design of Experiment (DOE)	60
3.4. Results and discussion.....	61
3.4.1. Optimization study of polymer blends and processing factors	61
3.4.2. Rheological assessment.....	62
3.4.3. Characterization studies of filaments and printed tablets	65
3.4.4. Design of Experiment (DOE).....	75
3.5. Conclusion.....	79
REFERENCES	81
CHAPTER IV	85
Tailoring immediate release FDM 3D printed tablets using a Quality by Design (QbD) approach.....	85
4.1. Abstract	86
4.2. Introduction	87
4.3. Materials and Methods.....	90
4.3.1. Materials.....	90
4.3.2. Screening study for setting up the level of components in DoE	90
4.3.3. Preparation of theophylline loaded filaments	90

4.3.4. Rheological measurements	90
4.3.6. Characterization studies of filaments and 3D printed tablets	91
4.3.7. Experimental design.....	93
4.4. Results and Discussion.....	94
4.4.1. Screening study for setting up the level of components in DoE	94
4.4.2. Rheological measurement	96
4.4.3. Characterization studies of filaments and 3D printed tablets	98
4.4.4. Design of Experiment	109
4.5. Conclusion	113
REFERENCES	115
CHAPTER V	120
CONCLUSION.....	120
5.1. Conclusion	120
5.2. Limitations	123
5.3. Suggestion and future work	124
REFERENCES	125
REFERENCES	127
APPENDIX A.....	128
RHEOLOGICAL STRAIN GRAPHS.....	128
APPENDIX B	130
IMAGES OF EXTRUDED FILAMENTS AND 3D PRINTED TABLETS	130
APPENDIX C	133
FT-IR SPECTRUM	133
APPENDIX D.....	135
POWDER X-RAY DIFFRACTOGRAM.....	135
APPENDIX E	137

RESULTS FROM DESIGN OF EXPERIMENT 137
VITA 141



LIST OF TABLES

	Page
Table 1. Optimization study with the filament properties.....	56
Table 2. D-optimal mixture design of FDM printed tablet formulations.....	60
Table 3. Drug content analysis of extruded filaments and printed tablets (n=3).....	72
Table 4. ANOVA results of 9-formulations design.	76
Table 5. Observed values of responses obtained from the D-optimal mixture design.	76
Table 6. Comparison of predicted and observed value of responses for the optimal formulation.	79
Table 7. D-optimal mixture design of FDM 3D printed tablet formulations.....	94
Table 8. Optimized filament formulations and hot melt extrusion (HME) conditions.	95
Table 9. Drug content analysis of filaments and printed tablets (n=3).....	106
Table 10. ANOVA results of the 17-formulations design.	109
Table 11. Observed values of responses obtained from the D-optimal mixture design.	110
Table 12. Comparison of predicted and observed value of responses for the optimal formulation.....	113

LIST OF FIGURES

	Page
Figure 1. Structure of indomethacin.	21
Figure 2. Structure of theophylline.	21
Figure 3. Energy pyramid of amorphous forms, amorphous solid dispersion, the crystalline form and their structural forms.....	24
Figure 4. Diagrammatic representation of salt formation process.....	26
Figure 5. The schematic diagram of hot melt extrusion process.	28
Figure 6. Chemical structure of cellulose ether derivatives.....	30
Figure 7. Chemical Structures of Soluplus.	31
Figure 8. Chemical Structures of Kollidon® VA 64.	31
Figure 9. Chemical structure of Eudragit, For Eudragit E: R1, R3=CH ₃ , R2=CH ₂ CH ₂ N(CH ₃) ₂ , R4=CH ₃ , C ₄ H ₉ , For Eudragit RL and Eudragit RS: R1=H, CH ₃ , R2=CH ₃ , C ₂ H ₃ , R3=CH ₃ , R4=CH ₂ CH ₂ N(CH ₃) ⁺ ₃ CL ⁻	33
Figure 10. The diagram illustrating elementary processing steps in spray drying process.....	35
Figure 11. Schematic diagram of the steps for implementation of pharmaceutical QbD. Legend: CPP = Critical Process Parameter, CMA = Critical Material Attribute, CQA = Critical Quality Attribute, DS = Design Space, QTPP = Quality Target Product Profile, CAP = Critical Analytical Parameter.	37
Figure 12. Examples of various optimized designs (A) full factorial design, (B) central composite design, (C) Box-Behnken design, (D) optimal design, and (E) mixture design.....	39
Figure 13. Complex viscosity of (a) combined polymers and (b) HPC-disintegrant blends, as a function of temperature.....	64
Figure 14. SEM images of (a) cross section, (b) cross section (x1000) of polymer blend filaments, (c) side view and (d) side view (x1000) of printed tablets.	65
Figure 15. Breaking distance and breaking stress of all extrudable and printable filaments: (a) HPC-polymer at 3:1 and 1:1 ratio (b) HPC-disintegrant at 3:1 ratio, obtained from the 3-point bend test.	67

Figure 16. FTIR spectrum of extruded filaments compared with IMC.	68
Figure 17. Thermogravimetric analysis of raw materials and HPC-disintegrant filaments (a, b) and DSC thermograms of raw materials, polymer blend filaments (3:1 ratio) and printed layers (c).	70
Figure 18. X-ray powder diffractograms of (a) raw materials, HPC-polymer and (b) HPC-disintegrant filaments and printlets.	71
Figure 19. In-vitro dissolution profiles of (a) HPC-polymer blend tablets, (b) two sizes of HPC-PVP/VA (3:1) tablets and (c) HPC-disintegrant blend tablets (n=3, mean \pm SD).	74
Figure 20. Main effect plot of all three independent factors (HPC, PVP/VA and SLP).	77
Figure 21. Contour plot depicting effect of variables on % drug release at 4, 12 and 24 h.	78
Figure 22. Temperature sweep analysis of different drug load mixtures (a) EPO-based mixtures (b) PVP/VA-based mixtures.	97
Figure 23. SEM images of HME filaments: (a) surface and (b) cross-section images of (1) E10 (2) E30 (3) E60 filaments; and FDM 3D printed tablets: (4a) cross section (x1000), (5a) side view (x50) and (5b) side view (x500) images of P30 printed tablets.	99
Figure 24. Breaking distance and breaking stress of all extrudable and printable filaments obtained from the 3-point bend testing.	100
Figure 25. FTIR spectrum of EPO-based filaments compared with the pure drug. .	102
Figure 26. Thermogravimetric analysis of (a) API and excipients, (b) extruded filaments, and (c) DSC thermogram of extruded filaments.	104
Figure 27. X-ray powder diffractograms of pure API, excipients and extruded filaments.	105

Figure 28. In-vitro drug release profiles of FDM 3D printed tablets from EPO (blue lines) and PVP/VA (green lines)-based filaments.	107
Figure 29. Main effect plot of all four independent variables (THY, EPO, HPC and SSG).	111
Figure 30. Contour plot depicting effect of variables on % drug release at 30 min. .	112
Figure 31. Strain curves (a) polymeric blends and (b) polymer-disintegrants formulations.	129
Figure 32. Strain curves (a) EPO-based formulations and (b) PVP/VA-based formulations.	129
Figure 33. Image of (a) different polymeric-blend (b) polymer-disintegrants filaments and printed tablets.	131
Figure 34. Image of different drug loads filaments and printed tablets (a) 10%, (b) 30% and (c) 60%.	131
Figure 35. SEM image of HPC-disintegrant filaments (a) cross-section (b) cross-section (x1000).	132
Figure 36. FT-IR spectrum of PVP-based extruded filaments	134
Figure 37. X-ray powder diffractograms of pure API, excipients and printed tablets.	136
Figure 38. Interaction plot for different formulation factors (EPO, HPC and SSG)	138
Figure 39. (a) In-vitro drug release studies of controlled release printed tablets obtained from DoE runs (b) Optimized formulation.	138
Figure 40. (a) In-vitro drug release studies of immediate release printed tablets obtained from DoE runs (b) Optimized formulation.	139
Figure 41. Contour plot depicting effect of variables on % drug release at 45 min. .	139

LIST OF ABBREVIATIONS

CCM	croscarmellose sodium
Cros PVP	cross povidone
DoE	design of experiment
DSC	differential scanning calorimetry
EPO	eudragit E
FDM	fused deposition modelling
HME	hot melt extrusion
HPC	hydroxypropyl cellulose
IMC	indomethacin
L-HPC	low substituted hydroxypropyl cellulose
LVR	linear viscoelastic region
MCC	microcrystalline cellulose
NSAIDs	nonsteroidal anti-inflammatory drug
SLP	soluplus
Pa.s	pascal
PVP/VA	polyvinyl pyrrolidone/vinyl acetate
SSG	sodium starch glycolate
PXRD	powder X-ray diffraction
QbD	quality by design
SEM	scanning electron microscopy
TGA	thermo gravimetric analysis
THY	theophylline
UV/Vis	ultraviolet/visible

CHAPTER I

INTRODUCTION

1.1. Introduction

The term “three-dimensional (3D) printing” is a rapid prototyping technique depended on the elements of additive manufacturing which has a wide range of applications in the area of pharmaceutical production. It allows the fabrication of sophisticated geometrical dosage forms, personalized drug products, and items made for immediate utilization (1). Thus, 3D printing techniques via fused deposition modelling (FDM) can be managed to generate a variety of dosage forms from immediate release tablets to osmotic drug delivery systems. This designates that theoretically all type of drug delivery system (DDS) is printable and can be manipulated to the patient’s needs relating with the size, drug load and release properties (2, 3).

The API-loaded filaments used in FDM printing could also be prepared via hot-melt extrusion (HME). Several studies have already shown that HME of 3D-printable filaments consisting of pharmaceutical polymers grade was feasible (4). In order to successful fabrication of 3D printed tablets containing amorphous solid dispersion by this technique, the extruding filaments of pharmaceutical grade polymers, which are very crucial step along with suitable miscibility of drug with the polymers (5), mechanical and rheological properties for manufacturing of dosage forms, are not yet fully available (6). The extruded polymers filaments are either fragile which break into pieces in the gear wheels or flexible that cannot be driven by the driving wheel possibly owing to very flexibility of filaments, leading to failing printing (1). Many types of polymer matrices that have been used in FDM printing for APIs are hydroxypropyl cellulose, methacrylate (4), polyvinyl alcohol (2, 7), polyvinylpyrrolidone (8), hydroxypropyl methylcellulose acetate succinate (HPMCAS) (9), polymers mixture (e.g., hydroxypropyl methylcellulose E5 and Soluplus or Eudragit L 100, hydroxypropyl cellulose LF and ethylcellulose N14 (1), ethyl cellulose (10). This study approached the polymeric blends with different ratios to adjust the printability of filaments and to control the drug release rate of the tablets. Moreover, we introduced the addition of different disintegrants to polymer matrix to

with different ratios for extrudability via hot melt extrusion and printing to ensure critical material attributes (CMA) . With respect to immediate release printed tablets, theophylline (THY) was used as a model drug because this drug is thermostable drug with high melting point (ca. 270.1°C) (4) and it is suitable for testing of drug release profiles due to its high solubility in various pH (15). Eudragit® EPO, Kollidon VA 64 were used as immediate release polymers containing different drug loads in combination with various ratios of superdisintegrant, SSG to enhance the dissolution rate whereas HPC was used as a flexibility modifier to improve the filament property in this immediate release system. Moreover, the processing parameters related with hot melt extrusion including temperature and screw speed, rheology of molten filaments as well as temperature for printing were optimized as critical processing parameters (CPP).

To keep the formulations relatively simple, no plasticizer was used for both systems. After defining the CMA and CPP via screening, the obtained filaments and produced dosage forms were methodically evaluated such as rheological analysis, mechanical property, content and mass uniformity, and drug release pattern to ensure the product quality attributes. Further on, DoE was again conducted to investigate the impact of formulation compositions as variables on drug release profile in both formulations. This work is substantiated an approach to obtain the better suited excipients combinations for printing and developing 3D printed dosage forms with improved characteristics, especially tailored drug release for manufacturing efficiency.

1.2. Background and rationale

Nowadays, a huge number of different additive manufacturing of 3D printing process are available (16). The most utilized and researched additive manufacturing technologies include materials jetting (e.g binder jetting) (17-19), material extrusion system (e.g fused deposition modelling) (9), powder bed fusion (e.g selective laser sintering) (20), photopolymerizations (e.g stereolithography) (21-23). The main differences between methods are deposition of layer materials to generate 3D objects and on the starting materials that are used. Some methods melt or soften the material to produce the layers, for example, fused deposition modeling (FDM), fused filament

fabrication (FFF) or selective laser sintering (SLS). Each method has its own benefits and weak points (24).

Of these techniques, fused deposition modelling (FDM) 3D printing is the most extensively applied as cost effective technique across various sectors (25-27) and one of the extrusion-based techniques which is dynamically utilized in the pharmaceutical sciences (23, 28-32). This technique is based on the extrusion of a molten polymeric filament through a heated nozzle, followed by deposition onto a moving platform into the required 3D objects. The important parameters in FDM are the qualities of the filament (23, 33) such as mechanical stability, consistent diameter and homogeneous API distribution.

In order to produce extruded filament, hot melt extrusion (HME) is a continuous, solvent free process (34) and one of the attractive methods in solid dispersion development (1, 35-37) in which the drug is molecularly dispersed in the molten polymer matrix to form amorphous solid dispersion (ASD) that enhance the bioavailability of such APIs (1, 38-41). The combination of two novel technologies has brought the prospective changes for pharmaceutical manufacturing of innovative dosage forms. The advantage of two combined processes is production of more complex-shaped dosage forms such as pellets (42), melt cast films (43), implants (43-45) scaffolds (46), capsule shells (47) and personalized manufacturing system (1, 48). Therefore, there is an emerging interest in developing the HME-FDM printing process technology for continuous manufacturing of 3D printed formulations.

Recently, research regarding the FDM printing have indicated many restrictions of the system which necessitate vigorous explorations for extensive applications in drug delivery (41). The extruded filaments of polymers were either too brittle, thus breaking in the driven gear or too soft, thus not being able to push by the gear wheels because of flexibility of filaments (1, 5, 49). The potential of the HME-FDM printing process to develop the filaments with mechanical stability (50, 51) has been less studied. Even though most of studies have used plasticizer in order to possibly decrease melt viscosity and thus reduce processing temperature for hot melt extrusion, the added plasticizer may not be miscible with the polymer and its existence may cause crystallization of drug from the system (52, 53). Therefore,

extruding the 3D printable filaments with the suitable mechanical property is a crucial step.

Another major constraint of 3D printing is that most of prepared tablets appeared to be faster drug release by either altering the internal structure (infill function) of FDM (2, 54, 55) or geometry of tablets (56). Hence, it is of great attention to adapt the 3D printing method which grants the different pharmaceutical devices with a variety of modification in dissolution profiles from one feedstock filament (1, 23, 33). In researchers' efforts to produce immediate release formulations of theophylline and dipyridamole by FDM printing, Okwuosa *et al.* (8) developed 3D printed formulations containing high amounts of talc and such active ingredients with 50%, where the drugs remained unchanged in crystalline state (8). The drug release from tablets was governed by the polymer matrix and the solubility of drugs (5).

The next important issue of the extruded filaments stems from the limitation in dosing amount which is a key element in the case of polypills dosage forms (50), fixed-dose tablets with the limitations of personalized medications (57-60), dissolvable and solid coated microneedles (24). Pietrzak *et al.* (4) made use of higher melting temperature drug, theophylline (273°C), at same ratio (1:1) with Eudragit® RL, E or RS to fabricate filaments with the aids of different plasticizers such as Tween® 80, PEG 400, triethyl citrate and triacetin to enhance the pliability of filaments, melt processing and reduce printing temperature (10, 61-63). Additionally, many research works associated with processing parameters of FDM including temperature, infill percentage and dimensions provided by DoE were reported in the last decade to improve the quality of FDM objects (64) and to tailor the drug release (65). However, there is still limited/no published report on the systematic identification of formulation compositions required to the FDM printed dosage forms. Therefore, it may be a challenging to investigate the effect of pharmaceutical excipients related with the suitability of FDM printing.

Research studies in many fields often apply Design of Experiments (DOE) techniques for process optimization and analysis procedure (64). Quality by design is a systematic quality tactic of conducting the testing by using the principles of statistical sciences, that provides in creating cause-and-effect relationship between the independent variables and dependent variables (66). Quality-by-design tool such as

mixture design is the most appropriate method used in optimizing the tablet compositions as the tablets are mixtures of active ingredients and other excipients containing fillers or disintegrants. In order to set up the optimum formulation composition, establishing a formulation design in which the constituents can be fluctuated to predict the best formulation with desired properties (67, 68). Furthermore, tiny fluctuations in formulation proportion can cause significant changes in their properties (37, 69).

The overall variability in a particular critical quality attributes (CQA) of the product has been contributed to be a combination of the variability of the API and the excipients as a critical material attribute (CMA), the production process parameter, and the interactions between these individual factors (70). Although the previous studies related with FDM printing focus on the development of FDM processing parameters (e.g., temperature, infill percentage and tablet geometry) experiment-based design, there has been no or little explorations into understanding how much variability in excipients impacts drug product performance relative to variability in API properties and processing parameters or method. Therefore, the present study provides a preliminary assessment of the relative impact of variability in polymers, disintegrants, API loadings to understand the critical material attributes and related critical processing parameters (CPP) that pursue safe and effective dosage form development. Then, a statistical design of experiments for investigating the impact of formulation factors on drug release profiles as independent variables is presented.

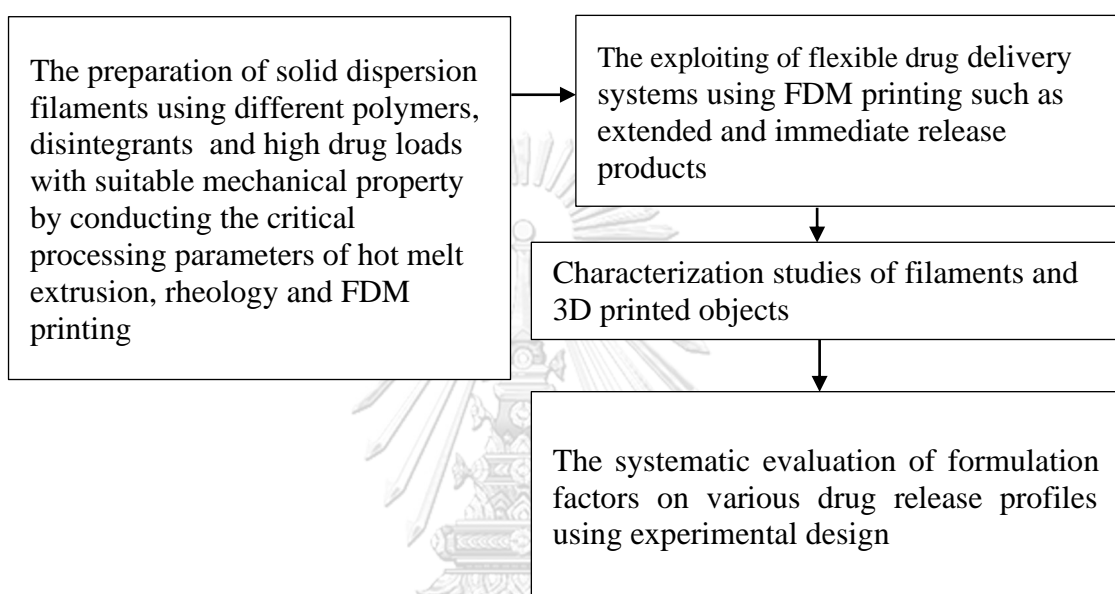
1.3. Objectives

1. To produce solid dispersion filaments by screening the effect of pharmaceutical excipients and drug loadings on FDM printability using hot melt extrusion
2. To investigate the rheological characterization of molten solid dispersions for processability
3. To evaluate the physicochemical and mechanical properties of the extruded filaments and 3D printed objects

- To develop the extended and immediate release 3D printed tablets by systematically investigating the formulation compositions and their potential interactions using Design of Experiments

1.4. Scope of the research

The scope of this research work will cover:



1.5. Expected benefits

- A variety of extrudable and printable filaments for FDM printing can be produced for extended and immediate oral drug delivery and can be extended to other applications.
- The obtained rheological data could be useful for optimizing HME and FDM process parameters.
- Researchers can apply the polymer mixture systems to further develop extended and immediate drug delivery.
- The platform of using D-optimal mixture design can be applied for other formulation development and HME-FDM applications.

REFERENCES

1. Zhang J, Feng X, Patil H, Tiwari RV, Repka MA. Coupling 3D printing with hot-melt extrusion to produce controlled-release tablets. *International Journal of Pharmaceutics*. 2017;519(1):186-97.
2. Goyanes A, Buanz ABM, Basit AW, Simon G. Fused-filament 3D printing (3DP) for fabrication of tablets. *International Journal of Pharmaceutics*. 2014;476(1):88-92.
3. Khaled SA, Burley JC, Alexander MR, Roberts CJ. Desktop 3D printing of controlled release pharmaceutical bilayer tablets. *International Journal of Pharmaceutics*. 2014;461(1):105-11.
4. Pietrzak K, Isreb A, Alhnan MA. A flexible-dose dispenser for immediate and extended release 3D printed tablets. *European Journal of Pharmaceutics and Biopharmaceutics*. 2015;96:380-7.
5. Solanki NG, Tahsin M, Shah AV, Serajuddin ATM. Formulation of 3D printed tablet for rapid drug release by fused deposition modeling: screening polymers for drug release, drug-polymer miscibility and printability. *Journal of Pharmaceutical Sciences*. 2018;107(1):390-401.
6. Korte C, Quodbach J. Formulation development and process analysis of drug-loaded filaments manufactured via hot-melt extrusion for 3D-printing of medicines. *Pharmaceutical Development and Technology*. 2018;23(10):1117-27.
7. Skowrya J, Pietrzak K, Alhnan MA. Fabrication of extended-release patient-tailored prednisolone tablets via fused deposition modelling (FDM) 3D printing. *European Journal of Pharmaceutical Sciences*. 2015;68:11-7.
8. Okwuosa TC, Stefaniak D, Arafat B, Isreb A, Wan K-W, Alhnan MA. A Lower temperature FDM 3D printing for the manufacture of patient-specific immediate release tablets. *Pharmaceutical Research*. 2016;33(11):2704-12.
9. Goyanes A, Fina F, Martorana A, Sedough D, Gaisford S, Basit AW. Development of modified release 3D printed tablets (printlets) with pharmaceutical excipients using additive manufacturing. *International Journal of Pharmaceutics*. 2017;527(1):21-30.
10. Kempin W, Franz C, Koster L-C, Schneider F, Bogdahn M, Weitschies W. Assessment of different polymers and drug loads for fused deposition modeling of drug loaded implants. *European Journal of Pharmaceutics and Biopharmaceutics*. 2017;115:84-93.
11. Tiwari SB, Murthy TK, Raveendra Pai M, Mehta PR, Chowdary PB. Controlled release formulation of tramadol hydrochloride using hydrophilic and hydrophobic matrix system. *The American Association of Pharmaceutical Scientists: Pharmaceutical Science and Technology*. 2003;4(3):18-23.
12. Gupta A, Hunt RL, Shah RB, Sayeed VA, Khan MA. Disintegration of highly soluble immediate release tablets: a surrogate for dissolution. *The American Association of Pharmaceutical Scientists: Pharmaceutical Science and Technology*. 2009;10(2):495-9.
13. Marto J, Gouveia LF, Gonçalves LM, Gaspar DP, Pinto P, Carvalho FA. A Quality by design (QbD) approach on starch-based nanocapsules: A promising platform for topical drug delivery. *Colloids and Surfaces B: Biointerfaces*. 2016;143:177-85.

14. Sovány T, Csordás K, Kelemen A, Regdon G, Pintye-Hódi K. Development of pellets for oral lysozyme delivery by using a quality by design approach. *Chemical Engineering Research and Design*. 2016;106:92-100.
15. Mengozzi G, Intorre L, Bertini S, Giorgi M, Soldani G. Comparative bioavailability of two sustained-release theophylline formulations in the dog. *Pharmacological Research*. 1998;38(6):481-5.
16. Jamróz W, Szafraniec J, Kurek M, Jachowicz R. 3D printing in pharmaceutical and medical application-recent achievements and challenges. *Pharmaceutical Research*. 2018;35(9):176.
17. Wang J, Goyanes A, Gaisford S, Basit AW. Stereolithographic (SLA) 3D printing of oral modified-release dosage forms. *International Journal of Pharmaceutics*. 2016;503(1):207-12.
18. Clark EA, Alexander MR, Irvine DJ, Roberts CJ, Wallace MJ, Sharpe S. 3D printing of tablets using inkjet with UV photoinitiation. *International Journal of Pharmaceutics*. 2017;529(1):523-30.
19. Kyobula M, Adedeji A, Alexander MR, Saleh E, Wildman R, Ashcroft I. 3D inkjet printing of tablets exploiting bespoke complex geometries for controlled and tuneable drug release. *Journal of Controlled Release*. 2017;261:207-15.
20. Fina F, Goyanes A, Gaisford S, Basit AW. Selective laser sintering (SLS) 3D printing of medicines. *International Journal of Pharmaceutics*. 2017;529(1):285-93.
21. Khaled SA, Burley JC, Alexander MR, Yang J, Roberts CJ. 3D printing of tablets containing multiple drugs with defined release profiles. *International Journal of Pharmaceutics*. 2015;494(2):643-50.
22. Goyanes A, Allahham N, Trenfield SJ, Stoyanov E, Gaisford S, Basit AW. Direct powder extrusion 3D printing: Fabrication of drug products using a novel single-step process. *International Journal of Pharmaceutics*. 2019;567:118471.
23. Jamróz W, Kurek M, Szafraniec-Szczęsny J, Czech A, Gawlak K, Knapik-Kowalczuk J. Speed it up, slow it dow. An issue of bicalutamide release from 3D printed tablets. *European Journal of Pharmaceutical Sciences*. 2020;143:105169.
24. Trenfield SJ, Awad A, Goyanes A, Gaisford S, Basit AW. 3D Printing Pharmaceuticals: Drug Development to Frontline Care. *Trends in Pharmacological Sciences*. 2018;39(5):440-51.
25. Vithani K, Goyanes A, Jannin V, Basit AW, Gaisford S, Boyd BJ. An Overview of 3D printing technologies for soft materials and potential opportunities for lipid-based drug delivery systems. *Pharmaceutical Research*. 2018;36(1):4.
26. Pham DT, Gault RS. A comparison of rapid prototyping technologies. *International Journal of Machine Tools and Manufacture*. 1998;38(10):1257-87.
27. Waldbaur A, Rapp H, Länge K, Rapp BE. Let there be chip-towards rapid prototyping of microfluidic devices: one-step manufacturing processes. *Analytical Methods*. 2011;3(12):2681-716.
28. Sakin M, Kiroglu YC. 3D printing of buildings: construction of the sustainable houses of the future by BIM. *Energy Procedia*. 2017;134:702-11.

29. Zein NN, Hanouneh IA, Bishop PD, Samaan M, Eghtesad B, Quintini C. Three-dimensional print of a liver for preoperative planning in living donor liver transplantation. *Liver Transplantation*. 2013;19(12):1304-10.
30. Kizawa H, Nagao E, Shimamura M, Zhang G, Torii H. Scaffold-free 3D bio-printed human liver tissue stably maintains metabolic functions useful for drug discovery. *Biochemistry and Biophysics Reports*. 2017;10:186-91.
31. Noor N, Shapira A, Edri R, Gal I, Wertheim L, Dvir T. 3D printing of personalized thick and perfusable cardiac patches and hearts. *Advanced Science*. 2019;6(11):1900344.
32. Jamróz W, Kurek M, Łyszczarz E, Szafraniec J, Knapik-Kowalczyk J, Syrek K. 3D printed orodispersible films with Aripiprazole. *International Journal of Pharmaceutics*. 2017;533(2):413-20.
33. Aho J, Bøtker JP, Genina N, Edinger M, Arnfast L, Rantanen J. Roadmap to 3D-printed oral pharmaceutical dosage forms: feedstock filament properties and characterization for fused deposition modeling. *Journal of Pharmaceutical Sciences*. 2019;108(1):26-35.
34. Almeida A, Claeys B, Remon JP, Vervaet CJ. Hot-melt extrusion developments in the pharmaceutical industry. *Laboratory of Pharmaceutical Technology*. 2012:43-69.
35. Sareen S, Mathew G, Joseph L. Improvement in solubility of poor water-soluble drugs by solid dispersion. *International Journal of Pharmaceutical Investigation*. 2012;2(1):12-7.
36. Sarode AL, Sandhu H, Shah N, Malick W, Zia H. Hot melt extrusion (HME) for amorphous solid dispersions: predictive tools for processing and impact of drug-polymer interactions on supersaturation. *European Journal of Pharmaceutical Sciences*. 2013;48(3):371-84.
37. Thiry J, Krier F, Evrard B. A review of pharmaceutical extrusion: critical process parameters and scaling-up. *International Journal of Pharmaceutics*. 2015;479(1):227-40.
38. Patil H, Tiwari RV, Repka MA. Hot-melt extrusion: from theory to application in pharmaceutical formulation. *American Association of Pharmaceutical Scientists: Pharmaceutical Science and Technology*. 2016;17(1):20-42.
39. Stanković M, Frijlink HW, Hinrichs WLJ. Polymeric formulations for drug release prepared by hot melt extrusion: application and characterization. *Drug Discovery Today*. 2015;20(7):812-23.
40. Puri V, Brancazio D, Desai PM, Jensen KD, Chun J-H, Myerson AS. Development of maltodextrin-based immediate-release tablets using an integrated twin-screw hot-melt extrusion and injection-molding continuous manufacturing process. *Journal of Pharmaceutical Sciences*. 2017;106(11):3328-36.
41. Perissutti B, Newton JM, Podczeczek F, Rubessa F. Preparation of extruded carbamazepine and PEG 4000 as a potential rapid release dosage form. *European Journal of Pharmaceutics and Biopharmaceutics*. 2002;53(1):125-32.
42. Follonier N, Doelker E, Cole ET. Evaluation of hot-melt extrusion as a new technique for the production of polymer-based pellets for sustained release

- capsules containing high loadings of freely soluble drugs. *Drug Development and Industrial Pharmacy*. 1994;20(8):1323-39.
43. Repka MA, Majumdar S, Kumar Battu S, Srirangam R, Upadhye SB. Applications of hot-melt extrusion for drug delivery. *Expert Opinion on Drug Delivery*. 2008;5(12):1357-76.
 44. Zema L, Loreti G, Melocchi A, Maroni A, Gazzaniga A. Injection molding and its application to drug delivery. *Journal of Controlled Release*. 2012;159(3):324-31.
 45. Li LC, Deng J, Stephens DJ. Polyamide implant for antibiotic delivery—from the bench to the clinic. 2002;54(7):963-86.
 46. Teng P-T, Chern M-J, Shen Y-K, Chiang Y-C. Development of novel porous nasal scaffold using injection molding. *Polymer Engineering & Science*. 2013;53(4):762-9.
 47. Zema L, Loreti G, Macchi E, Foppoli A, Maroni A, Gazzaniga A. Injection-Molded Capsular Device for Oral Pulsatile Release: Development of a Novel Mold. *Journal of Pharmaceutical Sciences*. 2013;102(2):489-99.
 48. Goole J, Amighi K. 3D printing in pharmaceuticals: A new tool for designing customized drug delivery systems. *International Journal of Pharmaceutics*. 2016;499(1):376-94.
 49. Hwang S, Reyes EI, Moon K-s, Rumpf RC, Kim NS. Thermo-mechanical characterization of metal/polymer composite filaments and printing parameter study for fused deposition modeling in the 3D printing process. *Journal of Electronic Materials*. 2015;44(3):771-7.
 50. Tidau M, Kwade A, Finke HJ. Influence of high, disperse API load on properties along the fused-layer modeling process chain of solid dosage forms. *Pharmaceutics*. 2019;11(4).
 51. Goyanes A, Chang H, Sedough D, Hatton GB, Wang J, Buanz A. Fabrication of controlled-release budesonide tablets via desktop (FDM) 3D printing. *International Journal of Pharmaceutics*. 2015;496(2):414-20.
 52. Solanki N, Gupta SS, Serajuddin ATM. Rheological analysis of itraconazole-polymer mixtures to determine optimal melt extrusion temperature for development of amorphous solid dispersion. *European Journal of Pharmaceutical Sciences*. 2018;111:482-91.
 53. Gumaste SG, Gupta SS, Serajuddin ATM. Investigation of polymer-surfactant and polymer-drug-surfactant miscibility for solid dispersion. *The American Association of Pharmaceutical Scientists: Pharmaceutical Science and Technology*. 2016;18(5):1131-43.
 54. Sadia M, Arafat B, Ahmed W, Forbes RT, Alhnan MA. Channelled tablets: an innovative approach to accelerating drug release from 3D printed tablets. *Journal of Controlled Release*. 2018;269:355-63.
 55. Tagami T, Fukushige K, Ogawa E, Hayashi N, Ozeki T. 3D Printing factors important for the fabrication of polyvinylalcohol filament-based tablets. *Biological and Pharmaceutical Bulletin*. 2017;40(3):357-64.
 56. Ibrahim M, Barnes M, McMillin R, Cook DW, Smith S, Halquist M. 3D printing of metformin hcl pva tablets by fused deposition modeling: drug loading, tablet design, and dissolution studies. *The American Association of*

- Pharmaceutical Sciences: Pharmaceutical Science and Technology. 2019;20(5):195.
57. Öblom H, Zhang J, Pimparade M, Speer I, Preis M, Repka M, et al. 3D-Printed Isoniazid Tablets for the Treatment and Prevention of Tuberculosis- Personalized Dosing and Drug Release. *The American Association of Pharmaceutical Sciences: Pharmaceutical Science and Technology*. 2019;20(2):52.
 58. Zema L, Melocchi A, Maroni A, Gazzaniga A. Three-dimensional printing of medicinal products and the challenge of personalized therapy. *Journal of Pharmaceutical Sciences*. 2017;106(7):1697-705.
 59. Sandler N, Preis M. Printed Drug-Delivery Systems for Improved Patient Treatment. *Trends in Pharmacological Sciences*. 2016;37(12):1070-80.
 60. Water JJ, Bohr A, Boetker J, Aho J, Sandler N, Nielsen HM. Three-Dimensional Printing of Drug-Eluting Implants: Preparation of an Antimicrobial Polylactide Feedstock Material. *Journal of Pharmaceutical Sciences*. 2015;104(3):1099-107.
 61. Alhijaj M, Belton P, Qi S. An investigation into the use of polymer blends to improve the printability of and regulate drug release from pharmaceutical solid dispersions prepared via fused deposition modeling (FDM) 3D printing. *European Journal of Pharmaceutics and Biopharmaceutics*. 2016;108:111-25.
 62. Melocchi A, Parietti F, Loreti G, Maroni A, Gazzaniga A, Zema L. 3D printing by fused deposition modeling (FDM) of a swellable/erodible capsular device for oral pulsatile release of drugs. *Journal of Drug Delivery Science and Technology*. 2015;30:360-7.
 63. Melocchi A, Parietti F, Maroni A, Foppoli A, Gazzaniga A, Zema L. Hot-melt extruded filaments based on pharmaceutical grade polymers for 3D printing by fused deposition modeling. *International Journal of Pharmaceutics*. 2016;509(1):255-63.
 64. Alafaghani Aa, Qattawi A. Investigating the effect of fused deposition modeling processing parameters using Taguchi design of experiment method. *Journal of Manufacturing Processes*. 2018;36:164-74.
 65. Palekar S, Nukala PK, Mishra SM, Kipping T, Patel K. Application of 3D printing technology and quality by design approach for development of age-appropriate pediatric formulation of baclofen. *International Journal of Pharmaceutics*. 2019;556:106-16.
 66. Fukuda IM, Pinto CFF, Moreira- CdS, Saviano AM, Lourenço FR. Design of Experiments (DoE) applied to pharmaceutical and analytical quality by design (QbD). *Brazilian Journal of Pharmaceutical Sciences*. 2018;54.
 67. doCarmo AM, Cunha-Filho MSS, Gelfuso GM, Gratieri T. Evolution of quality on pharmaceutical design: regulatory requirement? *Accreditation and Quality Assurance*. 2017;22(4):199-205.
 68. Gaikwad VL, Bhatia MS, Singhvi I. Experimental and chemoinformatics evaluation of some physicochemical properties of excipients influencing release kinetics of the acidic drug ibuprofen. *Chemosphere*. 2015;138:494-502.
 69. Malaquias LFB, Schulte HL, Chaker JA, Karan K, Durig T, Marreto RN. Hot melt extrudates formulated using design space: one simple process for both

- palatability and dissolution rate improvement. *Journal of Pharmaceutical Sciences*. 2018;107(1):286-96.
70. Kushner J, Langdon BA, Hicks I, Song D, Li F, Kathiria L, et al. A quality-by-design study for an immediate-release tablet platform: examining the relative impact of active pharmaceutical ingredient properties, processing methods, and excipient variability on drug product quality attributes. *Journal of pharmaceutical sciences*. 2014;103(2):527-38.



CHAPTER II

LITERATURE REVIEWS

2.1. Additive manufacturing

Additive layer manufacturing, also denominated three-dimensional printing (3DP), is a rapid modelling method that is defined as the set of production of joining materials to make a printed object from a digital design (1). In 3D printing, an object is fabricated by depositing additive layers of material on a plate. By applying a CAD program, a 3D object is created and changed into a .STL file. Such file is one of the most frequently utilized file format for 3D printing and comprises of the raw data for the design of an object. Initially, in the 3D printing techniques, the basement layers of the object are printed by depositing on the build plate in X-Y axis planes by travelling the nozzles. After that, the platform travels down along with Z-axis while depositing the adjacent layer on the initial layer and replicate till an object is manufactured (2). These techniques can be applied with a broad range of materials including liquids, metals, polymers, powders, pastes, solids, ceramics and plastics and it is substantially reliable to prepare complicated designs and structures (3-5).

Three-dimensional (3D) printing technologies are considered to revolutionize the personalization of dosage forms at the point of dispensing or use. These highly elegant technologies fabricate 3-dimensional objects of virtually any shape under the control of a computer software (6). 3D printing is a layer-by-layer production of 3D objects with the aid of computational design. It is also known as additive manufacturing (AM) (7). There has been five main 3DP technologies in researched areas, fused deposition modelling (FDM), binder jet printing, semi-solid extrusion (SSE), selective laser sintering (SLS) and stereolithography (8).

2.1.1. Fused deposition modelling (FDM)

Fused Deposition Modelling (FDM) is a 3D printing technique based on the melt-extrusion process. Typical FDM printers employ a thermoplastic material in the form of filament, which is then heated above its glass transition temperature (9). The extruded polymer filaments are molten into a semi-liquid state when passed through a heated nozzle. The softened filaments are then deposited onto a build platform in a layer-by-layer process to harden the soft filament. One of the advantages of this

technology is higher resolution compared with powder-bed printing, which form deposition of more complex scaffolds and to gain better dosing accuracy. FDM also provides advantages of good mechanical strength and the printed dosage forms can be designed to achieve different releases profile by changing the infill amount, 3D object design (8). In order to be smoothing the operating condition, materials must possess proper rheological effect. These properties are controlled by the pressure drop, nozzle diameter, and the feed rate, and other factors corresponding to the thermal properties of the feed material including density, thermal conductivity or glass transition temperature (T_g). It is one of the most widely applied 3D printing technique under many research due to its capacity to produce drugs with sophisticated geometries which affect the drug release profile (10).

2.1.2. Binder jet printing

Printing-based inkjet systems take into two types of methods: drop-on-demand (DOD) printing and continuous inkjet printing (CIJ). Both methods are based on the burst of a liquid stream. In such techniques, it is important to utilize a heat post-treatment of the 3D object to avoid solvents applied during the processing to remove solvent residuals and impurities within the printed drugs (10). Typical inkjet printing systems deposit droplets of binding material onto a powder bed resulting in the selective solidification of a layer onto a moving platform. After the completion of each layer, the moving platform lower and a new powder bed is appeared. Successive building of layers results to the structure designed (9).

2.1.3. Semi-solid extrusion

Alternative method of 3D printing involves layer by layer deposition of semisolids through a syringe-based tool head. Semi-solids (gel or pastes) are formulated by mixing optimal ratios of polymers and suitable solvents to obtain an appropriate rheology for printing. It has a wide range of applications the availability of bench top platforms that encourage its creative use in rapid prototyping of numerous objects (11).

2.1.4. Selective laser sintering (SLS)

In this 3D printing, a laser is travelled in a raster pattern over a powder bed. The heat generated by the laser melts and blends adjacent particles within the bed,

forming a solid object. The powder or starting materials that could be used include polyamide, polystyrene or polycarbonate. The use of SLS is well established in tissue engineering (11).

2.1.5. Stereolithography (SLA)

Stereolithography (SLA) is a 3D printing method that uses high energy of laser emissions or projections of light to selectively photopolymerize a liquid resin to create solid parts. These technologies are capable of the fabrication of structures through the consecutive layer-wise polymerization of UV-sensitive polymers, through a curing photo-polymerization (9). The major limitation of this technique is the need for photopolymerizable raw materials, which are relatively uncommon in pharmaceutical manufacturing and also, residual resin can represent a genotoxicity risk because the unprinted material may be chemically diverse and contain functional groups that are probably affect for genes (12). SLA is superior regarding manufacturing, drug release, the morphological features of the printed object and the stability due to high resolution over other methods and that heating is lowered during printing, which permits for the application of thermolabile drug unlike FDM (10).

2.2. Oral solid dosage forms using 3D printing

Oral delivery of drugs is the most convenient and preferred route of administration for patients because of its flexibility of administration, good patient compliance, cost effectiveness, low sterility restraints, and simplicity of dosage form design. When a drug is consumed orally, it is necessary to possess good solubility or dissolution properties within the biological system to be permeation across the membrane, and first pass metabolism to obtain the desired therapeutic effect via systemic circulation (13, 14). The conventionally produced solid oral delivery systems are related to limitation in producing of individualized or complex oral tablets (15, 16) and the multiple unit processes including sieving, granulation, compression, and coating that make the high cost of manufacturing methods. The 3D printing technology can skip these processes over conventional methods by providing prospects which aim at increasing the speed of production, reducing the number of steps and being capable of fabrication of the innovative complex and individualized dosage forms (17) which have improved safety, better efficacy. It is evident that the

first 3D-printed drug product, Spiritam, is encouraged by the approval of U.S FDA, in the month of August 2015 (18-20).

2.2.1. Immediate release tablets

An immediate release formulation could be formulated by producing a drug-loaded filament using a water-soluble polymer with or without plasticizers. Such polymer could be selected from the widely used polymers including povidone, hydroxypropyl methylcellulose, hydroxypropyl cellulose or grafted polymers such as Soluplus[®], Kollidon[®]VA 64 or Eudragit[®] EPO. These filaments are used in FDM printer to prepare an immediate release tablet (21, 22). Okwuosa et al. produced and studied immediate release tablets made of dypridamole and theophylline applying polyvinyl pyrrolidone (PVP) polymer, triethyl citrate (TEC) as a plasticizer and talc as a filler with the ratio of 10, 50, 12.5, and 27.5 % wt. Over 90% of the API was found to release in 30 min for both the drugs with 10% loading, exhibiting the ability of printing in producing an immediate release tablet (23). Kempin et al. explored that five different immediate release polymers, namely polyvinylpyrrolidone (PVP K12), Kollidon[®]VA 64, polyethylene glycol 20,000 (PEG 20,000), polyethylene glycol 6000 (PEG 6000) and poloxamer 407 were perfectly melt extruded to drug loaded filaments and printed to tablets containing the thermo-sensitive drug pantoprazole sodium at temperatures below 100°C. A rapid drug release from printed tablets that was completed within 10 min and 29 min was found for PVP K12 and PEG 6000 tablets, respectively (24).

2.2.2. Floating tablets

Chai et al. reported that the application of FDM printing to produce a floating dosage form. In such technique, shells and infill are the main parameters which identify the inner support and outline structure of dosage form. One shell, at least, is required to construct an item, and the adding shells provide body's strength and weight that last more time and materials. Likewise, infill level is next parameter, that can be modified from 0% to 100%, making the item from completely void to totally solid filled structure. By maintaining the structure hollow, the overall density can be reduced that makes buoyancy. In this study, the optimized tablet design with 2 shells and 0% infill exhibits the density of 0.77 g/cm³, which had the floating ability for

over 10 h in dissolution medium, while produced tablets with shells over 3 or infill level over 20% had densities over 0.9 g/cm³ that caused them to sink in less than 1 h. The drug release rate was longer for 12 h that is neither considerably affected by the number of shells nor the infill amount (25).

2.2.3. Monolithic sustained release tablets

Sustained release tablets of 5-aminosalicylic acid, were produced by preparing drug loaded polyvinyl alcohol (PVA) filaments. The drug-loaded filament was prepared by soaking the commercially available polyvinyl alcohol (PVA) filaments in its ethanolic solution containing the drug. The filament was observed to be 0.06% w/w and 0.25% w/w for 5-ASA and 4-ASA, respectively. Dissolution test of tablets containing 5-ASA in modified bicarbonate buffer managed by an Auto pH System™ depicted that tablets made of 90% infill illustrated drug release (100%) extended over 4 h period. Reducing in the infill percentage increased the drug release. It was seemed that 50% of 4-ASA destroyed during printing possibly due to high extrusion temperature (210 °C) for such filament. Therefore, this process may not be appropriate for thermo-sensitive drugs. Another polymer with lessen extrusion temperature can assist in lowering degradation of drug due to temperature (26).

2.2.4. Pulsatile drug release tablets

Chrono Caps® are example of pulsatile delivery systems that depended on capsular type. Capsules of changing thickness are developed, applying injection molding technique, using water-soluble polymers which offers different fluctuation of time lag [29]. These devices could be developed applying FDM printing of HPC filaments. Melocchi et al. explored the situation of such capsular devices fabricated by 3D printing and injection molding (27). It was noticed that the printed objects demonstrated a lag time before release of the drug. In addition, the morphological transformations were in comparison with the system constructed utilizing injection molding. This study demonstrates that the 3D printing is alternatively useful with injection molding method (28).

2.2.5. Enteric release tablets

Goyanes et al. produced enteric release tablets containing paracetamol using one type of enteric polymers like hydroxypropyl methylcellulose acetate succinate

(HPMCAS). Drug-loaded filaments were prepared applying hot melt extrusion. These filaments were produced into 3D printed tablets with a single filament using fused deposition modeling (FDM) printing. Drug loading up to 50% was maintained while prolonging the enteric protection (29). This can be advantageous as an alternative opportunity compared to conventional enteric coating process using organic solvent and safety concerns as well.

2.2.6. Nano-capsule based formulation

Beck et al. prepared 3D printed tablets with polymeric nano-capsules of deflazacort with a particle size of 138 nm. In this work, the 3D printed tablets were manufactured using the filaments made of Eudragit® RL100 (EUD) and poly(ϵ -caprolactone) (PCL) with or without mannitol and the fused deposition modeling (FDM) was used as a tablet production technique. The printed tablets were then immersed into a determined quantity of suspension containing polymeric nanoparticles and then, made them dried at 30°C over 24 h. It was observed that up to 0.62% drug was loaded by soaking the tablet for 24 h. The study showed that long soaking time, up to 24 h increases drug loading (30).

2.2.7. Medicines used in 3D printing

Printing technologies are capable of the personalization of medicines with complicated dosage regimes, especially for narrow therapeutic index (TI) drugs (31, 32). Narrow TI medicines are those that have a small gap between the therapeutic and toxic dose, thereby unsuitable dosing can cause the ineffective treatment outcomes or adverse effects. Instead of producing conventional fixed-dose formulations, 3DP may generate a printlet containing a specific dose of drug, simplicity of administration and lowering the issues of dose deviation and medication errors. Therefore, 3DP could also be gained using FDM printing to adjust the desired drug release for medicines that require delayed release to reduce the dose related adverse effect including indomethacin (33) or flexible dose changes such as theophylline (34).

2.2.7.1. Indomethacin

Indomethacin (IMC) is a member of NSAID class, analgesic agent with anti-inflammatory and antipyretic properties. Such properties have been used in several

conditions such as rheumatoid arthritis, gout attacks and osteoarthritis, tendonitis and ankylosing spondylitis. It can be administered orally that causes various adverse effects, mainly related to the gastrointestinal malfunctions (33, 35). It is a non-selective cyclooxygenase 1 and 2 (COX-1 and COX-2) inhibitor and is also an indole derivative assigned chemically as 1-(p-chlorobenzoyl)-5-methoxy- 2-methyl-1H-indole-3-acetic acid. and. IMC is pale yellow to yellow crystalline material and an odorless. It is a poor aqueous solubility and a weak dissolution rate which confined both its therapeutic usefulness and efficacy (36, 37). Nonetheless, it is lipid-soluble and sparingly soluble in alcohol. IMC possesses a pKa of 4.5 and is stable in slightly acidic media or neutral and decomposes in strong alkaline (33).

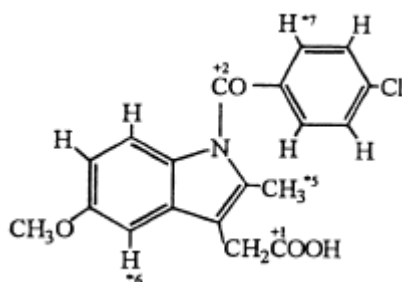


Figure 1. Structure of indomethacin.

2.2.7.2. Theophylline

Theophylline, called as 1,3-dimethylxanthine, is a methylxanthine agent used in treatment for respiratory diseases such as asthma and chronic obstructive pulmonary disease (COPD). The drug is a muco-active substance with numerous properties including secretomotoric and secretolytic activities used in the treatment of respiratory syndrome associated with viscid or excessive mucus (39).

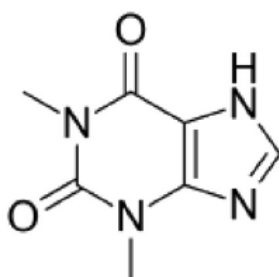


Figure 2. Structure of theophylline.

It has been widespread application in various controlled release systems such as compressed tablets (40), spray dried matrices (41) and flexible dose system including 3D printed tablets. In addition, it possesses an excellent thermal stability (melting ca. 270°C), and high solubility in various pH, which are suitable effects for drug release tests. However, the release adjustment to maintain the optimal theophylline level is needed owing to a narrow therapeutic range (10-20 µg/ml) and overdose causes cardiac arrhythmia, hyperglycemia and metabolic acidosis (42).

2.3. Strategies for drug dissolution/solubility enhancement

When a drug is consumed orally, it requires to possess good solubility or dissolution properties within the biological system to be permeation across the membrane, and first pass metabolism to achieve the desired therapeutic effect via systemic circulation. However, most of the new chemical entities in the development phases show either poor solubility or dissolution, or both (13, 43). There are numerous approaches greatly popular to enhance the dissolution rate of poorly soluble drugs methods including solid dispersion, salt formation, liquid-solid techniques, complexation, cocrystals, particle size reduction, and the use of additives in the crystallization process in overcoming this challenge (44-47). Historically, spray drying (SDD) and hot-melt extrusion (HME) have been widely applied methods to develop ASDs in the pharmaceutical industry and has resulted in successful improvements of solubility and bioavailability of poorly soluble APIs (48, 49).

2.3.1. Solid dispersion

Solid dispersions technology was firstly discovered by Sekiguchi and Obi in 1961, who noted that eutectic mixtures increase the release rate of poorly water soluble drugs (50). Preparation of the drugs as solid dispersions offers a wide range of processing and excipient selections that allow for an efficient approach when manufacturing the oral delivery systems for poorly water-soluble drugs (13, 51) and hence increase the oral bioavailability of APIs being formulated this way (52, 53). Solid dispersions is termed as molecular or amorphous mixtures of poorly water soluble drugs that is dispersed/dissolved in hydrophilic carriers and show as a one phase powder, with molecularly tiny particles that could be accomplished with mechanical grinding methods (54-59). The fine dispersion of drug within the

hydrophilic excipient, result in enhanced dissolution (60) in which the polymer properties occupy an important role in the drug dissolution pattern (50, 54).

The enhancement of the dissolution of drugs from solid dispersions can mainly be attributed to one of the different mechanisms: eutectic mixture formation, the improved wettability of the drug due to direct contact with the hydrophilic carriers, the increased in particles surface area, alteration of a metastable crystalline form of API and changing of the crystalline nature to the complete soluble amorphous state (52, 61, 62). This strategy is one of the most efficient way to improve the bioavailability of drugs with low water solubility (50, 63). The different type of the solid dispersion is influenced by the physical state of excipient (crystalline or amorphous) and drug and can be distinguished into amorphous, crystalline solid dispersions, and crystalline-amorphous solid dispersions.

Initially, crystalline solid dispersions, the eutectic mixtures, were actually the first identified solid dispersions (58). Eutectic mixtures are formed by simultaneously heating up and melting a mixture at suitable weight proportions, followed by a cooling-down phase (64). Each component possesses its specific melting temperature but when used in a particular weight proportion the mixture can melt simultaneously (13) and the temperature at which is called the eutectic temperature (64). Because the eutectic temperature is lower than the melting temperature of the individual constituents of the mixture, the production temperature can be decrease which is notably merit for thermal sensitive compounds. The advantage of eutectic mixture is that drug and excipient are more uniformly mixed than in physical mixtures that undergoes in higher drug dissolution (44). Another form of crystalline solid dispersion is solid solution. In solid solution, a crystalline drug is “dissolved” in a crystalline excipient which results in a single-phase powder because the excipient and drug molecules are positioned in the lattice of the crystal. Solid solutions contain minute particles than pure crystalline forms and are higher homogenous than physical mixtures. This renders to higher drug dissolution and absorption. For instance, griseofulvin-polyethylene glycol 4000 solid solution provided in two times greater in vivo study compared to crystalline griseofulvin (65).

In an amorphous solid dispersion, the drug disperses in an amorphous polymer/excipient turning into in a single amorphous phase (66). The amorphous state

of the mixture, homogeneously blended with a molecular level, the hydrophilic nature of the excipient and the increase surface area render in improvement of dissolution and absorption (58). For instance, the antiviral drug, telaprevir, is formulated as an amorphous solid dispersion showing 32 times enhanced dissolution and 10 times higher bioavailability (67). The limitation of amorphous solid dispersions is that they could not be stable because amorphous materials can transform to crystalline forms (64). With respect to a glass suspension of ASD, an amorphous drug is not completely dispersed in an amorphous polymer (66). Instead, the drug is dissolved as amorphous clusters or is partly amorphous and partly crystalline (64).

Glass suspensions may take place when the percentage of drug in the polymer matrix is substantially high (P35%). Recrystallization of drug is expected to appear under storage condition, and this causes negative effect on stability than glass solutions. Therefore, amorphous solid dispersions need more cautious handling and storage than crystalline solid dispersions (66). Regarding the amorphous precipitates, the drug precipitates out as an amorphous form and is dissolved in a crystalline excipient (13). The amorphous form of the drug and the hydrophilic character of the excipient render towards higher dissolution of drug. For instance, an amorphous solid dispersion of ritonavir in crystalline polyethylene glycol 8000 presented in a 3.5-5 times higher dissolution and 11-22 times increased absorption in comparison with a crystalline physical mixture of ritonavir-polyethylene glycol 8000 (54, 68).

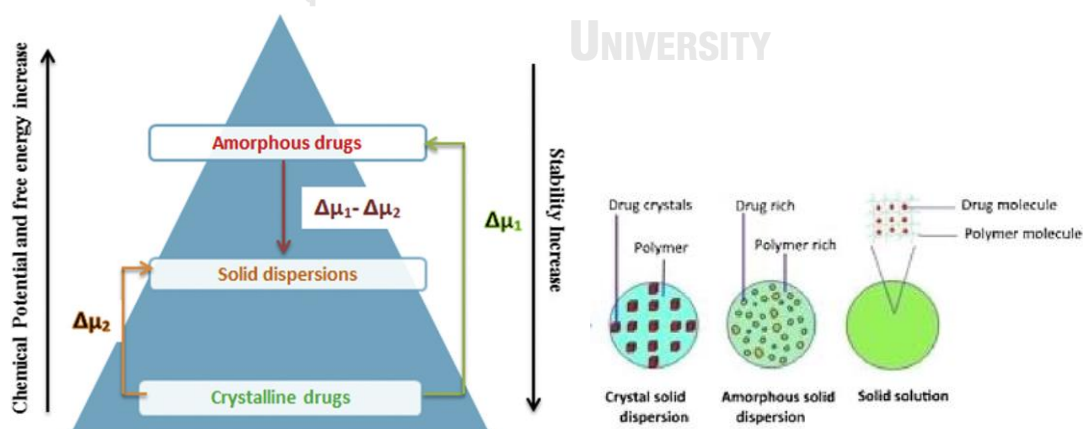


Figure 3. Energy pyramid of amorphous forms, amorphous solid dispersion, the crystalline form and their structural forms.

2.3.1.1. Stability of amorphous solid dispersion

Polymers are chemically made of repeating structural units known as monomers which are connected with each other making a long structural framework. Owing to their complicated 3D structures with many intrachain or interchain cross links, entrapping of amorphous drugs into these networks delay their molecular mobility. This reduces the chemical possibility of the amorphous drug and closer to that of the crystalline form. As a result, polymers hamper devitrification thereby preserving the stability of the amorphous state over the shelf life. The number of features, such as thermodynamic property, environmental stress, molecular mobility, preparation methods play an important role in the chemical/physical stability of the amorphous drug.

In thermodynamics, it is stated as an event which causes a higher in T_g of the material which enhances the free energy involved by the amorphous drug to change into the crystalline form. Blending a low- T_g amorphous drug with a high- T_g polymer at the molecular level happens to the formation of polymeric amorphous solid dispersion (PASD) with a middle T_g of such two components. In other words, the polymer undertakes plasticization while the T_g of the drug enhances, and it renders antiplasticized effect. Next, the drug molecules may interrelate with the polymer molecules via numerous weak forces such as hydrogen bonding, van der Waals forces, electrostatic, ionic, or hydrophobic. Such intermolecular bonds prohibit the molecular mobility of the drug molecules in the polymer matrix and render stability to the system (127).

2.3.2. Salt formation

Salt formations have grown increasing interests during recent years that it can provide many advantages. Salts are a class of crystalline materials with definite stoichiometry, leading to better solid-state stability and more predictable physical properties than amorphous solids to improve the dissolution rate of the poorly soluble drug (69). The method of salt formation is relatively simple and comprise of pairing the parent drug molecule with a suitable counterion. The essential step is the attachment of ionizable functional groups in the drug's structure that permits enough ionic interaction between the drug and the salt former (70).

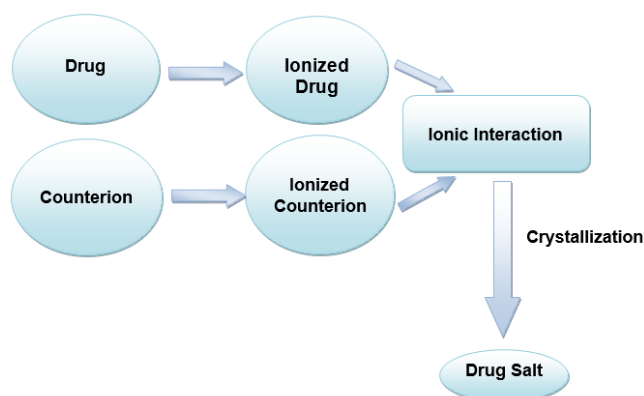


Figure 4. Diagrammatic representation of salt formation process.

2.3.3. Co-crystals

Cocrystals are necessarily neutral single-phase solids composing of two or more ingredients in a specific stoichiometric ratio held together via a wide range of noncovalent interactions including hydrogen bonds. Pharmaceutical cocrystals are multicomponent solid forms composing of an API and GRAS (Generally Regarded as Safe) partner molecules. The chemical and biological efficacy of API does not alter since these cocrystals are held together by noncovalent interactions. Secondly, it has been uniformly observed that co-former with higher solubility range make cocrystals enhanced solubility regarding parent APIs (71). In some cases, co-crystal formation is readily apparent from the resulting physical properties of the new material. For instance, formation of a co-crystal from acetaminophen and 2,4- pyridine dicarboxylic acid is immediately apparent from the red color of the co-crystal, although components are white solids. As fraction of the whole hydrogen-bonded crystal-packing arrangement, with associated reduction of the p-p* energy gap, the red color happens from the fact that the pyridine dicarboxylic acid transforms to the zwitterionic form in the co-crystal (72).

2.4. Techniques applied for amorphous solid dispersion

There are two main distinct methods such as melting and solvent evaporation to produce amorphous solid materials. Both types have been exhibited useful at the industrial and laboratorial scales. Some mechanical processes, such as ball milling or grinding, also enable to induce some amorphization (73). However, degree and robustness of amorphization are very low and, thus, of limited usefulness in these

mechanical methods (63, 73). As for melting process, a physical mixture of drug and polymer is melted by heating to form a molten mixture where a drug is dispersed or dissolved in a molten of amorphous polymer(s). The resulted molten material is further hardened by cooling that forms an amorphous solid dispersion (63, 74).

Solvent evaporation methods consist of the solubilizing of drug substance and carrier(s) in a single solvents or solvent mixture followed by solvent removal to gain a solid dispersion (73, 75). This technique is capable of yielding a molecular level mixing which is preferred to improve the solubility and stability of the product. The major advantage of such method is that the thermal decomposition of drug and polymer can be protected since low temperatures are typically used to evaporate organic solvents (76). The most appropriate technologies for the production of solid dispersions are melting of excipients via hot melt extrusion (13), solvent evaporation method by means of spray drying.

2.4.1. Hot melt extrusion (HME)

The pharmaceutical use of HME is currently promoted as a method for increasing the release rate of poorly water-soluble APIs. The bioavailability of such APIs are enhanced by melt-mixing them with hydrophilic, water-soluble polymers (7). HME is a robust method that could allow for solvent-free manufacturing of amorphous solid dispersion. Furthermore, it is a continuous process and can be easily scaled up from a small-scale laboratory extruder to a production-scale equipment. HME is based on the solid materials transfer through the heated barrel, designed with single or twin screws that can be either co-rotating or counter-rotating (Fig. 5) (14). The major application of HME is to disperse the APIs in a polymer matrix at the molecular level inside the heated barrel with rotating screw, thus forming solid solutions. HME has been used for various applications, such as (i) enhancing the dissolution rate and bioavailability of poorly soluble drugs by forming a solid dispersion or solid solution, (ii) controlling or modifying the release of the drug, (iii) taste masking of bitter APIs, and (iv) formulation of various thin films (6).

The machine is composed of several components, namely, feeder that bring the mixture inside a heating barrel at a controlled rate (“feed rate”), the screw(s) with a defined speed (“screw speed”) and at the end, the die. The screws have various

functions such as conveying, kneading elements. These elements and their design are of utmost importance in the manufacturing process and may have a strong influence on the final formulation. At the end of the screws, the die can have different shapes and diameters. Again, the temperature range can be selected in the different heating zones during the process. Therefore, the important processing parameters of this method are the screw design, the screw speed, the feed rate and the extrusion temperature. These parameters should be well managed and it is mandatory to optimize their effect on quality attributes of the final product such as drug homogeneity and drug release (6).

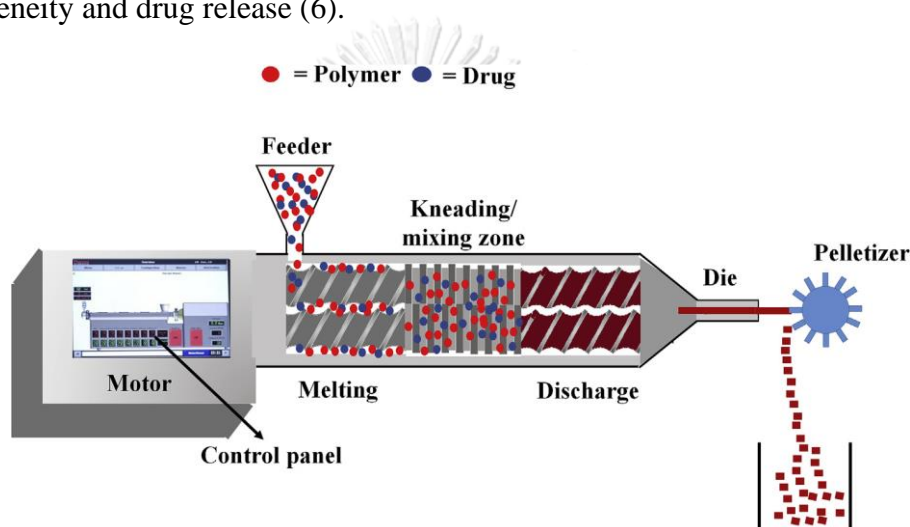


Figure 5. The schematic diagram of hot melt extrusion process.

2.4.2. Materials used in hot-melt extrusion

Major ingredients used in HME process comprise of molten materials like polymeric carriers or low melting waxes, plasticizers and other additive materials such as drug release modifiers, super disintegrants, thickening agents and antioxidants. The materials used in HME process must be thermally stable in addition to acceptable physical and chemical stability.

2.4.2.1. Active ingredient

HME renders many benefits over traditional processing techniques. The melt extrusion process is anhydrous, protecting any possible drug degradation due to hydrolysis. In addition, poorly compactable materials can be blended into one tablets

produced by cutting an extruded rod, eliminating any potential tableting problems happened in traditional compressed dosage forms (78).

2.4.2.2. Polymeric system

The selection of polymer for hot-melt extrusion process mainly depends on drug-polymer miscibility, polymer stability and function of final dosage form (78). Polymers for HME must have thermoplastic property in order to be easy the operating condition and they also show to be thermally stable under the extrusion temperatures. Other related properties should include proper glass transition temperature (T_g , 50-180°C), no toxicity and hygroscopicity as the high quantity of polymers are applied in the formulation (79). Most widely used polymeric carriers include cellulosic polymers. Such polymeric carriers include ethyl cellulose (EC) and hydroxypropyl cellulose (HPC) (80).

(I) Cellulose-based polymers

Cellulose is the most plentiful and inexhaustible biopolymeric material with a fascinating structure as the main structural component of plants in the world. Cellulose is a highly hydrophilic polymer, having hydrophilic-lipophilic balance (HLB) number at 12.45. However, due to its strong intermolecular and intramolecular hydrogen bonding between the individual chains and a high range of crystallinity (in the range of 40%-60%), it is insoluble in water in its native form. Hence, cellulose is chemically transformed to water-soluble cellulose ester or ether derivatives. In cellulose ethers, fraction of the hydrogen atoms of the three hydroxyl groups on the glucose repeating unit is modified by alkyl or combined alkyl groups (Fig. 6).

A group of polymers commonly termed as cellulose ethers could be synthesized from alkylation of cellulose. Hydroxypropyl cellulose (HPC), Ethylcellulose (EC), Methylcellulose (MC) and Hydroxypropyl methylcellulose (HPMC) are the most extensively used cellulose ethers in pharmaceutical fields (Fig 6). Cellulose esters and ethers are of particular important for producing amorphous solid dispersions because of their physicochemical properties such as high molecular weight and resistance to hydrolysis which protects the absorption of most cellulose ethers and esters in the GI tract (81, 82). The adaptable properties of cellulose ethers

are their aqueous solubility, enhanced viscosity, and water retention ability have been widely employed for various applications (83).

HPC is one of the most commonly used cellulose ethers for generation of amorphous solid dispersion because of their physicochemical properties such as high molecular weight and relatively hydrolytically stable which remain unchanged under GI conditions that ascertains beneficial in oral drug delivery systems (81, 82). This water-soluble cellulose ether is not pH-responsive and lacks very strong hydrogen bond donor and acceptor groups (84). These cellulosic polymers have the higher efficiency inhibition of the crystallization of the lipophilic drugs due to their amphiphilic nature because of their greater ability to interact with the molecules and thereby efficiently block the growth sites (85). Different ratios of Hydroxypropyl cellulose & Polyethylene oxide polymers using clotrimazole as model drug were investigated to study the effect on drug release, bioadhesive and mechanical properties, and stability of melt-extruded formulations. Hydroxypropyl cellulose was observed to improve the physical stability of PEO and clotrimazole (86).

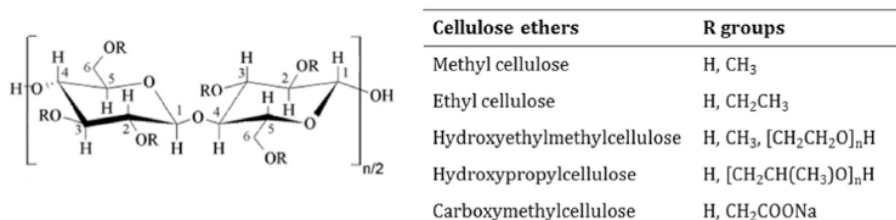


Figure 6. Chemical structure of cellulose ether derivatives.

(II) Soluplus[®]

Soluplus[®] (Polyvinyl caprolactam–polyvinyl acetate–polyethylene glycol graft copolymer) is a novel polymer with amphiphilic property and developed for solid solutions (Fig. 7). Unlike other typical solubilizers, namely, Cremophore RH40 and Solutol HS15, Soluplus[®] with its bifunctional character such as a matrix former for solid dispersion and an active solubilizer through micelle formation in water that can be regarded as the fourth generation of solid dispersions (87). Its solubility does not alter along with the gastrointestinal tract as it is hydrophilic and nonionic. It has a slightly surface-active property which can be useful to keep supersaturation of poorly soluble drugs in the gastrointestinal tract. Soluplus[®] demonstrates good solubilizing

property having low Tg about 70°C and provides the fabricating of solid solutions of numerous drugs with poor solubility applying extrusion techniques (87).

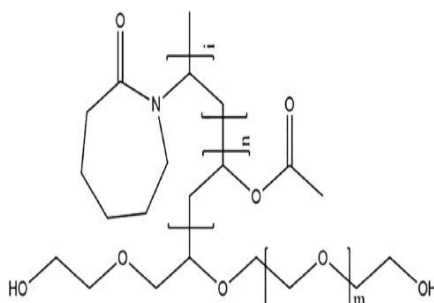


Figure 7. Chemical Structures of Soluplus.

(III) Kollidon® VA 64

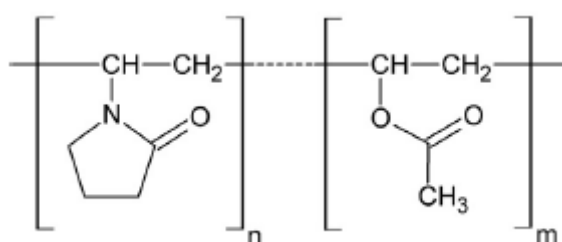


Figure 8. Chemical Structures of Kollidon® VA 64.

Kollidon VA 64 is a poly (vinylpyrrolidone-co-vinyl acetate) (Fig 8) and one of the most popular polymers for their high hydrophilicity which increases wettability of the formulation pointing to an increased dissolution rate in comparison with amorphous API and the pure crystalline (89, 90). As expected, those formulations imbibe large amounts of water when exposed to humid environment. The water moistens the formulation and decreases form stability and physical stability (90-94). High API solubilizing abilities and high glass-transition temperatures of PVP/VA (107.1°C) showed in high physical stability of ASDs as the absorption of moisture is kept small. That was reported in literature for many APIs such as naproxen (NAP) (91, 93), acetaminophen (APAP) (93), indomethacin (95) and nifedipine (96). Even low amounts of this polymer can stabilize some amorphous APIs including felodipine (97, 98), indomethacin (99), and APAP (100) which can be received from stronger

molecular interactions between APIs and these polymers than the modified celluloses had weaker interactions with some APIs therefore inhibit crystal growth from an amorphous API effectively (97, 98, 100, 101).

(IV) Eudragit[®] polymers

The Eudragit[®] range of polymers are polymethacrylates composed of synthetic anionic and cationic polymers of dimethyl aminoethyl methacrylic acid, methacrylic acid esters and methacrylate in different ratios (Fig .9). Several types are marketed and may be available as aqueous dispersion, the dry powder and organic solution. Polymethacrylates are mainly used as film-coating agents in tablet and capsule dosage forms. Moreover, present studies reported that polymethacrylates have been widely applied in the formulation of taste masking, better permeation across skin, dissolution improvement, bioavailability enhancement, enteric coating, intestinal epithelium and corneal permeation, pH dependent release, sustain release and colon targeting etc. Therefore, polymethacrylates play a significant role in formulation and development of various dosage forms with novel applications (102).

Of these series, Eudragit[®] EPO is cationic copolymer based on dimethyl aminoethyl methacrylate, methyl methacrylate and butyl methacrylate. It can be utilized in formulations such as solid dispersions, orally disintegrating tablets, nanosuspensions, nanoparticles, stabilization of liposomes, superior moisture protection for solid dosage forms. It has a molecular weight of approximately (47,000 g/mole), alkali value (180 mg KOH/g of polymer) and a glass transition temperature of 48°C. It is soluble in gastric pH until to 5.0. high pigment binding capacity, low viscosity, low polymer weight and good adhesion are specific features of Eudragit E series (102).

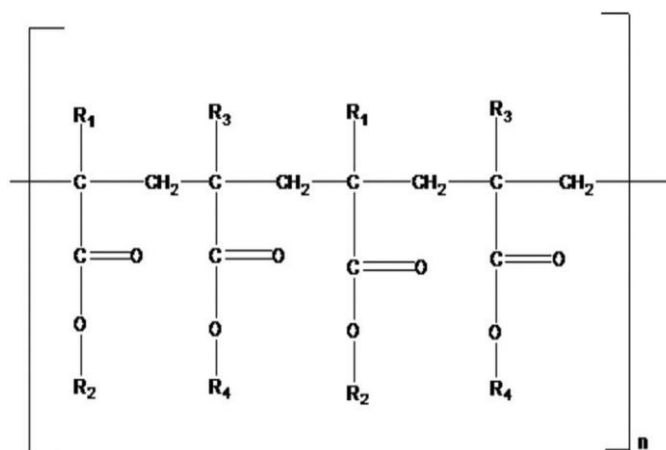


Figure 9. Chemical structure of Eudragit, For Eudragit E: $R_1, R_3=CH_3$, $R_2=CH_2CH_2N(CH_3)_2$, $R_4=CH_3, C_4H_9$, For Eudragit RL and Eudragit RS: $R_1=H, CH_3$, $R_2=CH_3, C_2H_5$, $R_3=CH_3$, $R_4=CH_2CH_2N(CH_3)^+_3CL^-$.

Eudragit RL and RS are copolymers of ethyl acrylate, methyl methacrylate and a low content of methacrylic acid ester with quaternary ammonium groups. The ammonium groups exist as salts which cause the polymers permeable. Molecular weight of these polymers is approximately 32,000 g/mol and their glass transition temperatures are 40°C and 55°C. They are mainly used for personalized release profile by combination of RL and RS grades in different ratios and they are also suitable for matrix structures. Furthermore, they were also used for formulation of patch. Patches could extend the drug release up to 12 h, with muco-adhesion. Sahoo et al. (103) generated solid dispersion of verapamil using Eudragit RLPO or Kollidon SR to prepare sustain drug release system which showed extended the drug release up to 12 h was maintained in terms of Eudragit RLPO (102).

(V) Other additional ingredients

Plasticizers can improve the operating conditions during the production of the extruded dosage form (104) by enhancing the practicability and feasibility of the polymer reducing the melt viscosity, glass transition temperature (T_g) and elastic modulus of a polymeric film. Moreover, the addition of plasticizers may lower the processing temperatures needed in hot-melt extrusion, thereby reducing drug and excipients degradation (78). Commonly used plasticizers in HME include tributyl citrate (TBC), triethyl citrate (TEC) (105), triacetin (80) and glycol derivatives

including propylene glycol and PEG (106). The decreasing in polymer T_g is reliant upon the plasticizer ratio and type. The reduction of operating temperatures may increase the stability effect of the active ingredient and that of the polymeric carrier. However, the liquid plasticizers, for instance, TEC (107) have certain disadvantages like non-uniform mixing, pre-plasticization and evaporation/loss of plasticizers.

Apart from the plasticizers, some additional excipients such as drug release modifiers (croscarmellose sodium), super disintegrants, thermal lubricant and thickening agents may also be utilized in the HME process based on the needs. Drug release profile of diltiazem hydrochloride has been improved by increasing the permeability of the pellet during dissolution (107). The burst release effect was restricted by adding the viscosity inducing agents. Super disintegrants and swelling agents such as AcDiSol and Explotab have also been employed to control drug release. Chorpheniramine melete (CPM) tablets containing lipophilic thermal lubricant are prepared by hot melt extrusion and studied the effect of such lubricant on the processing conditions. The incorporation of either TEC or glyceryl monostearate (GMS) into the powder blend decreased the drive amperes and the torque values during the hot-melt extrusion process. An increase in GMS amount in the Eudragit RS PO system resulted in higher rate of drug release from the formulation since GMS reduced the high melt viscosity of the methacrylic polymer (108). Thickening agents like MCC have been added into PEG 8000 matrices in order to increase the formulation viscosity and the plasticity of the obtained tablets developed by injection molding (109).

2.4.3. Spray drying

A relatively efficient solvent evaporation-based technology is spray drying (SD), since it permits for very rapid solvent evaporation, leading to a fast conversion of the API to the crystallized and/or amorphized form dissolve within solid carrier during the processing (110). The operating parameters of spray drying are inlet temperature, feed rate humidity and flow rate of drying gas and atomization conditions (110-112) (Fig. 10). The type and size of the spray nozzles strongly influences to the amorphous solid dispersion, in particularly to the particle size, but also smoothness and texture (113, 114). Additionally, the solid content may have an

effect on the solution viscosity and subsequently the drying process and the final product (114). Furthermore, solid concentration in the feed, viscosity, solvent type, and surface tension of the solution as well as formulation variables such as composition (drug, carrier, solvent) are important for manufactured goods properties. Mahlin et al. (115) and Baird et al. (116) have investigated using the different drug compounds showing that generating an amorphous form is reliant on the chemical nature of the drugs rather than on the processing variables. Spray drying has become the most reliable solvent-based method, as it provides strong control of the powder characteristics and due to cheaper production costs, simplicity of scale-up, and unvarying batch manufacture (66).

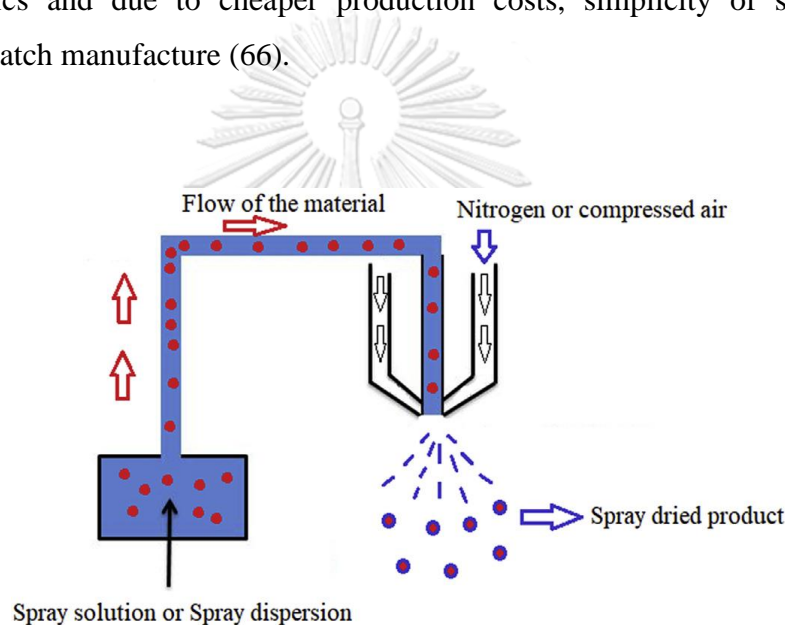


Figure 10. The diagram illustrating elementary processing steps in spray drying process.

2.5. Quality by Design (QbD)

QbD is “a systematic strategy to pharmaceutical development that enables understanding in depth in the pharmaceutical manufacturing process at various stages of the initial product development based on sound science and quality risk assessment (117, 118). Through this system, it would scientifically provide better comprehending of the product design (119), its process and further evolutions such as the scale-up parameters and optimize and control steps, therefore improving the proficiency of the operating conditions and the value of the product (118).

Pharmaceutical QbD goals may comprise: a) to gain excellent items with quality arrangements; b) to increase processing ability and decrease product variability; c) to improve pharmaceutical development and manufacturing efficiencies; and d) to heighten cause-effect analysis and regulatory flexibility (117). Commonly used QbD elements are specified in the ICH Q8 and explain in the following section for each element.

2.5.1. Quality target product profile (QTPP)

Quality Target Product Profile (QTPP) is a summary of quality features of pharmaceutical goods that must be achieved to guarantee safety and efficacy and superiority of the final product (119). Instances of QTPP include intended clinical application, administration delivery, therapeutic dosage, pharmaceutical dosage form, drug delivery system, packing container, factors affecting pharmacokinetic parameters (119, 120) and quality principles of the final goods, such as stability during storage, sterility and drug release (e.g. prolonged or immediate) (121).

2.5.1.1. Critical quality attributes (CQAs)

CQAs are generally relevant to the choice of correct amounts of excipients and drug. Additionally, CQA may include assay, identity, content uniformity, degradation, products, residual solvents, drug release or dissolution, moisture content, microbial limits, and physical properties including color, shape, size, and friability. Potential CQA derived from QTPP are utilized to point out the product and process development (119, 120).

2.5.1.2. Critical material attributes (CMAs)

The properties of materials such as the solid-state form and particle size are the main critical material attributes (122) that should meet adequate limits to guarantee the quality of excipients, drugs and other materials used during the process which lead to ensuring the desired CQA (120).

2.5.1.3. Critical process parameters (CPPs)

Critical Process Parameters (CPP) are part of the manufacturing or operating parameters such as temperature, mixing time, stirring speed, air flow, among others

that must be controlled prior or during the preparation process to ensure the desired CQA (120, 121).

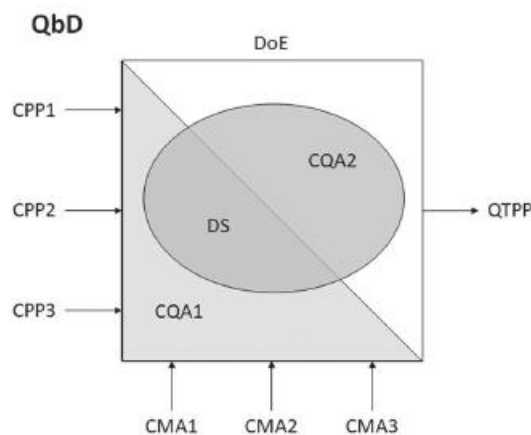


Figure 11. Schematic diagram of the steps for implementation of pharmaceutical QbD. Legend: CPP = Critical Process Parameter, CMA = Critical Material Attribute, CQA = Critical Quality Attribute, DS = Design Space, QTPP = Quality Target Product Profile, CAP = Critical Analytical Parameter.

2.6. Design of Experiment

Design of experiments (DoE) is a systematic study of performing the experiments by using the principles of science and statistics, which supports the relationship between the input factors and output responses.¹ In other words, it helps in establishing cause-and-effect relationships among the factors and response(s). Such information is necessary to manage the input control for rationally optimizing the end effects in the form of output. In simplest way, an experimental design aims at expecting the outcome on the basis of model built with the aids of experiments by bringing a change of the preconditions, which is represented by one or more independent factors, also referred to as “input variables.” The change in one or more independent variables can result an alteration in one or more dependent variables, also referred to as “output variables” or “response variables.” The experimental designs not only include the selection of appropriate independent and dependent variables, but also the arrangement of the experiments under statistically optimal conditions. In order to give a better understand of DoE application, the experimental designs can be

generally categorized into two types, such as screening designs and response surface designs, which have been discussed below in detail (124, 125).

2.6.1. Screening design

Screening designs are a proficient way to identify the main effects of the variables. The term “screening” refers to an experimental run that is intended to search the few significant factors from a listing of many possible ones (126). The most used screening designs are two-level full factorial designs, fractionate factorial designs, and Plackett -Burman designs because of their cost-effectiveness. These experimental designs permit one to study a wide range of input variables with lower numbers of experiments. However, they also have some restrictions that should be considered in order to realize the effects of input factors on responses (124, 125).

2.6.1.1. Two-level full factorial designs

Two-level full factorial designs are the most powerful screening designs, once they allow to predict main effects of input factors and their related interactions on output responses. The main limitations of two-level full factorial designs rely on the large number of experiments required, in comparison with fractionate factorial designs and Plackett-Burman designs. The number of experiments needed for two-level full factorial designs may be calculated as 2^k , where k is the number of input factors to be studied (124, 125).

2.6.1.2. Fractionate factorial designs

Fractionate factorial designs are one of the most applicable methods for screening plans, because these designs may successfully evaluate a large number of input factors with a lower number of experiments. This may be obtained by fractionating a full factorial 2^k design into a 2^{k-p} design, where p is the number of generators selected to fractionate the design. For example, when investigating four input variables, a half-fraction factorial design ($2^{4-1} = 8$ experiments) may be achieved (124, 125).

2.6.1.3. Plackett-Burman designs

Plackett-Burman designs are particular types of two-level fractionate designs, which allow one to study up to $N-1$ input factors with N experiments (N should be multiple of 4) (124, 125).

2.6.2. Optimizing designs

The most popular optimized designs are three-level full factorial designs, central composite designs (CCD), Box-Behnken designs (BBD) (123) and mixture designs (126) are because they allow modeling complex response surface (123).

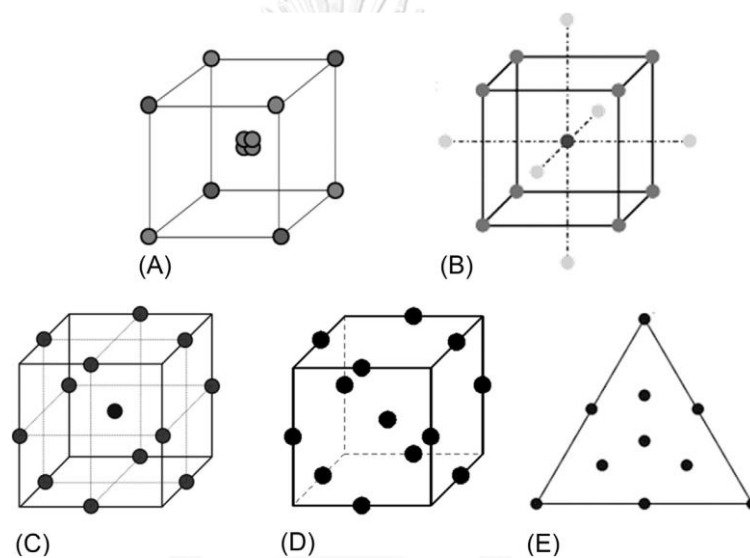


Figure 12. Examples of various optimized designs (A) full factorial design, (B) central composite design, (C) Box-Behnken design, (D) optimal design, and (E) mixture design.

2.6.2.1. Full factorial design

Three-level full factorial experiment are often used only when two or more input variables require to be performed (123). These designs may be calculated by X_k , where X represents number of factors and k indicates number of levels. A full factorial design may also be called a fully crossed design and creates experimental runs based on the factorial points and a linear polynomial model. Moreover, use of adding center points also assists in increasing for better estimation of the design

space. Such design provides the experimenter to understand the impact of each factor on the output variables, as well as the interrelated effects between the factors on the responses (126).

2.6.2.2. Central composite designs

Central composite designs (CCD) are one of the most effective optimization designs because they use second-order (quadratic) model for the response variable with a reduced number of experiments, when compared to three-level full factorial design (124, 125). CCD is regarded as a supplementary form of three-level factorial design paired with star points or axial points. It is applied when factorial designs perceive the existence of curvature in the data, thus needs augmentation from a former linear design to the quadratic response surface design (126).

2.6.2.3. Box-Behnken design

Box-Behnken designs are special types of independent quadratic designs, which permit 1st and 2nd order response surfaces modeling. These designs are lower-cost than three-level full factorial designs, particularly for large number of input factors (124, 125). In this design, the experimental combinations are at the center of edges of the processing space and at the middle. The designs have limited capacity for orthogonal blocking in comparison with the CCDs. However, it can be alternatively selected for fitting quadratic models that is necessary three levels of each factor and is quite in rotation to supply symmetry to the design (126).

2.6.2.4. Optimal Designs

The optimality of a design is dependent upon the statistical model and is assessed in terms of a statistical factor, which is correlated to the variance-matrix of the predictor. Both functions such as specifying an appropriate model and a suitable criterion necessitate to understand the statistical theory and practical information with designing experiments. Moreover, optimal designs are of various types such as D-optimal, A-optimal and I-optimal. These designs exploit three levels for each factor and are most generally applied for factor optimization study (126).

(A) Mixture Designs

In a mixture experiment, the independent variables are proportions of various constituents of a blend. In other word, such proportions of the different factors must be 100% in total. Mixture designs can be categorized into simplex-lattice designs, simplex-centroid designs, and optimal designs. Among these variants of mixture designs, optimal design is the most commonly useful for optimization of factors (126).



REFERENCES

1. Gross BC, Erkal JL, Lockwood SY, Chen C, Spence DM. Evaluation of 3D printing and its potential impact on biotechnology and the chemical sciences. *Analytical Chemistry*. 2014;86(7):3240-53.
2. Goole J, Amighi K. 3D printing in pharmaceuticals: A new tool for designing customized drug delivery systems. *International Journal of Pharmaceutics*. 2016;499(1):376-94.
3. Vithani K, Goyanes A, Jannin V, Basit A, Gaisford S, Boyd B. An overview of 3D printing technologies for soft materials and potential opportunities for lipid-based drug delivery systems. *Pharmaceutical Research*. 2019;36.
4. Trenfield SJ, Awad A, Goyanes A, Gaisford S, Basit AW. 3D printing pharmaceuticals: drug development to frontline care. *Trends in Pharmacological Sciences*. 2018;39(5):440-51.
5. Prasad L, Smyth H. 3D printing technologies for drug delivery: a review. *Drug Development and Industrial Pharmacy*. 2015;42:1-35.
6. Maniruzzaman M, Boateng JS, Snowden MJ, Douroumis D. A review of hot-melt extrusion: process technology to pharmaceutical products. *Improvement Science Research Network Pharmaceutics*. 2012;2012.
7. Zhang J, Feng X, Patil H, Tiwari RV, Repka MA. Coupling 3D printing with hot-melt extrusion to produce controlled-release tablets. *International Journal of Pharmaceutics*. 2017;519(1-2):186-97.
8. Trenfield SJ, Awad A, Goyanes A, Gaisford S, Basit AW. 3D printing pharmaceuticals: drug development to frontline care. *Trends in Pharmacological Sciences*. 2018.
9. Economidou SN, Lamprou DA, Douroumis D. 3D printing applications for transdermal drug delivery. *International Journal of Pharmaceutics*. 2018.
10. Konta AA, García-Piña M, Serrano DR. Personalised 3D printed medicines: which techniques and polymers are more successful? *Bioengineering*. 2017;4(4):79.
11. Sadia M, Alhnan MA, Ahmed W, Jackson MJ. 3D printing of pharmaceuticals. *Micro and Nanomanufacturing Volume II: Springer*; 2018. p. 467-98.
12. Norman J, Madurawe RD, Moore CM, Khan MA, Khairuzzaman A. A new chapter in pharmaceutical manufacturing: 3D-printed drug products. *Advanced Drug Delivery Reviews*. 2017;108:39-50.
13. Baghel S, Cathcart H, O'Reilly NJ. Polymeric amorphous solid dispersions: a review of amorphization, crystallization, stabilization, solid-state characterization, and aqueous solubilization of biopharmaceutical classification system class II drugs. *Journal of Pharmaceutical Sciences*. 2016;105(9):2527-44.
14. Genina N, Hadi B, Löbmann K. Hot melt extrusion as solvent-free technique for a continuous manufacturing of drug-loaded mesoporous silica. *Journal of Pharmaceutical Sciences*. 2018;107(1):149-55.
15. Yang C, Yu D-G, Pan D, Liu X-K, Wang X, Bligh SWA. Electrospun pH-sensitive core-shell polymer nanocomposites fabricated using a tri-axial process. *Acta Biomaterialia*. 2016;35:77-86.

16. Yu D-G, Li X-Y, Wang X, Yang J-H, Bligh SWA, Williams GR. Nanofibers fabricated using triaxial electrospinning as zero order drug delivery systems. *American College Surgeon Applied Materials & Interfaces*. 2015;7(33):18891-7.
17. Skowyrza J, Pietrzak K, Alhnan MA. Fabrication of extended-release patient-tailored prednisolone tablets via fused deposition modelling (FDM) 3D printing. *European Journal of Pharmaceutical Sciences*. 2015;68:11-7.
18. Sadia M, Sośnicka A, Arafat B, Isreb A, Ahmed W, Kelarakis A. Adaptation of pharmaceutical excipients to FDM 3D printing for the fabrication of patient-tailored immediate release tablets. *International Journal of Pharmaceutics*. 2016;513(1):659-68.
19. Melocchi A, Parietti F, Maroni A, Foppoli A, Gazzaniga A, Zema L. Hot-melt extruded filaments based on pharmaceutical grade polymers for 3D printing by fused deposition modeling. *International Journal of Pharmaceutics*. 2016;509(1):255-63.
20. Norman J, Madurawe RD, Moore CM, Khan MA, Khairuzzaman AJA. A new chapter in pharmaceutical manufacturing: 3D-printed drug products. *Advanced Drug Delivery Reviews*. 2017;108:39-50.
21. Alhijaj M, Belton P, Qi S. An investigation into the use of polymer blends to improve the printability of and regulate drug release from pharmaceutical solid dispersions prepared via fused deposition modeling (FDM) 3D printing. *European Journal of Pharmaceutics and Biopharmaceutics*. 2016;108:111-25.
22. Ilyés K, Kovács NK, Balogh A, Borbás E, Farkas B, Casian T. The applicability of pharmaceutical polymeric blends for the fused deposition modelling (FDM) 3D technique: Material considerations-printability-process modulation, with consecutive effects on in vitro release, stability and degradation. *European Journal of Pharmaceutical Sciences*. 2019;129:110-23.
23. Okwuosa TC, Stefaniak D, Arafat B, Isreb A, Wan K-W, Alhnan MA. A lower temperature fdm 3d printing for the manufacture of patient-specific immediate release tablets. *Pharmaceutical Research*. 2016;33(11):2704-12.
24. Kempin W, Domsta V, Grathoff G, Brecht I, Semmling B, Tillmann S. Immediate release 3D-printed tablets produced via fused deposition modeling of a thermo-sensitive drug. *Pharmaceutical Research*. 2018;35(6):124.
25. Chai X, Chai H, Wang X, Yang J, Li J, Zhao Y. Fused deposition modeling (FDM) 3D printed tablets for intragastric floating delivery of domperidone. *Scientific Reports*. 2017;7(1):2829.
26. Goyanes A, Buanz ABM, Hatton GB, Gaisford S, Basit AW. 3D printing of modified-release aminosalicylate (4-ASA and 5-ASA) tablets. *European Journal of Pharmaceutics and Biopharmaceutics*. 2015;89:157-62.
27. Melocchi A, Parietti F, Loreti G, Maroni A, Gazzaniga A, Zema L. 3D printing by fused deposition modeling (FDM) of a swellable/erodible capsular device for oral pulsatile release of drugs. *Journal of Drug Delivery Science and Technology*. 2015;30:360-7.
28. Khatri P, Shah MK, Vora N. Formulation strategies for solid oral dosage form using 3D printing technology: A mini-review. *Journal of Drug Delivery Science and Technology*. 2018;46:148-55.

29. Goyanes A, Fina F, Martorana A, Sedough D, Gaisford S, Basit AW. Development of modified release 3D printed tablets (printlets) with pharmaceutical excipients using additive manufacturing. *International Journal of Pharmaceutics*. 2017;527(1):21-30.
30. Beck RCR, Chaves PS, Goyanes A, Vukosavljevic B, Buanz A, Windbergs M. 3D printed tablets loaded with polymeric nanocapsules: an innovative approach to produce customized drug delivery systems. *International Journal of Pharmaceutics*. 2017;528(1):268-79.
31. Alomari M, Mohamed FH, Basit AW, Gaisford S. Personalised dosing: printing a dose of one's own medicine. *International Journal of Pharmaceutics*. 2015;494(2):568-77.
32. Vuddanda PR, Alomari M, Dodoo CC, Trenfield SJ, Velaga S, Basit AW. Personalisation of warfarin therapy using thermal ink-jet printing. *European Journal of Pharmaceutical Sciences*. 2018;117:80-7.
33. Gupta NV, Gowda DV, Balamuralidhara V, Khan MS. Preparation and comparative bioavailability studies of indomethacin-loaded cetyl alcohol microspheres. *Journal of Pharmaceutics*. 2013;2013:109837.
34. Pietrzak K, Isreb A, Alhnan MA. A flexible-dose dispenser for immediate and extended release 3D printed tablets. *European Journal of Pharmaceutics and Biopharmaceutics*. 2015;96:380-7.
35. Froelich A, Osmalek T, Snela A, Kunstman P, Jadach B, Olejniczak M. Novel microemulsion-based gels for topical delivery of indomethacin: Formulation, physicochemical properties and in vitro drug release studies. *Journal of Colloid and Interface Science*. 2017;507:323-36.
36. Löbenberg R, Amidon GL. Modern bioavailability, bioequivalence and biopharmaceutics classification system. New scientific approaches to international regulatory standards. *European Journal of Pharmaceutics and Biopharmaceutics*. 2000;50(1):3-12.
37. Hirasawa N, Ishise S, Miyata H, Danjo K. Physicochemical characterization and drug release studies of nilvadipine solid dispersions using water-insoluble polymer as a carrier. *Drug Development and Industrial Pharmacy*. 2003;29(3):339-44.
38. Yamamura S, Gotoh H, Sakamoto Y, Momose Y. Physicochemical properties of amorphous precipitates of cimetidine-indomethacin binary system. *European Journal of Pharmaceutics and Biopharmaceutics*. 2000;49(3):259-65.
39. Kalyani L, Rao CVN. Simultaneous spectrophotometric estimation of Salbutamol, Theophylline and Ambroxol three component tablet formulation using simultaneous equation methods. *Karbala International Journal of Modern Science*. 2018;4(1):171-9.
40. Ceballos A, Cirri M, Maestrelli F, Corti G, Mura P. Influence of formulation and process variables on in vitro release of theophylline from directly-compressed Eudragit matrix tablets. *Il Farmaco*. 2005;60(11):913-8.
41. Asada M, Takahashi H, Okamoto H, Tanino H, Danjo K. Theophylline particle design using chitosan by the spray drying. *International Journal of Pharmaceutics*. 2004;270(1):167-74.

42. Mengozzi G, Intorre L, Bertini S, Giorgi M, Soldani G. Comparative bioavailability of two sustained-release theophylline formulations in the dog. *Pharmacological Research*. 1998;38(6):481-5.
43. Colombo P, Sonvico F, Colombo G, Bettini R. Novel platforms for oral drug delivery. *Pharmaceutical Research*. 2009;26(3):601-11.
44. Leuner C, Dressman J. Improving drug solubility for oral delivery using solid dispersions. *European Journal of Pharmaceutics and Biopharmaceutics*. 2000;50(1):47-60.
45. Adebisi AO, Kaialy W, Hussain T, Al-Hamidi H, Nokhodchi A, Conway BR. An assessment of triboelectrification effects on co-ground solid dispersions of carbamazepine. *Powder Technology*. 2016;292:342-50.
46. Adebisi AO, Kaialy W, Hussain T, Al-Hamidi H, Nokhodchi A, Conway BR. Solid-state, triboelectrostatic and dissolution characteristics of spray-dried piroxicam-glucosamine solid dispersions. *Colloids and Surfaces B: Biointerfaces*. 2016;146:841-51.
47. Tan X, Li G, Zhao Y, Hu C. Effect of preparation method on the surface properties and activity of Ni_{0.7}Cu_{0.3}Fe₂O₄ nanoparticles. *Journal of Alloys and Compounds*. 2010;493(1):55-63.
48. Khadka P, Ro J, Kim H, Kim I, Kim JT, Kim H. Pharmaceutical particle technologies: An approach to improve drug solubility, dissolution and bioavailability. *Asian Journal of Pharmaceutical Sciences*. 2014;9(6):304-16.
49. Shah VP, Amidon GL. G.L. Amidon, H. Lennernas, V.P. Shah, and J.R. Crison. A theoretical basis for a biopharmaceutic drug classification: the correlation of in vitro drug product dissolution and in vivo bioavailability, *Pharmaceutical Research* 12, 413-420, 1995-Backstory of BCS. *The American Association of Pharmaceutical Scientists: Pharmaceutical Science and Technology*. 2014;16(5):894-8.
50. Eloy JO, Marchetti JM. Solid dispersions containing ursolic acid in Poloxamer 407 and PEG 6000: A comparative study of fusion and solvent methods. *Powder Technology*. 2014;253:98-106.
51. Volkova TV, Perlovich GL, Terekhova IV. Enhancement of dissolution behavior of antiarthritic drug leflunomide using solid dispersion methods. *Thermochimica Acta*. 2017;656:123-8.
52. Beneš M, Pekárek T, Beránek J, Havlíček J, Krejčík L, Šimek M. Methods for the preparation of amorphous solid dispersions - A comparative study. *Journal of Drug Delivery Science and Technology*. 2017;38:125-34.
53. Dong Z, Chatterji A, Sandhu H, Choi DS, Chokshi H, Shah N. Evaluation of solid state properties of solid dispersions prepared by hot-melt extrusion and solvent co-precipitation. *International Journal of Pharmaceutics*. 2008;355(1):141-9.
54. Sawicki E, Schellens JHM, Beijnen JH, Nuijen B. Inventory of oral anticancer agents: Pharmaceutical formulation aspects with focus on the solid dispersion technique. *Cancer Treatment Reviews*. 2016;50:247-63.
55. Kawabata Y, Wada K, Nakatani M, Yamada S, Onoue S. Formulation design for poorly water-soluble drugs based on biopharmaceutics classification system: Basic approaches and practical applications. *International Journal of Pharmaceutics*. 2011;420(1):1-10.

56. Stuurman FE, Nuijen B, Beijnen JH, Schellens JHM. Oral Anticancer Drugs: Mechanisms of Low Bioavailability and Strategies for Improvement. *Clinical Pharmacokinetics*. 2013;52(6):399-414.
57. Alam MA, Ali R, Al-Jenoobi FI, Al-Mohizea AM. Solid dispersions: a strategy for poorly aqueous soluble drugs and technology updates. *Expert Opinion on Drug Delivery*. 2012;9(11):1419-40.
58. Bikiaris DN. Solid dispersions, Part I: recent evolutions and future opportunities in manufacturing methods for dissolution rate enhancement of poorly water-soluble drugs. *Expert Opinion on Drug Delivery*. 2011;8(11):1501-19.
59. Craig DQM. The mechanisms of drug release from solid dispersions in water-soluble polymers. *International Journal of Pharmaceutics*. 2002;231(2):131-44.
60. Janssens S, Van den Mooter G. Review: physical chemistry of solid dispersions. *Journal of Pharmacy and Pharmacology*. 2009;61(12):1571-86.
61. Frizon F, Eloy JdO, Donaduzzi CM, Mitsui ML, Marchetti JM. Dissolution rate enhancement of loratadine in polyvinylpyrrolidone K-30 solid dispersions by solvent methods. *Powder Technology*. 2013;235:532-9.
62. de Waard H, Hinrichs WLJ, Visser MR, Bologna C, Frijlink HW. Unexpected differences in dissolution behavior of tablets prepared from solid dispersions with a surfactant physically mixed or incorporated. *International Journal of Pharmaceutics*. 2008;349(1):66-73.
63. Vasconcelos T, Sarmiento B, Costa P. Solid dispersions as strategy to improve oral bioavailability of poor water soluble drugs. *Drug Discovery Today*. 2007;12(23):1068-75.
64. Vo CL-N, Park C, Lee B-J. Current trends and future perspectives of solid dispersions containing poorly water-soluble drugs. *European Journal of Pharmaceutics and Biopharmaceutics*. 2013;85(3, Part B):799-813.
65. Dannenfelser R-M, He H, Joshi Y, Bateman S, Serajuddin ATM. Development of clinical dosage forms for a poorly water soluble drug I: Application of polyethylene glycol-polysorbate 80 solid dispersion carrier system. *Journal of Pharmaceutical Sciences*. 2004;93(5):1165-75.
66. Srinarong P, de Waard H, Frijlink HW, Hinrichs WLJ. Improved dissolution behavior of lipophilic drugs by solid dispersions: the production process as starting point for formulation considerations. *Expert Opinion on Drug Delivery*. 2011;8(9):1121-40.
67. Kwong AD, Kauffman RS, Hurter P, Mueller P. Discovery and development of telaprevir: an NS3-4A protease inhibitor for treating genotype 1 chronic hepatitis C virus. *Nature Biotechnology*. 2011;29(11):993-1003.
68. Law D, Schmitt EA, Marsh KC, Everitt EA, Wang W, Fort JJ. Ritonavir-PEG 8000 Amorphous Solid Dispersions: In vitro and In vivo Evaluations. *Journal of Pharmaceutical Sciences*. 2004;93(3):563-70.
69. Fu Q, Lu H-D, Xie Y-F, Liu J-Y, Han Y, Gong N-B. Salt formation of two BCS II drugs (indomethacin and naproxen) with (1R, 2R)-1,2-diphenylethylenediamine: Crystal structures, solubility and thermodynamics analysis. *Journal of Molecular Structure*. 2019;1185:281-9.
70. Makary P, editor *Principles of Salt Formation*. 2014.

71. Bhattacharya B, Das S, Lal G, Soni SR, Ghosh A, Reddy CM. Screening, crystal structures and solubility studies of a series of multidrug salt hydrates and cocrystals of fenamic acids with trimethoprim and sulfamethazine. *Journal of Molecular Structure*. 2020;1199:127028.
72. Sander JRG, Bučar D-K, Henry RF, Baltrusaitis J, Zhang GGZ, Macgillivray LR. a red zwitterionic co-crystal of acetaminophen and 2,4-pyridinedicarboxylic acid. *Journal of Pharmaceutical Sciences*. 2010;99(9):3676-83.
73. Sóti PL, Bocz K, Pataki H, Eke Z, Farkas A, Verreck G. Comparison of spray drying, electroblowing and electrospinning for preparation of Eudragit E and itraconazole solid dispersions. *International Journal of Pharmaceutics*. 2015;494(1):23-30.
74. Ghebremeskel AN, Vemavarapu C, Lodaya M. Use of surfactants as plasticizers in preparing solid dispersions of poorly soluble API: Selection of polymer–surfactant combinations using solubility parameters and testing the processability. *International Journal of Pharmaceutics*. 2007;328(2):119-29.
75. Passerini N, Calogerà G, Albertini B, Rodriguez L. Melt granulation of pharmaceutical powders: A comparison of high-shear mixer and fluidised bed processes. *International Journal of Pharmaceutics*. 2010;391(1):177-86.
76. Serajuddin AT. Solid dispersion of poorly water-soluble drugs: early promises, subsequent problems, and recent breakthroughs. *Journal of Pharmaceutical Sciences*. 1999;88(10):1058-66.
77. Mendonsa N, Almutairy B, Kallakunta VR, Sarabu S, Thipsay P, Bandari S. Manufacturing strategies to develop amorphous solid dispersions: An overview. *Journal of Drug Delivery Science and Technology*. 2020;55:101459.
78. Chokshi R, Zia H. Hot-melt extrusion technique: a review. *Iranian Journal of Pharmaceutical Research*. 2010;3-16.
79. Zi P, Zhang C, Ju C, Su Z, Bao Y, Gao J. Solubility and bioavailability enhancement study of lopinavir solid dispersion matrixed with a polymeric surfactant - Soluplus. *European Journal of Pharmaceutical Sciences*. 2019;134:233-45.
80. Madan S, Madan S. Hot melt extrusion and its pharmaceutical applications. *Asian Journal of Pharmaceutical Sciences*. 2012;7(1).
81. Edgar KJ, Buchanan CM, Debenham JS, Rundquist PA, Seiler BD, Shelton MC. Advances in cellulose ester performance and application. *Progress in Polymer Science*. 2001;26(9):1605-88.
82. Liu H, Taylor LS, Edgar KJ. The role of polymers in oral bioavailability enhancement; a review. *Polymer*. 2015;77:399-415.
83. Sharma P, Modi SR, Bansal AK. Co-processing as a tool to improve aqueous dispersibility of cellulose ethers. *Drug Development and Industrial Pharmacy*. 2015;41(11):1745-58.
84. Chavan RB, Rathi S, Jyothi VGSS, Shastri NR. Cellulose based polymers in development of amorphous solid dispersions. *Asian Journal of Pharmaceutical Sciences*. 2019;14(3):248-64.

85. Xie T, Taylor LS. Dissolution performance of high drug loading celecoxib amorphous solid dispersions formulated with polymer combinations. *Pharmaceutical Research*. 2016;33(3):739-50.
86. Repka MA, Battu SK, Upadhye SB, Thumma S, Crowley MM, Zhang F. Pharmaceutical applications of hot-melt extrusion: part II. *Drug Development and Industrial Pharmacy*. 2007;33(10):1043-57.
87. Nagy ZK, Balogh A, Vajna B, Farkas A, Patyi G, Kramarics Á. Comparison of electrospun and extruded soluplus[®]-based solid dosage forms of improved dissolution. *Journal of Pharmaceutical Sciences*. 2012;101(1):322-32.
88. Lehmkemper K, Kyeremateng SO, Bartels M, Degenhardt M, Sadowski G. Physical stability of API/polymer-blend amorphous solid dispersions. *European Journal of Pharmaceutics and Biopharmaceutics*. 2018;124:147-57.
89. Itai S, Nemoto M, Kouchiwa S, Murayama H, Nagai T. Influence of wetting factors on the dissolution behavior of flufenamic acid. *Chemical & Pharmaceutical Bulletin*. 1985;33(12):5464-73.
90. Qian F, Wang J, Hartley R, Tao J, Haddadin R, Mathias N. Solution behavior of PVP-VA and HPMC-as-based amorphous solid dispersions and their bioavailability implications. *Pharmaceutical Research*. 2012;29(10):2766-76.
91. Prudic A, Ji Y, Luebbert C, Sadowski G. Influence of humidity on the phase behavior of API/polymer formulations. *European Journal of Pharmaceutics and Biopharmaceutics*. 2015;94:352-62.
92. Hancock BC, Zografi G. The Relationship Between the Glass Transition Temperature and the Water Content of Amorphous Pharmaceutical Solids. *Pharmaceutical Research*. 1994;11(4):471-7.
93. Lehmkemper K, Kyeremateng SO, Heinzerling O, Degenhardt M, Sadowski G. Long-term physical stability of PVP- and PVPVA-amorphous solid dispersions. *Molecular Pharmaceutics*. 2017;14(1):157-71.
94. Konno H, Taylor LS. Ability of different polymers to inhibit the crystallization of amorphous felodipine in the presence of moisture. *Pharmaceutical Research*. 2008;25(4):969-78.
95. Yuan X, Xiang T-X, Anderson BD, Munson EJ. Hydrogen bonding interactions in amorphous indomethacin and its amorphous solid dispersions with poly (vinylpyrrolidone) and poly (vinylpyrrolidone-co-vinyl acetate) studied using ¹³C solid-state NMR. *Molecular Pharmaceutics*. 2015;12(12):4518-28.
96. Theil F, Anantharaman S, Kyeremateng SO, van Lishaut H, Dreis-Kühne SH, Rosenberg J. Frozen in time: kinetically stabilized amorphous solid dispersions of nifedipine stable after a quarter century of storage. *Molecular Pharmaceutics*. 2017;14(1):183-92.
97. Konno H, Taylor LS. Influence of different polymers on the crystallization tendency of molecularly dispersed amorphous felodipine. *Journal of Pharmaceutical sciences*. 2006;95(12):2692-705.
98. Kestur U, Taylor L. Role of polymer chemistry in influencing crystal growth rates from amorphous felodipine. *Crystengcomm*. 2010;12.
99. Matsumoto T, Zografi G. Physical Properties of solid molecular dispersions of indomethacin with poly(vinylpyrrolidone) and poly(vinylpyrrolidone-co-

- vinyl-acetate) in relation to indomethacin crystallization. *Pharmaceutical Research*. 1999;16(11):1722-8.
100. Trasi N, abbou oucherif K, Litster J, Taylor L. Evaluating the influence of polymers on nucleation and growth in supersaturated solutions of acetaminophen. *Cryst Eng Comm*. 2014;17.
 101. Kothari K, Ragoonanan V, Suryanarayanan R. The Role of drug-polymer hydrogen bonding interactions on the molecular mobility and physical stability of nifedipine solid dispersions. *Molecular Pharmaceutics*. 2015;12(1):162-70.
 102. Patra C, Priya R, Swain DS, Jena G, Panigrahi K, Ghose D. Pharmaceutical significance of Eudragit: A review. *Future Journal of Pharmaceutical Sciences*. 2017;3.
 103. Sahoo J, Murthy PN, Biswal S, Manik. Formulation of sustained-release dosage form of verapamil hydrochloride by solid dispersion technique using Eudragit RLPO or Kollidon[®]SR. *AAPS PharmSciTech*. 2009;10(1):27-33.
 104. Crowley MM, Zhang F, Repka MA, Thumma S, Upadhye SB, Kumar Battu S. Pharmaceutical applications of hot-melt extrusion: part I. *Drug Development and Industrial Pharmacy*. 2007;33(9):909-26.
 105. Repka MA, Gerding TG, Repka SL, McGinity JW. Influence of plasticizers and drugs on the physical-mechanical properties of hydroxypropylcellulose films prepared by hot melt extrusion. *Drug Development and Industrial Pharmacy*. 1999;25(5):625-33.
 106. Zhang F, McGinity JW. Properties of sustained-release tablets prepared by hot-melt extrusion. *Pharmaceutical Development and Technology*. 1999;4(2):241-50.
 107. Schilling SU, Shah NH, Waseem Malick A, McGinity JW. Properties of melt extruded enteric matrix pellets. *European Journal of Pharmaceutics and Biopharmaceutics*. 2010;74(2):352-61.
 108. Follonier N, Doelker E, Cole ET. Various ways of modulating the release of diltiazem hydrochloride from hot-melt extruded sustained release pellets prepared using polymeric materials. *Journal of Controlled Release*. 1995;36(3):243-50.
 109. Cuff G, Raouf FJ. A preliminary evaluation of injection molding as a technology to produce tablets. 1998;22:96-106.
 110. Paudel A, Worku ZA, Meeus J, Guns S, Van den Mooter G. Manufacturing of solid dispersions of poorly water soluble drugs by spray drying: Formulation and process considerations. *International Journal of Pharmaceutics*. 2013;453(1):253-84.
 111. Paudel A, Loyson Y, Van den Mooter G. An Investigation into the effect of spray drying temperature and atomizing conditions on miscibility, physical stability, and performance of naproxen-PVP K 25 solid dispersions. *Journal of Pharmaceutical Sciences*. 2013;102(4):1249-67.
 112. Gu B, Linehan B, Tseng Y-C. Optimization of the Büchi B-90 spray drying process using central composite design for preparation of solid dispersions. *International Journal of Pharmaceutics*. 2015;491(1):208-17.
 113. Thybo P, Hovgaard L, Lindeløv JS, Brask A, Andersen SK. Scaling up the spray drying process from pilot to production scale using an atomized droplet size criterion. *Pharmaceutical Research*. 2008;25(7):1610-20.

114. Dobry DE, Settell DM, Baumann JM, Ray RJ, Graham LJ, Beyerinck RA. A Model-based methodology for spray-drying process development. *Journal of Pharmaceutical Innovative*. 2009;4(3):133-42.
115. Mahlin D, Ponnambalam S, Heidarian Höckerfelt M, Bergström CAS. Toward in silico prediction of glass-forming ability from molecular structure alone: a screening tool in early drug development. *Molecular Pharmaceutics*. 2011;8(2):498-506.
116. Baird JA, Santiago-Quinonez D, Rinaldi C, Taylor LS. Role of viscosity in influencing the glass-forming ability of organic molecules from the undercooled melt state. *Pharmaceutical Research*. 2012;29(1):271-84.
117. Yu LX, Amidon G, Khan MA, Hoag SW, Polli J, Raju GK. Understanding pharmaceutical quality by design. *The American Association Pharmaceutical Scientists: Pharmaceutical Science and Technology*. 2014;16(4):771-83.
118. Mendonsa NS, Pradhan A, Sharma P, Prado RMB, Murthy SN, Kundu S. A quality by design approach to develop topical creams via hot-melt extrusion technology. *European Journal of Pharmaceutical Sciences*. 2019;136:104948.
119. Sangshetti JN, Deshpande M, Zaheer Z, Shinde DB, Arote R. Quality by design approach: Regulatory need. *Arabian Journal of Chemistry*. 2017;10:S3412-S25.
120. Zhang L, Mao S. Application of quality by design in the current drug development. *Asian Journal of Pharmaceutical Sciences*. 2017;12(1):1-8.
121. Cunha S, Costa CP, Moreira JN, Sousa Lobo JM, Silva AC. Using the quality by design (QbD) approach to optimize formulations of lipid nanoparticles and nanoemulsions: A review. *Nanomedicine: Nanotechnology, Biology and Medicine*. 2020;28:102206.
122. Soni G, Kale K, Shetty S, Gupta MK, Yadav KS. Quality by design (QbD) approach in processing polymeric nanoparticles loading anticancer drugs by high pressure homogenizer. *Heliyon*. 2020;6(4):e03846.
123. Fukuda I, Pinto C, Moreira C, Saviano A, Lourenço F. Design of experiments (DOE) applied to pharmaceutical and analytical quality by design (QbD). *Brazilian Journal of Pharmaceutical Sciences*. 2018;54.
124. S NP, Colombo P, Colombo G, D MR. Design of experiments (DoE) in pharmaceutical development. *Drug Devery of Indian Pharmacy*. 2017;43(6):889-901.
125. Vera Candioti L, De Zan MM, Cámara MS, Goicoechea HC. Experimental design and multiple response optimization. Using the desirability function in analytical methods development. *Talanta*. 2014;124:123-38.
126. Beg S, Swain S, Rahman M, Hasnain MS, Imam SS. Chapter 3 - Application of design of experiments (DoE) in pharmaceutical product and process optimization. In: Beg S, Hasnain MS, editors. *Pharmaceutical Quality by Design*: Academic Press; 2019. p. 43-64.
127. Baghel S, Cathcart H, Reilly NJO. Polymeric amorphous solid dispersions: a review of amorphization, crystallization, stabilization, solid-state characterization, and aqueous solubilization of biopharmaceutical classification system class II drugs. *Journal of Pharmaceutical Sciences*. 2016;105:2527-2544.

CHAPTER III

(Submitted manuscript to the European Journal of Pharmaceutics and Biopharmaceutics on 29th November 2020)

Research paper

Statistical Design of Experiment (DoE)-based formulation development and optimization of FDM 3D printed oral controlled release drug delivery with multi target product profile

Yee Mon Than¹, Varin Titapiwatanakun^{1,*}

¹ Department of Pharmaceutics and Industrial Pharmacy, Faculty of Pharmaceutical Sciences, Chulalongkorn University

254 Phayathai road, Pathumwan, Bangkok, 10330, Thailand

*Corresponding author: Varin Titapiwatanakun

Department of Pharmaceutics and Industrial Pharmacy, Faculty of Pharmaceutical Sciences, Chulalongkorn University

254 Phayathai road, Pathumwan, Bangkok, 10330, Thailand

E-mail address: varin.t@pharm.chula.ac.th

3.1. Abstract

Fused deposition modelling 3D printing is the most broadly applied 3D printing technology because of its low cost and non-solvent application. The objectives of this study were to produce a novel controlled release 3D printed tablets from the polymer blends by rationally exploring the impact of formulation excipients on drug release using the Design of Experiment. Firstly, optimization study of various mixtures was conducted stepwise to set up the suitable critical material attribute in DoE. This showed that the use of polymeric blends using five pharmaceutical polymers (hydroxy propyl cellulose (HPC), Kollidon[®] VA 64 (PVP/VA), Soluplus[®] (SLP), Eudragit[®] RL and RS) and five disintegrants (sodium starch glycolate, croscarmellose sodium, crospovidone, microcrystalline cellulose and low substituted hydroxypropyl cellulose) were successfully hot melt-extruded and FDM printed with the support of HPC at ratio 3:1 and 1:1, 10% indomethacin (IMC) loading and no plasticizer. Rheological assessment was performed to further understand the critical process parameters whereas the mechanical property of extrudable and printable filaments was determined by 3-point test for the formulation development. Critical quality attributes were investigated by a range of solid-state characterizations. Controlled-release dissolution profiles were obtained. D-optimal mixture design suggested that drug release was significantly affected by the combined action of different polymers and could predict the optimum formulation (IMC: HPC: PVA/VA: SLP as 10.00: 49.97: 19.09: 20.94) with the required quality target product profile at 4, 12 and 24 h. Therefore, this work could provide the practical scenario of controlled release printed tablets with QbD design and more robust filament preparation formulations for FDM printing technology.

Keywords: extended-release tablets, FDM 3D printing, hot melt extrusion, dissolution, DoE, hydroxy propyl cellulose

3.2. Introduction

Nowadays, the interest for the Quality by Design (QbD) concept has rapidly directed towards pharmaceutical field since it is a prospective tool to realize the sources of alterations in product formulation and to develop a product with advanced properties (1). The guidance for Abbreviated New Drug Application was released in 2012 by U.S FDA where it was further affirmed and scrutinized the impact of material excipients property along with manufacturability as a momentous aspect of Quality-by-design (QbD) on drug product critical quality attributes (CQA) (2). The initial step of product CQA includes physicochemical, biological, or microbiological properties that should be the suitable limit or distribution to guarantee the desirable product quality (3). The overall variability has been proposed to be an amalgamation of the variability of the excipient, API, production methods and interactions of any of these solitary factors (4). Current studies have focused on the development of FDM printed dosage forms for determining the processing factors such as infill percentage and patterns on drug release performance (5). Despite the advancements of QbD in diverse drug delivery approach, QbD on 3D printed oral controlled delivery has been still no reported on optimizing the levels of formulation components to control the drug release pattern.

One major attention of pharmaceutical research has been recognized on the low solubility APIs and to solve such problems, various formulation strategies such as particle size reduction, amorphous solid dispersion, co-crystal formation have been applied to improve aqueous solubility (6). Among these techniques, hot melt extrusion (HME) is considered to be one of the most reliable, versatile processing methods in amorphous solid dispersion in which the dispersion of one or more active ingredients in a molten polymer matrix by the action of high temperature and shear mixing of the screw speed which offer forming glassy drugs for enhanced the release rate of poorly water soluble API leading to increasing bioavailability. Moreover, HME can be effectively paired with other technologies such as fused deposition modelling printing, high pressure homogenization, high-pressurized carbon-dioxide.

Fuse deposition modelling (FDM) is the most extensively applied in the pharmaceutical sciences owing to the low cost fabrication, diverse choice of

excipients and ease of producing dosage forms even with complex geometries, which have good patient compliance (7, 8). The FDM process involves a polymer or polymer-drug mixture strand melted and extruded through a thermal nozzle tip which can be moved into different XYZ directions (9, 10), followed by solidification onto a build plate into the desired geometry as dictated by the computer software. Thus, FDM printers have been applied in producing drug products including immediate, extended, and time-released tablets. However, only a restricted number of feeding materials, i.e. filaments, are obtainable for printing items for human consumption (11). Additionally, the physical properties of the filament such as brittle, stiffness, plastic and strength are necessary to be sufficient to prevent filament breakage and enable the printer to operate (12). To fulfill this gap, many researchers have attempted to expand filaments using a single or a combination of pharmaceutical polymers, including hydroxy propyl cellulose (13), ethyl vinyl acetate (14), ethyl cellulose (15), hydroxypropyl methylcellulose acetate succinate (16), and hydroxypropyl methylcellulose (17); however, limited work has been reported regarding polymer blending.

In this study, hydroxy propyl cellulose (HPC) was revealed as a parent polymer due to their versatility in achieving controlled, swelling-driven release of a drug upon contact with water or physiological fluids (18). Lately, Solanki developed polymer blending (Kollidon[®] VA 64 combined with Affinisol[™] 15 cp or HPMCAS) with improved mechanical property of filaments and good miscibility of the polymers (19). Moreover, numerous studies have conducted to develop controlled release printed tablets using Eudragit RL PO and RS PO combined with triethyl citrate (TEC) and triacetin as plasticizers to improve the mechanical effect of the filaments (13, 20). Yet, the potential of HPC-based filaments, produced in combined with other polymers, have not been fully explored to increase the ability of filaments; especially, the feasibility of the disintegrant. For those reasons, our group assessed for the various polymers applied for the controlled release (HPC, Kollidon[®] VA 64 (PVP/VA), Soluplus[®] (SLP), Eudragit[®] RL and Eudragit[®] RS polymers) together with various disintegrants (sodium starch glycolate, croscarmellose sodium, croscopolidone, microcrystalline cellulose and low substituted hydroxypropyl) to form a solid

dispersion filament with the adequate mechanical properties via HME, without the need of plasticizer.

The objectives of the present work were to develop extended release printed tablets for oral delivery system with multi target product profile using statistical Design of Experiment. Initially, optimization study of various polymers was performed to establish the influence of factors composition with proper limit in DoE along with rheology investigation to obtain optimal HME and FDM process conditions. Meanwhile, a series of characterizations including physicochemical and mechanical properties of the solid dispersion systems were evaluated to ensure the product quality attributes. Further, mixture design was used to explore the optimized formulation and the effect of formulations factors on multi target drug release profile as generally required in pharmacopoeia for extended-release tablets.

3.3. Materials and methods

3.3.1. Materials

Indomethacin (IMC), a model drug, was obtained from Sigma-Aldrich. Hydroxy propyl cellulose (HPC), semi-crystalline Kollidon[®] VA 64 (MW. 67,000 g/mol; PVP/VA), Soluplus[®] (MW. 120,000 g/mol; SLP), Eudragit[®] RS PO and Eudragit[®] RL PO (MW. 45,000 g/mol; Eu RS and Eu RL) were purchased from BASF SE (Ludwigshafen, Germany) and used as matrix former. Sodium starch glycolate (SSG), croscarmellose sodium (CCM), cros povidone (Cros PVP), microcrystalline cellulose (MCC) and low substituted hydroxypropyl cellulose (L-HPC) were used as disintegrant. All other materials and reagents were of analytical grade.

3.3.2. Optimization study of polymer blends and processing factors

Different excipients were screened prior to developing a design of experiment (DoE). In the initial step, single polymer extrusion was performed while polymer blending with 3:1 and 1:1 ratios was conducted in 2nd stage. In the 3rd stage, a series of superdisintegrants was assessed in the combination of the polymer (chosen from the 2nd stage) as it is necessary to select the suitable polymer and other functional

excipient besides the drug (21) to guarantee the successful printing of solid dosage forms (Table 1). Physical properties of melt-extruded filaments (section 2.3) and the printability of such filaments (section 2.4) were examined to understand the critical material and process attributes.

Table 1. Optimization study with the filament properties.

Step	Formulation	HME temp. (°C)/screw speed (rpm)	Physical property	Printability at 200°C
Step I (single polymer)	HPC	140/30	soft	NP
	PVP/VA	140/30	brittle	NP
	SLP	120/30	brittle	NP
	Eu RS	120/30	brittle	NP
	Eu RL	120/30	brittle	NP
Step II (combined polymers)	HPC:PVP/VA (3:1)	150/35	stiffness	P
	HPC:SLP (3:1)		stiffness	P
	HPC:Eu RS (3:1)		stiffness	P
	HPC:Eu RL (3:1)		stiffness	P
	HPC:PVP/VA (1:1)		stiffness	P
	HPC:SLP (1:1)		stiffness	P
	HPC:Eu RS (1:1)		brittle	NP
	HPC:Eu RL (1:1)		brittle	NP
Step III (polymer combined with disintegrant)	HPC:SSG (3:1)	150/35	stiffness	P
	HPC:MCC (3:1)		stiffness	P
	HPC:Cros PVP (3:1)		stiffness	P
	HPC:CCM (3:1)		stiffness	P
	HPC:L-HPC (3:1)		stiffness	P

P= printable, NP= not printable

The filament feeding efficiency was carried out by printing filaments with fine quality features (i.e. consistent diameter and acceptable surface smoothness) into tablets (n=6). Filament that passed this test was referred to as being “printable” (10). In addition, the process parameters were optimized using rheology investigation (section 3.3.5) of the polymer blends. Then, the HME filaments and FDM printed tablets were evaluated an array of characterizations (section 3.3.6) to ensure the

critical quality attributes of the product. The independent and dependent factors levels in DoE were finally assigned.

3.3.3. Preparation of indomethacin-loaded filaments via hot melt extrusion

The powder of polymer and indomethacin (IMC) physical mixture was manually mixed in a mortar and pestle for 15 min and loaded into a single-screw filament extruder (Noztek®, England). The rotating speed of screw was operated at 30-35 rpm and the barrel temperatures were set at 120-150°C which is above the glass transition temperature (T_g) of polymers used and close to the melting point of indomethacin (160°C). Then, the mixture was extruded through a 1.75 mm diameter nozzle to obtain drug loaded filament in the range of 1.65 to 1.70 mm fit to the nozzle of the FDM printer. The drug loading percentage was fixed at 10% for all formulations (Table 1 and Table 2).

3.3.4. Fabrication of 3D printed tablets

Devices were fabricated from the drug-loaded filaments using a commercial fused-deposition modelling 3D printer, MakerBot Replicator 2x (MakerBot Inc., USA). Tablets were printed using the nozzle temperatures set at 200°C and the temperature of build plate was set at 90°C. The other printing settings were as follows: speed while extruding (90 mm/s), speed while travelling (150 mm/s), layer height (0.2 mm) and number of shells (2). The selected geometry of the dosage forms was flat faced round shape tablets with the following two different of dimensions: XYZ (10×10×4 mm) and (13×13×5 mm) which are therapeutically related doses of indomethacin (25 and 50 mg).

3.3.5. Oscillatory rheology experiment

A rotary rheometer (MARS, Germany) equipped with a parallel plate with a diameter of 25 mm was utilized to investigate the melt viscosity and processing parameters as a function of temperature for HME and 3D printing process optimization. The gap between the plate and the base was calibrated. 500-mg disc (25 mm diameter and 1 mm thickness) of each mixture was tested upon melting the sample. Amplitude sweep test was carried out to analyze the linear viscoelastic region

(LVR), followed by temperature sweep test at an amplitude strain of 1% (within the LVR region) and frequency of 1 Hz.

3.3.6. Characterization of the filaments and 3D printed objects

3.3.6.1. Macro and microscopic studies

The appearance including color, transparency of filaments and 3D printed dosage forms were examined by visual. A digital caliper (VWR1, PA, U.S.) was applied to quantify the diameters of the filaments (1.65 ± 0.05) and the dimensions of produced tablets ($10\times 10\times 4$ and $13\times 13\times 5\pm 0.02$). The topography of the drug-loaded filaments and dosage forms was observed using a Scanning Electron Microscope and Energy Dispersive X-ray Spectrometer (SEM-EDS, IT 300) at 3.0 nm resolution (1.5 KV) after being coated with a gold coater under a vacuum.

3.3.6.2. Mechanical evaluation

The flexibility and brittleness were examined by 3-point bend test to identify the mechanical properties of the extrudable and printable filaments (22). A universal TA analyzer (Texture Technologies Corp, New York, NY, USA) and the TA-95N probe set with a 25 mm supporting gap were used. The extruded filament samples were cut into rods with a length of 50 mm, then placed on the sample holder. The blades moved with a speed of 10 mm/s until reaching a maximum distance of 15 mm below the supported sample. Testing for each single filament formulation was repeated three times. The breaking distance and load force/stress data were recorded and analyzed in triplicate using the Exponents software.1.

3.3.6.3. Attenuated total reflectance-Fourier transform infrared spectroscopy (ATR-FTIR)

The molecular interactions between drug and polymer of extruded samples and physical mixtures was identified using a Varian 600 series FTIR spectrophotometer (ThermoFisher, Nicolet iS10, U.S.A) equipped with an ATR unit. Data was collected using 64 scans over a $650-4000\text{ cm}^{-1}$ range at a resolution of 6 cm^{-1} .

3.3.6.4. Thermal analysis

Thermogravimetric analysis (TGA) was measured to determine the decomposition temperature of all materials used and the produced filaments upon melt extrusion and printing. TG-DTA analyzer (Rigaku Thermo plus EVO2, Japan) was heated from 30 to 300 °C at a rate of 10 °C/min under an air atmosphere (40 mL/min). In addition, differential scanning calorimetry (Mettler Toledo, DSC822 STAR System, Germany) was used to analyze phases transformation including drug crystallization and thermal behavior of the polymer matrix. Samples (3–5 mg) from drug-loaded filaments and from layer of 3D printed tablets were placed and hermetically sealed in aluminium pans with a punched lid. Heating was set from 30 to 300°C using a heating rate of 10°C/min and nitrogen flow rate of 10 ml/min.

3.3.6.5. Powder X-ray diffraction (PXRD)

The presence of crystallinity of raw materials, extrudates and fabricated printed dosage forms was identified using a powder X-ray diffractometer (Rigaku model MiniFlex II, Japan), operated with a copper anode tube at the generator voltage and the current of 30 kV and 30 mA, respectively. Samples were scanned with the diffraction angle increasing from 5° to 45° 2θ at a step of 0.02° and a scan speed of 2 s/step.

3.3.6.6. Determination of drug content in filaments and 3D printed tablets

Indomethacin content in filaments was tested by cutting the samples of 100 mg from three different spots of the filament to ensure uniform distribution of indomethacin in the entire filament. The samples were dissolved in phosphate buffer solution (pH=7.2) and the drug content was analyzed by UV/Vis Spectrometry (Shimadzu, Japan) at the wavelength of 318 nm without disturbance from polymers and other additives. The similar procedure was performed for printed tablets.

3.3.6.7. In-vitro dissolution study

Drug release profiles of printed tablets were conducted in a USP I (Basket) dissolution apparatus (Vankel 7000, U.S.A), 900 ml phosphate buffer (pH- 7.2) medium at $37 \pm 0.5^\circ\text{C}$ with paddle speed of 50 rpm for 24 hours in triplicate. Samples

were withdrawn at 0.5, 1, 2, 4, 6, 8, 12, 14 and 24 hours. The amount of released indomethacin in sample was analyzed by UV/VIS spectrophotometer (Shimadzu, Japan) at the wavelength of 318 nm.

3.3.7. Statistical Design of Experiment (DOE)

Based on the critical quality attributes of the products, three key variables (0-55% HPC, 0-45% PVP/VA and 0-45% SLP) were designed to study the influence of main factors on drug release and the optimized formulation using D-optimal mixture design (Table 2). The measured responses (three dependent variables) were the percent drug release at 4 h (Y_1), 12 h (Y_2) and 24 h (Y_3) to closely monitor the influence of DoE factors on different phases of dissolution testing.

Table 2. D-optimal mixture design of FDM printed tablet formulations.

Formulation	X ₁ : HPC (%w/w)	X ₂ : PVP/VA (%w/w)	X ₃ : SLP(%w/w)
1	52.50	27.50	10.00
2	45.00	45.00	0
3	45.00	0	45.00
4	50.00	20.00	20.00
5	47.50	32.50	10.00
6	55.00	0	35.00
7	55.00	35.00	0
8	52.50	10.00	27.50
9	47.50	10.00	32.50

The percent drug release at the predetermined time (quality target product profile) was measured according to the range specified in Test IV, USP dissolution topic. The tolerances of dissolution are specified as follow: 35-55% at 4h, 60-80% at 8h and not less than 75% at 24h. Filaments and tablets were prepared under the same optimized process parameters, identified in the previous sections. ANOVA analysis from Minitab software was applied to evaluate the experimental results including the statistical coefficients of the factors (linear regression (R^2), predicted R^2 and adjusted R^2) and subsequently create the design space with the optimized formulation.

3.4. Results and discussion

3.4.1. Optimization study of polymer blends and processing factors

As shown in the Table. 1, in the initial step of single polymer extrusion, HPC was selected as the platform polymer and first produced as feed filaments for FDM 3D printing (as a backbone polymer). However, the hot melt extrusion with this polymer yielded too flexible profile which lacked the stiffness property for the continuous FDM 3D printing (22). It was seen that the PVP/VA, SLP, Eu RL and Eu RS filaments were very brittle and fractured easily even under low loads and not suitable for the printing steps. Filament splintering in the hot tip of the printer must be avoided because diameter variations, either obtaining from non-uniform filament or broken strands, would lead to inaccurate dosing (23). Although bendable filament assists coiling of flex after HME, it can be an obstruction when it comes to the printing process. The more resistance to stress of the material, the more force can be applied by the filament via drive gear, with less likelihood of bend or slip events upon loading (24).

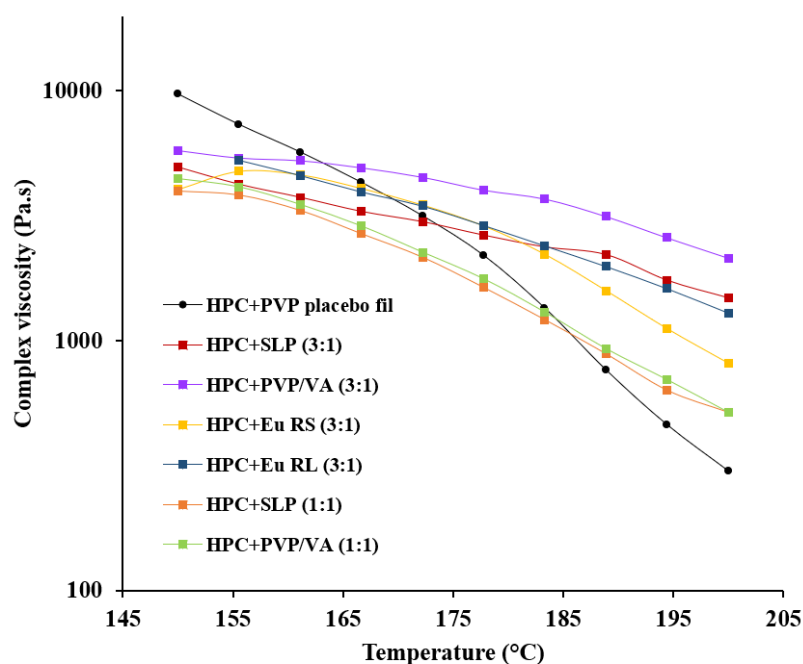
Therefore, for the second stage of the formulation optimization, PVP/VA, SLP, Eu RS and Eu RL were blended at two different ratios of HPC to improve mechanical property of the filaments for 3D printing. It was observed that all filaments produced by the mixture of higher amount of HPC with PVP/VA, SLP, Eu RL and RS (3:1 ratio) and the 1:1 ratio mixture of HPC with PVP/VA and SLP exhibited optimal mechanical property that perfectly printed into tablets. Hence, HPC was found to be a suitable polymer for printing applications in the range of 45–67.5% (w/w). This was likely attributed to the beta relaxation, in other words, the movement of propyl side groups in HPC (25) is responsible for the increased flexibility of the polymer, which is desired for successful FDM 3D printing (26). Herein, polymer blending demonstrated to be one solution to achieve the processability of materials of feeding filaments for FDM printing (27, 28).

In the third stage, based on aforementioned results, higher concentration of HPC was then combined with various disintegrants at the fixed ratio of 3:1. Expectedly, this type of filaments would improve the stiffness of the filaments that

were easily printed without breakage of the filament and clogging of the nozzle. Thus, optimization studies provided the printable filaments of polymer mixtures which have appropriate flexibility and mechanical strength upon the specific extrusion temperature at 150°C and screw speed at 35 rpm.

3.4.2. Rheological assessment

The role of temperature in the melt viscosity of various blends containing IMC was determined over the HME-FDM processing temperature (150-200°C). The starting temperature of 150°C was selected in the vicinity of melting temperature of the drug to obtain plasticization effect of IMC and to enhance the drug solubility in mixture as seen from the decreased viscosity of the IMC system than the placebo (black line). Such lower viscosity allowed IMC dispersion in the polymer matrix leading to its molecular dispersion (29). The viscosity for all blends at 150°C was in range of 5,000 to 8,000 Pa.s, in accordance with the optimal viscosity (1,000 to 10,000 Pa.s) for melt extrusion previously reported (29), and was found to reduce gradually with an increasing temperature (Fig. 13a). It seems possible to use the higher temperature to extrude drug-polymer mixtures; however, 150°C is preferred as the optimal condition due to the higher shear rate provided by the melt extruder (19). At above 180°C, some had the viscosity less than 1000 Pa s, which the extrudability could be considered as fluid-like because the polymer chains completely disentangled. From an extrusion side, such fluid-like polymer is not acceptable and could not definitely shape the desired diameter of filaments for successful extrusion and FDM printing (29).



It is readily seen that the complex viscosity of HPC-blends containing various disintegrants was high (except the polymer blends with MCC) at 150°C (Fig. 13b). Increasing the extrusion temperature offered reduced viscosity and could facilitate the extrusion, nevertheless, this was not possible in this case as the increasing temperature led to undersized filaments which were not fit to the printing nozzle. Thus, the optimized extrusion at 150°C under the viscosity of 7,000-11,000 Pa.s (higher value than previously reported at the upper limit of 10,000 Pa.s) can be noted. Likewise, in the case of the small viscosity of MCC system (ca. 1,200 Pa.s at 150°C), less temperature than 150°C could offer less free-flowing system for appropriate extrusion but the oversized filaments were produced. Therefore, this work highlighted the broad viscosity range of 1,200-11,000 Pa.s specific for additive HME-FDM manufacturing by considering both temperature and filament diameter factors.

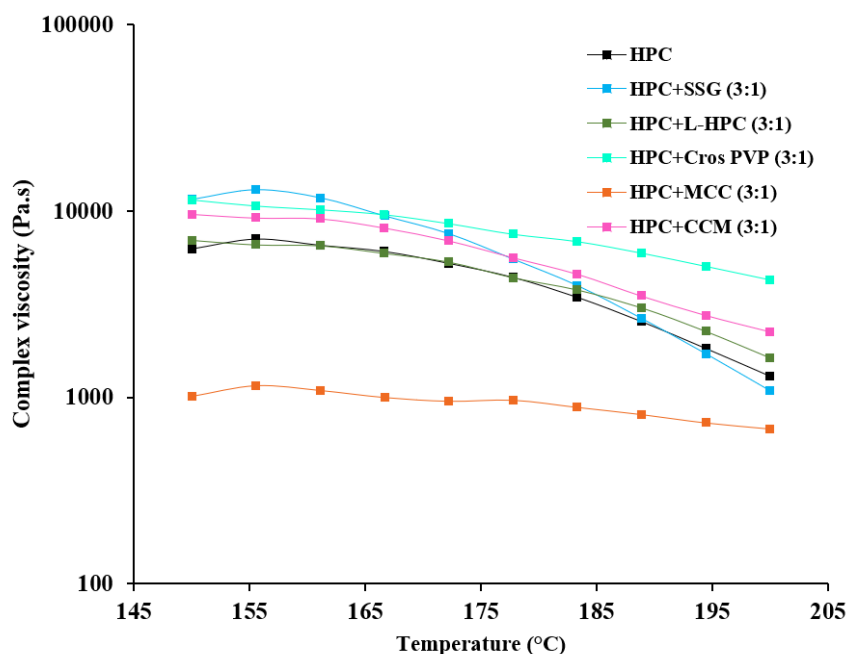


Figure 13. Complex viscosity of (a) combined polymers and (b) HPC-disintegrant blends, as a function of temperature.

In terms of FDM printing process, it tends to require lower viscosity of the mixture than the HME to induce the flow of molten filament through the smaller nozzle (0.4 mm: one-fourth diameter of the HME nozzle), so the higher temperature should be used due to the limited shear rate in the small tip to reach the optimal viscosity (19). The balance between setting temperature and product quality had to be optimized. The temperature of 200°C guaranteed the optimal melt viscosity in the range of 515 to 2,144 Pa.s for solidifying the polymer blends (Fig. 13a) and of 1,000 to 2,000 Pa.s for disintegrant filled systems, except HPC-MCC formulation (678 Pa.s) (Fig. 13b). In this work, less viscosity (515-4,291 Pa.s) was revealed to achieve high quality product (proper adhesion between printed layers for no-defect objects), compared with the previous study (less than 8,000 Pa.s, required to achieve FDM printing) (30).

3.4.3. Characterization studies of filaments and printed tablets

3.4.3.1. Macro and microscopic studies

The diameter of the produced filaments is of high importance to achieve accurate and successful printing (26) and was controlled at 1.68 ± 0.05 mm herein. The extruded indomethacin-loaded filaments were of good quality, smooth and uniform. The polymeric filaments became light yellow color with a smooth surface while HPC-disintegrant filaments was slightly whitish yellow. The tablets were yellow with a stack of small strips observed from the side view due to printed deposited layer of filament (10). The tablet's weight of small dimension was 273 ± 2 mg while the large one lied within 560 ± 1.5 mg with a small variation in the range of 0.5 to 2 % which lied within the recommended range of the pharmacopoeia.

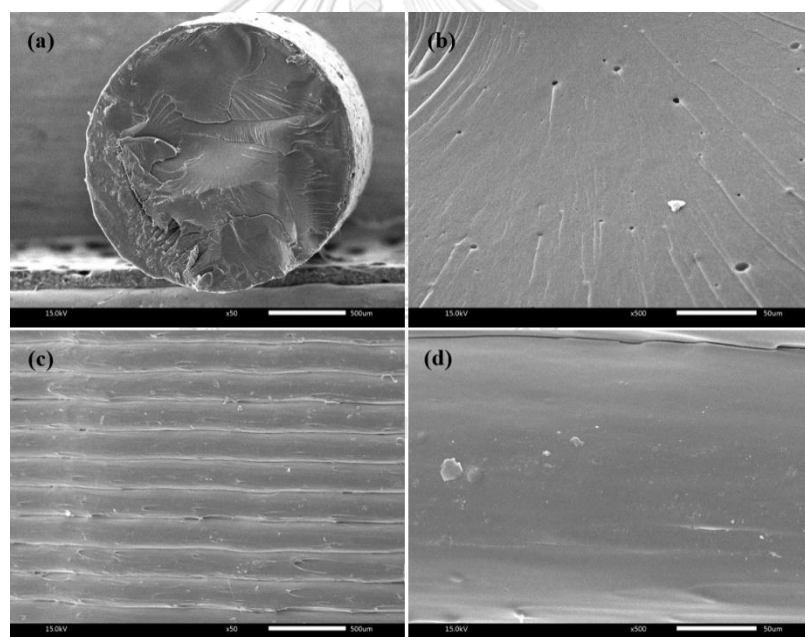


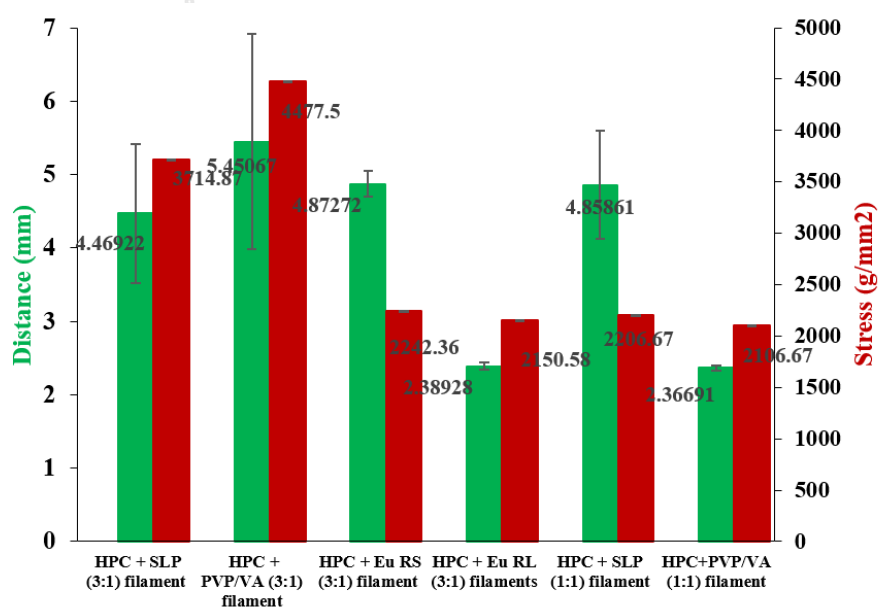
Figure 14. SEM images of (a) cross section, (b) cross section (x1000) of polymer blend filaments, (c) side view and (d) side view (x1000) of printed tablets.

SEM images of all produced filaments (Fig. 14a) revealed a compact filament with smooth surface, containing a small number of tiny pores (x1000, Fig. 14b) and without drug crystal implying homogenous solid dispersion. While the addition of disintegrant led to small roughness with tiny voids (Appendix B, Fig. 35). The side

view (Fig. 14c and 14d) of 3D printed tablets showed conjugation and adhesion between orderly printed strands.

3.4.3.2. Mechanical evaluation of filaments

Feedstock material should possess adequate stiffness and toughness (without being brittle) to assure a good feeding performance in FDM printer (10). Breaking distance can identify the flexibility of the filaments whereas force/stress determine the toughness/brittleness of the filaments. Comparing to the too-flexible polymer HPC alone, its blend with SLP, PVP/VA, Eu RL and Eu RS at 3:1 ratio offered mechanical improvement, exhibited adequate flexibility and toughness, and thus could be printed perfectly. The breaking distance values lied from 2.37-5.45 mm, corresponding to Zhang' work (>1 mm). Whereas the breaking stress for the printable filaments was in the range of 2,206.67-4,677.5 g/mm², not in accordance with Zhang' report (>2942 g/mm²) (17). Another work reported that the filaments with the breaking distance less than 1.5 mm seems to be brittle to be loaded while the breaking stress for printable filaments were in the range of 3126-7638 g/mm²) (26). In Fig. 15a, it can be assumed that Eu RS and Eu RL hold brittleness (easily broken inside the printer) than SLP and PVP/VA as seen from the lower stress values. Hence, it was not possible to use high ratio (about 45% w/w in mixture) of Eu RS and Eu RL to form a printable filament but turned to possible in the case of 45% SLP and PVP/VA with the aiding of HPC.



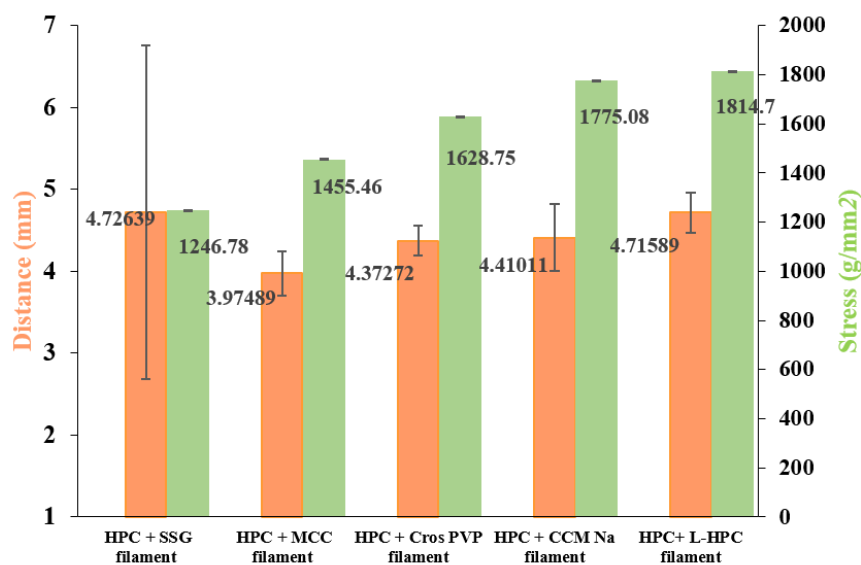


Figure 15. Breaking distance and breaking stress of all extrudable and printable filaments: (a) HPC-polymer at 3:1 and 1:1 ratio (b) HPC-disintegrant at 3:1 ratio, obtained from the 3-point bend test.

Regarding 3:1 HPC:disintegrant printable filaments, they showed the breaking distance of 3.97-4.72 mm (Fig. 15b) which is comparable to 3:1 HPC:polymer filaments and reflecting the flexibility pattern to more stiffness which become withstand more pressure from the gear in printed head. This could be attributed to the effect of the solid particles of the disintegrant disperse in the polymer matrix. By contrast, the relatively brittle filaments showed the lower stress values of 1246.78-1814.7 g/mm² (Fig. 15b) than both 3:1 and 1:1 HPC:polymer filaments. These advanced findings of HPC-disintegrant blends could propose that the stiff but rather brittle filaments are possible for successful FDM printing.

3.4.3.3. Attenuated total reflectance-Fourier-transform infrared spectroscopy (ATR-FTIR)

In all mixture systems (Fig. 16), shifts to lower wavenumber were found from the crystalline γ -form IMC at 1717 and 1692 cm⁻¹ to amorphous IMC at 1710 and 1684 cm⁻¹, corresponding to the asymmetric carboxylic acid C=O stretching of cyclic dimers and benzoyl C=O stretching, respectively (31). While the interaction of amorphous IMC and polymer was observed from the peak shift to high wavenumber

(e.g. to 1715 cm^{-1} in HPC-SLP and 1716 cm^{-1} in HPC-PVP/VA, to 1725 in HPC-Eu RL), which assigned for the non-hydrogen bonded C=O stretching (31). Different ratios between 3:1 and 1:1 in all the HPC:polymer systems showed the same shifting trends, likewise with all 3:1 HPC:disintegrant systems. The miscibility and intermolecular interactions between IMC and polymeric blends were confirmed by alterations in the wavenumber and peak shape (32).

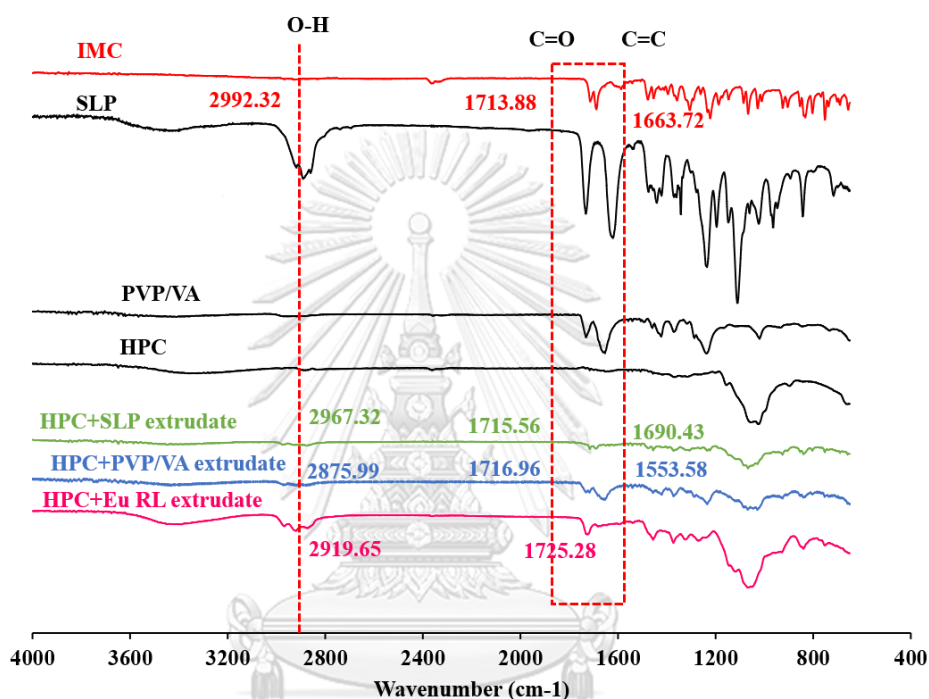
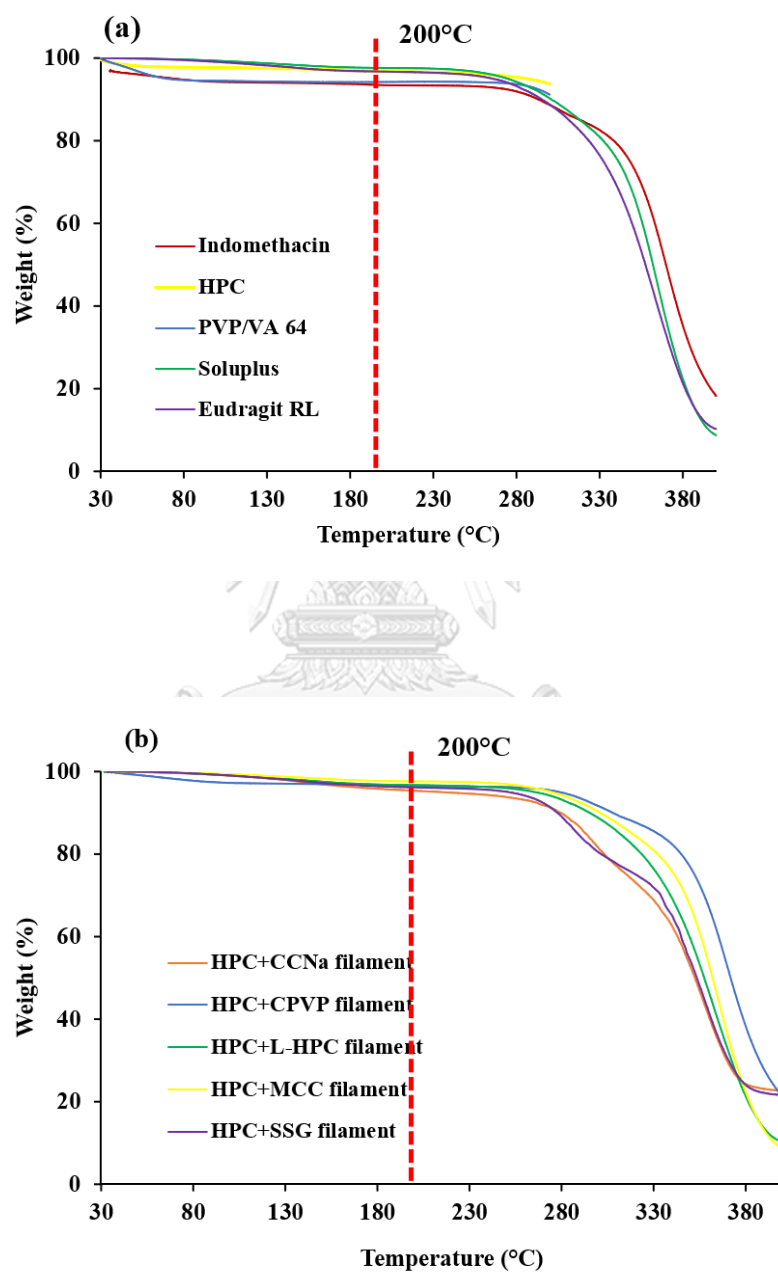


Figure 16. FTIR spectrum of extruded filaments compared with IMC.

3.4.3.4. Thermal analysis

The TGA curve (Fig. 17a) did not show a significant weight loss of all materials over the HME temperature (150°C) and printing temperature (200°C), suggesting that the drug and polymer matrix would not have thermal degradation. All the pure excipients were shown to be stable up to 250°C . HPC displayed the minimal weight loss of 2.89% around 53°C probably due to the loss of moisture and also small molecules removed from the structure followed by a plateau, indicating no further change in weight, while PVP/VA was stable up to 280°C with no or little weight loss of 0.84%. The weight change of SLP after heating until 220°C was 2.30%, possibly due to the loss of weakly bound water molecules (33). Eu RL is stable up to 170°C , where slow degradation process initiated (34). The indomethacin with a minimal

weight loss started from 40 to 130°C which is in agreement with the release of water in the structure (35). Likewise, the HPC:disintegrants filaments, (Fig. 17b) behaved in the similar manner, major differences showed only above 250 °C which was out of the domain of experiment.



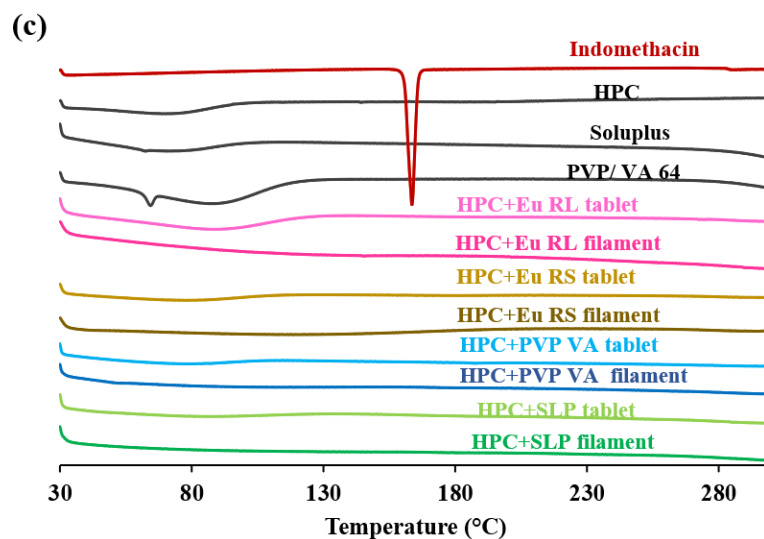


Figure 17. Thermogravimetric analysis of raw materials and HPC-disintegrant filaments (a, b) and DSC thermograms of raw materials, polymer blend filaments (3:1 ratio) and printed layers (c).

DSC thermogram (Fig. 17c) confirmed the miscibility of the active ingredient in a formulation to identify the amorphous solid dispersion of IMC by HME and FDM. IMC crystals displayed a sharp melting peak at ca. 161°C whereas all filaments and tablets clearly exhibited broaden curves, reflecting the complete conversion of crystalline IMC nature to the amorphous state during processing. This was verified by PXRD (section 3.4.3.5).

3.4.3.5. Powder X-ray diffraction (PXRD)

PXRD data showed the crystallinity of raw materials and all HME-FDM formulations (Fig. 18). The diffraction peaks for γ -form IMC were at $2\theta = 11.6^\circ$, 19.6° , 21.9° , 26.6° and 29.1° ; those for α -form IMC were at $2\theta = 8.4^\circ$, 11.9° , 14.4° , 18.0° and 22.1° . The peak positions of IMC crystals were consistent with those in a previous study (36). The PXRD pattern of all polymers showed no peaks, suggesting no X-ray scattering due to their amorphous nature of the polymers. All produced filaments demonstrated tiny peaks with very low intensity at 11.6° , 16.4° , 18.0° and 24.6° , indicating that most of indomethacin was dispersed in amorphous form with a small amount remaining in a crystalline nature.

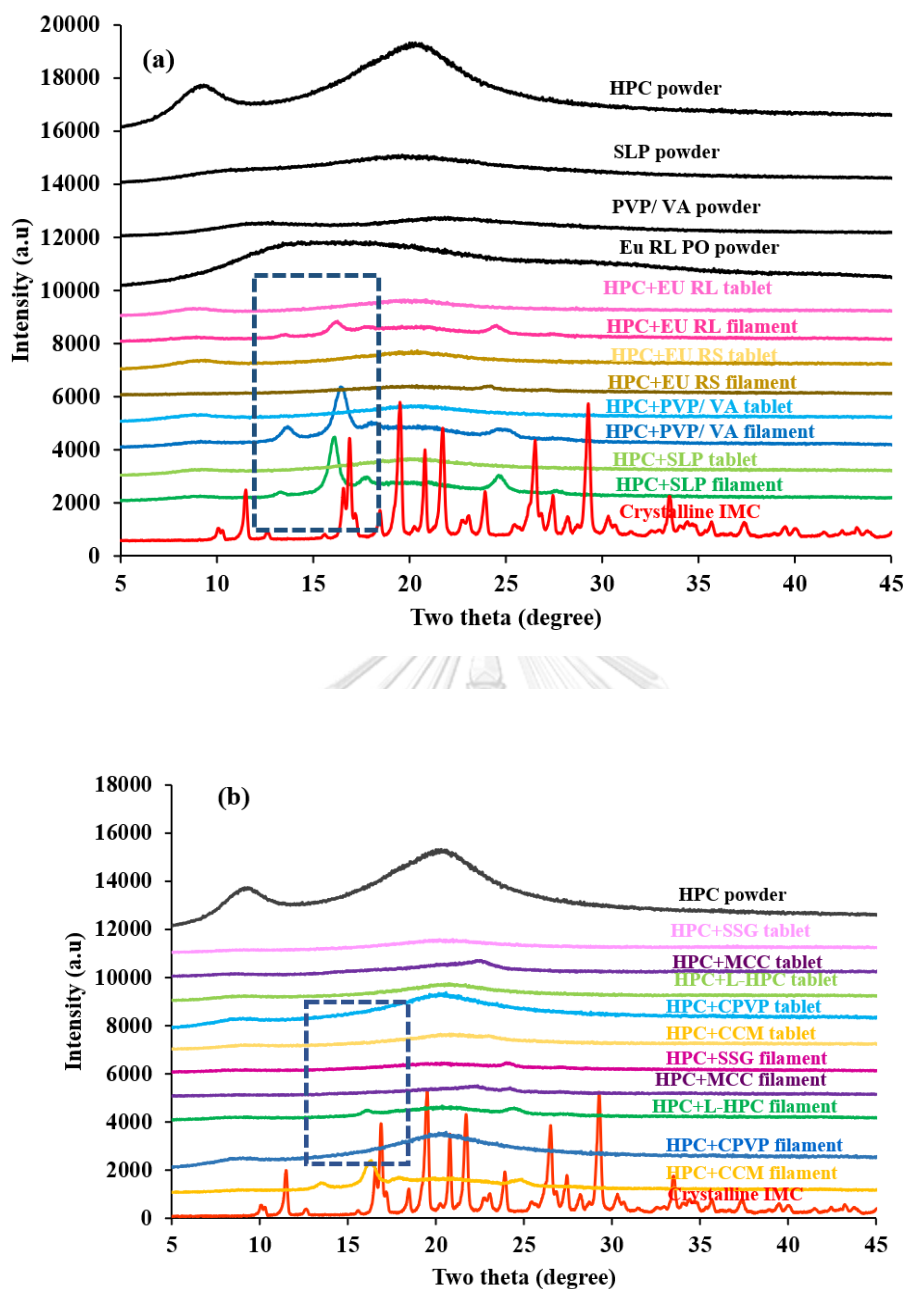


Figure 18. X-ray powder diffractograms of (a) raw materials, HPC-polymer and (b) HPC-disintegrant filaments and printlets.

HPC-disintegrant filaments had more amorphous ratio than HPC-polymer systems due to the less numbers of diffraction peaks. Noticeably, printing process converted all systems to be completely amorphous solid dispersions with smooth the halo pattern. This is likely a sign of melt-quenched amorphous indomethacin (36)

owing to the high printing temperature (above the melting point of IMC) with a shear rate at the narrow printing nozzle -to-the low temperature at the printing platform.

3.4.3.6. Drug content analysis in filaments and 3D printed tablets

All extruded filaments had a target drug load of 10% (w/w) indomethacin in order to get a sufficient amount of drug in the printed tablets. The results showed uniform distribution of the drug throughout the filament as well as in the tablets, indicating that the extrusion temperature (150°C), closely below the API melting point (160°C), was sufficient to dissolve the API completely in the polymer matrix as a desirable amorphous solid dispersion (37) with no drug loss (Table 3). The drug content was not specifically 100% because of subtle lot-to-lot variations (38). In general, there is an acceptable range to release drug product according to its specification. It is noted that printing process had a small effect on drug content in terms of content and deviation, possibly ascribed to the not-fully deposited strips of printed tablets as seen in the SEM image (Fig. 14c) comparing to the fully compact filaments (Fig. 14a).

Table 3. Drug content analysis of extruded filaments and printed tablets (n=3).

Formulation	Drug content in extruded filament (%)	Drug content in printed tablets (%)
HPC:SLP (3:1)	100.41 ± 0.689	99.96 ± 1.246
HPC:PVP/VA (3:1)	100.06 ± 0.908	98.67 ± 0.577
HPC:Eu RL (3:1)	101.65 ± 1.567	97 ± 1.791
HPC:Eu RS (3:1)	100.62 ± 0.765	100.36 ± 1.403
HPC:SLP (1:1)	100.81 ± 1.356	99.00 ± 2.549
HPC:PVP/VA (1:1)	99.94 ± 1.212	98 ± 2.354

3.4.3.7. In-vitro dissolution study

The previous research showed that 3D-printed tablets exhibited slower drug release rate than the conventional compressed tablets due to their smooth surface and compact structure from the melt extrusion (17). In addition, their dissolution rate is different from other conventional tablets where dissolution is initiated by water imbibition and swelling, therefore, the disintegration and dissolution of printed may be dominated by erosion and diffusion mechanisms (40). The appearance of the tablet showed an expansion during the dissolution process and then, became fragmentation of the tablet into smaller fractions in the medium. Herein, a wide range of extended-release profiles from various polymer-blended tablets was revealed (Fig. 19a). The faster IMC release was observed from HPC-PVP/VA > HPC-SLP > HPC-Eu RL > HPC-Eu RS based tablets. At 3:1 ratio, HPC:PVP/VA system exhibited 90 % release in 12 h whereas HPC:SLP system displayed 65%, representing the strong extended drug release rate from the SLP polymer matrix with double molecular weight than PVP/VA. Thus, with an increase in SLP, 1:1 HPC:SLP system offered the slower release. On the other hand, PVP/VA has more highly water-soluble components (polyvinyl pyrrolidone) in the structure, acting as a pore former (28) that could possibly provide rapid drug release; hence, a complete drug release within 8 h occurred with the increasing PVP/VA to 1:1 HPC:PVP/VA system. In case of the HPC-Eu RS and Eu RL-based tablets, IMC release exhibited the slowest drug release profiles ca. 22% over 24 h. It was likely evident that these formulations were a combination of hydrophilic (HPC) and hydrophobic polymers showing a more controlled drug release rate than other formulations. Furthermore, this is because both Eu RL and Eu RS are water-insoluble but rather permeable which render a sustained release of IMC (39).

Next, in order to manipulate the drug release profile upon the size of tablets, two dimensions of HPC-PVP/VA (3:1) tablets were fabricated and revealed that rapid release pattern was demonstrated in smaller dimension tablet (273 mg) compared to the larger one (597 mg) (Fig. 19b). This is likely to increase surface/mass ratio with the smaller tablets, which improved water imbibition and drug diffusion. The similar profile from theophylline release was reported with Eu RL based 3D printed tablets

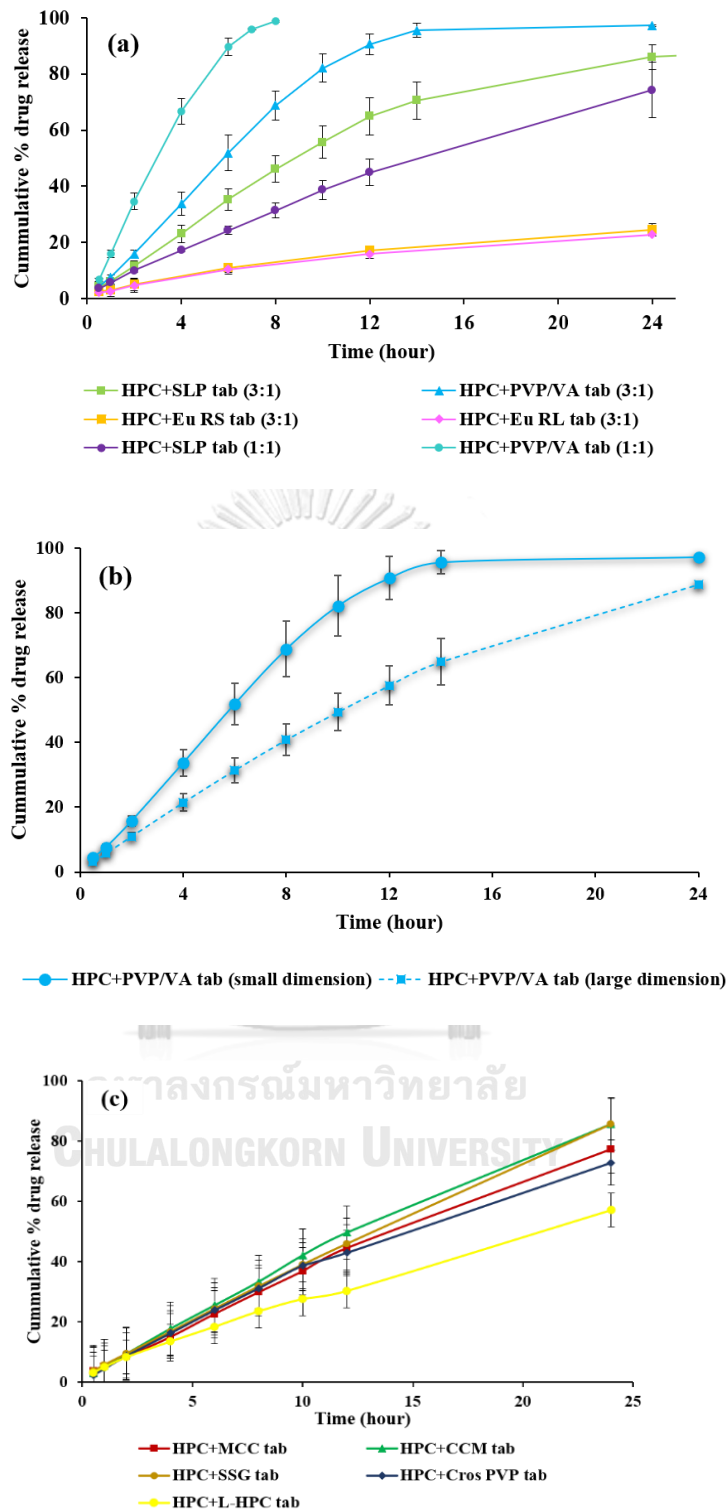


Figure 19. In-vitro dissolution profiles of (a) HPC-polymer blend tablets, (b) two sizes of HPC-PVP/VA (3:1) tablets and (c) HPC-disintegrant blend tablets ($n=3$, mean \pm SD).

(13). However, regarding the amount of the drug released from these two sized tablets, it was comparably similar.

Prominently, all the HPC-disintegrant mixtures in Fig. 19c showed the more sustained drug release than the HPC-polymer blends, ranging from 60% to 80% drug release over 24 h period. All the five disintegrants in polymer matrix could not outweigh their functions such as disintegration and swelling. This may be owing to the high content of HPC in tablet matrix inducing the inability of the disintegrant. In addition, it can be assumed that during HME molten HPC has coated the disintegrant particles, covered their pores and restricted their swelling upon dissolution testing (40). Upon 24 h, the formulation containing HPC-SSG and HPC-CCM showed the similar IMC release (approximately 80%) and the more-accelerated pattern than HPC-MCC (70%), HPC-cros PVP (70%) and L-HPC (60%) which may be explained by the fact that L-HPC is a modified hydrophilic and water insoluble disintegrant.

3.4.4. Design of Experiment (DOE)

The dissolution studies demonstrated that different polymers concentrations have a considerably effect on drug release manner and indicated that the mixtures of HPC-PVP/VA and HPC-SLP could be effective for tailoring of extended-release oral dosage form by varying the polymeric matrix compositions. While the tablets made of HPC-Eu RS, HPC-Eu RL and HPC-disintegrant are less suitable for oral dosage forms due to its incomplete drug release over 24 h. Therefore, HPC, PVP/VA and SLP polymers were selected as main formulation factors in DoE and the effect of such combined polymers was comprehensively substantiated by D-optimal mixture design on the drug release at specified timepoints.

The ANOVA proposed highly significant full quartic model of all responses ($p < 0.05$). All the three responses exhibited high values of R^2 , ranging from 0.97 to 0.99, which showed the best fit of the generated model polynomials to the response data (Table 4). The response contour plots displayed the variables and their interactions, presenting the effect of combined-formulation factors on the IMC release. The Minitab software generated 9 runs and the results of different dissolution

profiles were illustrated in Table 5. The polynomial equations of three response obtained were depicted in the followings:

$$Y_1 = 14878X_1 + 67045X_2 - 14808X_3 - 163579X_1 * X_2$$

$$Y_2 = 1889X_1 + 1345X_2 - 1798X_3 - 20170X_1 * X_2$$

$$Y_3 = 97X_1 + 100X_2 - 40X_3 + 194X_1 * X_3$$

The equations represent the quantitative effect of factors (X_1 , X_2 , and X_3) and their interactions on the responses (Y_1 , Y_2 and Y_3). The equations showed as a linear term that X_1 , X_2 positively affected the drug release, while X_3 had negatively effect on drug release, probably because the increase in the amount of X_3 (SLP) resulted in decreasing drug release of the formulations.

Table 4. ANOVA results of 9 formulations design.

Responses	Model	F-value	p-value	R ²	R ² (predicted)	R ² (adjusted)
Y ₁	Full quartic	941.12	0.021	99.99%	75.16%	99.95%
Y ₂	Full quartic	54.14	0.018	99.89%	96.13%	99.55%
Y ₃	Full quartic	21.41	0.01	97.29%	52.70%	94.57%

Table 5. Observed values of responses obtained from the D-optimal mixture design.

Formulation	Y ₁	Y ₂	Y ₃
1	25.66	50.31	88.09
2	66.72	99.72	99.75
3	35.07	45.76	77.88
4	44.66	57.87	84.16
5	45.44	57.59	86.14
6	39.78	52.70	82.97
7	53.05	70.07	97.88
8	42.58	54.78	81.78
9	40.84	51.79	80.00

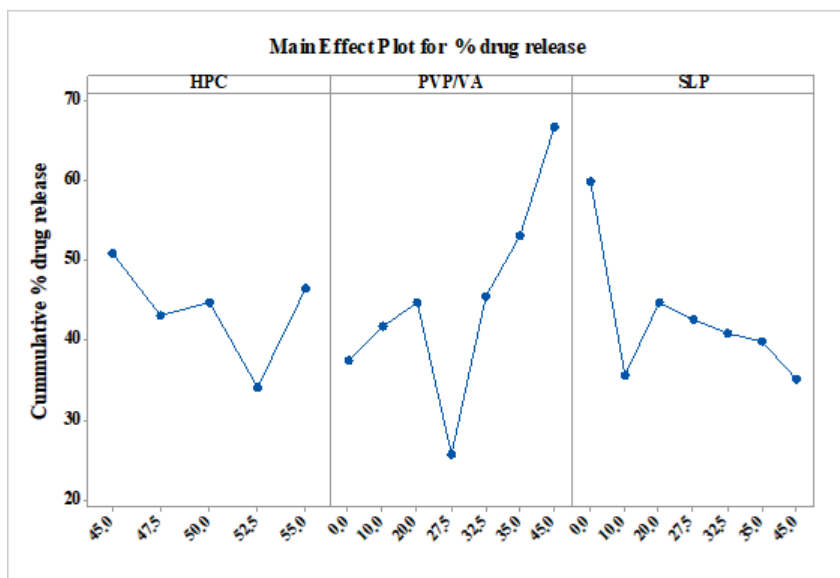


Figure 20. Main effect plot of all three independent factors (HPC, PVP/VA and SLP).

In Fig. 20, the main effect plot of three factors on the IMC release was illustrated. Apparently, an increase in drug release at specified timepoints was observed when increasing amount of PVP/VA and decreasing amount of SLP.

The relationship between the factors and response variables were further elucidated using contour plot (Fig. 21). Light green (with 40-50% release), green (with 50-80% release) and dark green (with >80% release) areas were tailored at 4, 12 and 24 h for extended-release system, respectively. The significant effects of formulation on the release were mainly found at 4 h timepoint. It can be seen that the required drug release can be obtained with the combined effect of ca. 47.5-50% HPC and 10-30% PVP/VA (Fig. 21a), 47.5-50% HPC and 20-30% SLP (Fig. 9b), and 10-20% PVP/VA and 20-30% SLP (Fig. 21c) while pale green areas (<40% release) should be avoided. Nevertheless, the results of drug release at 12 h (Y_2) and 24 h (Y_3) applied the same rationale as presented in Fig. 21.

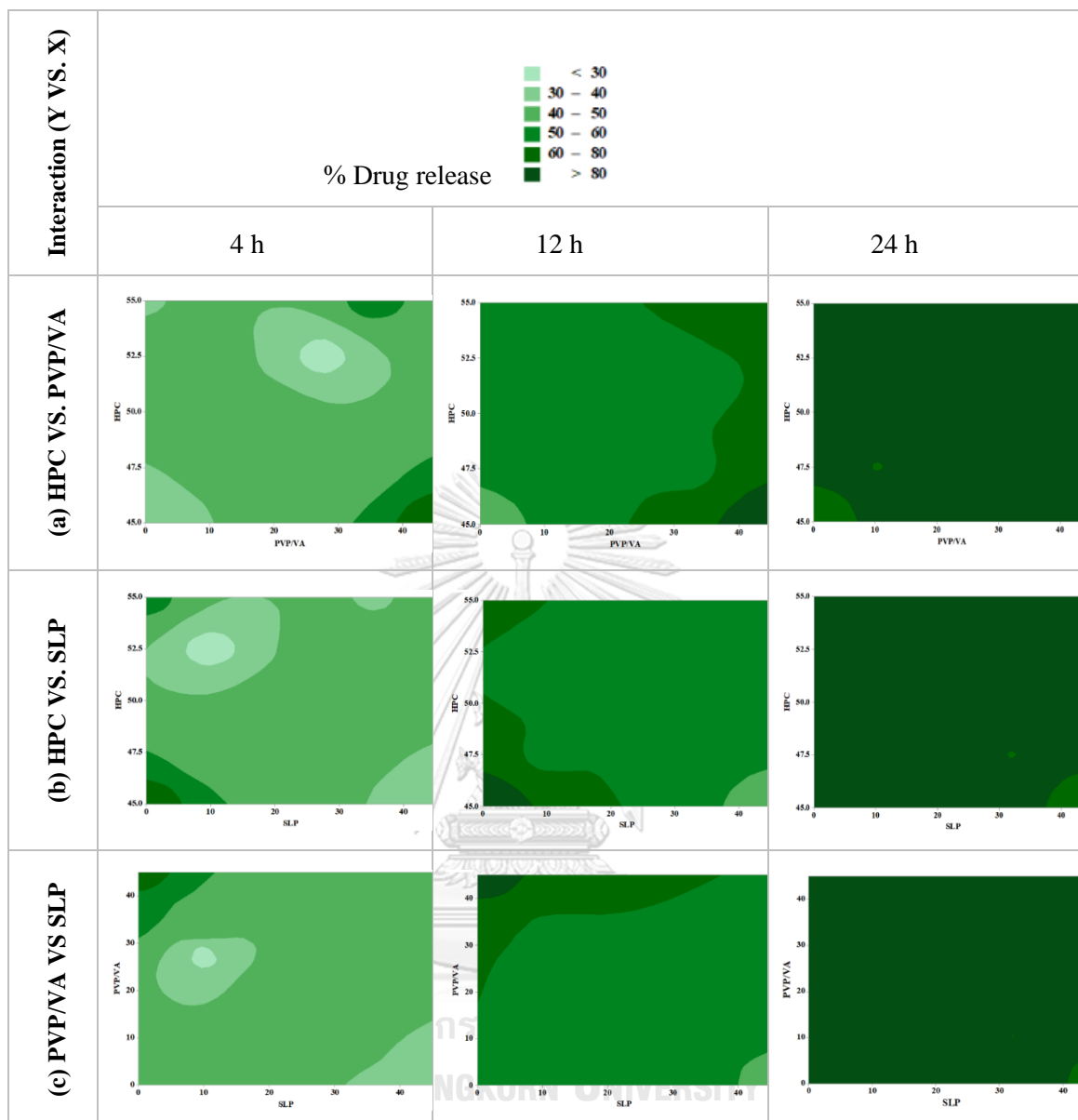


Figure 21. Contour plot depicting effect of variables on % drug release at 4, 12 and 24 h.

Finally, to obtain the optimal formulation of the final product, the response optimization analysis was conducted, and the optimized formulation ratios of 3D printed tablets of X_1 (HPC), X_2 (PVA/VA) and X_3 (SLP) were 49.97%, 19.09% and 20.94%, respectively. These values were ascertained by a desirability values as illustrated in Table 6. When the predicted values were compared with the observed values, it was found to be in rationally close agreement for all the responses which had low % error.

Table 6. Comparison of predicted and observed value of responses for the optimal formulation.

Responses	Predicted value (%)	Observed valued (%)	Desirability	% error
Y₁	45.00	41.24	0.99955	-8.35
Y₂	58.13	61.85	0.81316	6.40
Y₃	82.97	84.54	0.99438	1.90

3.5. Conclusion

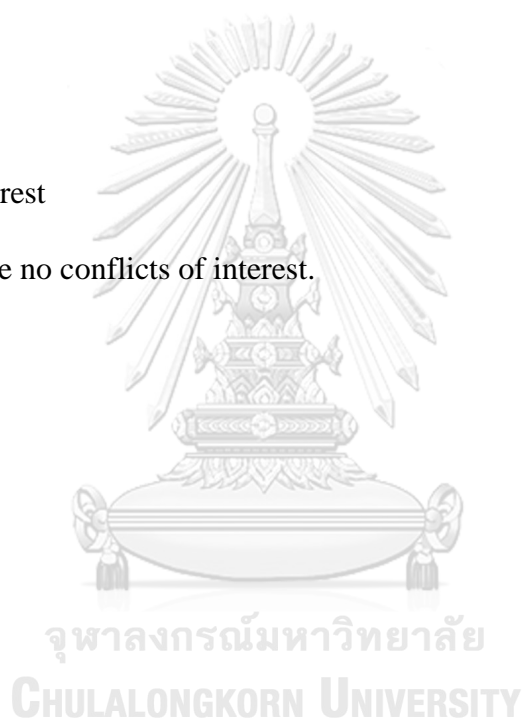
The manufacture of extended release printlets using 9 different combinations of hydroxy propyl cellulose (HPC) and polymer blends (Kollidon[®] VA 64 (PVP/VA), Soluplus[®] (SLP), Eudragit[®] RL and RS), HPC and disintegrant blends (sodium starch glycolate, croscarmellose sodium, croscroscopovidone, microcrystalline cellulose and low substituted hydroxypropyl cellulose) at 3:1 ratio with 2 additional blends of HPC-PVP/VA and HPC-SLP at 1:1 ratio were achieved, characterized, and further optimized by using statistical DoE. The definite range of complex viscosity of all the blends were highlighted and used for HME-FDM printing. Interestingly, the mechanical properties of all filaments were considerably enhanced by incorporating of HPC as a flexible modifier. All printable filaments and tablets showed qualified physicochemical characterizations while printed tablets offered the complete amorphous solid dispersion with a wide range of extended-release profiles. D-optimal mixture design demonstrated the effects of polymers on multi targeted drug release and generated the models from a small number of formulations together with the optimum formulation for extended-release tablets as determined in the pharmacopoeia. To conclude, this platform contributes to a number of printable API-loaded filaments and successful printed tablets which could be advantageous for the fabrication of extended-release dosage forms with multi drug release targets fitting to the patient's needs.

Acknowledgements

This work was financially supported by Chulalongkorn University-ASEAN (CU-ASEAN), Thailand; Graduate School Thesis Grant, Chulalongkorn University; a research fund (Grant number Phar2561-RGI-04 and Phar2562-RGI-01) to V.T.; and T.F., Department of Molecular Pharmaceutics, Meiji Pharmaceutical University. We also thank Pharmaceutical Research Instrument Center, Faculty of Pharmaceutical Sciences, Chulalongkorn University and to Chulalongkorn University Centenary Academic Development Project for supporting powder X-ray diffractometer within CU.D.HIP.

Declaration of interest

The authors declare no conflicts of interest.



REFERENCES

1. Marto J, Gouveia L.F, Gonclave L M, Gaspar DP, Pinto P, Carvalho FA, Oliveira E. A Quality by design (QbD) approach on starch-based nanocapsules: A promising platform for topical drug delivery. *Colloids and Surfaces B: Biointerfaces*. 2016;143:177-85.
2. Yu LX. Pharmaceutical Quality by Design: Product and Process Development, Understanding, and Control. *Pharmaceutical Research*. 2008;25(4):781-91.
3. Hales D, Luran V, Porav SA, Bodoki, Barbu T, Achim M A. A quality by design (QbD) study on enoxaparin sodium loaded polymeric microspheres for colon-specific delivery. *European Journal of Pharmaceutical Sciences*. 2017;100:249-61.
4. Rafati H, Talebpor Z, Adlnasab L, Ebrahimi SN. Quality by design: Optimization of a liquid filled pH-responsive macroparticles using Draper-Lin composite design. *Journal of Pharmaceutical Sciences*. 2009;98(7):2401-11.
5. Palekar S, Nukala PK, Mishra SM, Patel K. Application of 3D printing technology and quality by design approach for development of age-appropriate pediatric formulation of baclofen. *International Journal of Pharmaceutics*. 2019;556:106-16.
6. Surikutchi BT, Patil SP, Shete G, Patel S, Bansal AK. Drug-excipient behavior in polymeric amorphous solid dispersions. *Journal of Excipients and Food Chemicals*; Vol 4 No 3 (2013). 2013.
7. Goyanes A, Buanz ABM, Basit, Gaisford S. Fused-filament 3D printing (3DP) for fabrication of tablets. *International Journal of Pharmaceutics*. 2014;476(1):88-92.
8. Goole J, Amighi K. 3D printing in pharmaceutics: A new tool for designing customized drug delivery systems. *International Journal of Pharmaceutics*. 2016;499(1):376-94.
9. Norman J, Madurawe RD, Moore CMV, Khan MA, Khairuzzaman A. A new chapter in pharmaceutical manufacturing: 3D-printed drug products. *Advanced Drug Delivery Reviews*. 2017;108:39-50.
10. Verstraete G, Samaro A, Grymonpré W, Vanhoorne V, Van Snick B, Boone MN. 3D printing of high drug loaded dosage forms using thermoplastic polyurethanes. *International Journal of Pharmaceutics*. 2018;536(1):318-25.
11. Genina N, Boetker JP, Colombo S, Harmankaya N, Rantanen J, Bohr A. Anti-tuberculosis drug combination for controlled oral delivery using 3D printed compartmental dosage forms: From drug product design to in vivo testing. *Journal of Controlled Release*. 2017;268:40-8.
12. Prasad E, Islam MT, Goodwin DJ, Megarry AJ, Halbert GW, Florence AJ. Development of a hot-melt extrusion (HME) process to produce drug loaded Affinisol™ 15LV filaments for fused filament fabrication (FFF) 3D printing. *Additive Manufacturing*. 2019;29:100776.
13. Pietrzak K, Isreb A, Alhnan MA. A flexible-dose dispenser for immediate and extended release 3D printed tablets. *European Journal of Pharmaceutics and Biopharmaceutics*. 2015;96:380-7.
14. Genina N, Holländer J, Jukarainen H, Mäkilä E, Salonen J, Sandler N. Ethylene vinyl acetate (EVA) as a new drug carrier for 3D printed medical

- drug delivery devices. *European Journal of Pharmaceutical Sciences*. 2016;90:53-63.
15. Kempin W, Franz C, Koster L-C, Schneider F, Bogdahn M, Weitschies W. Assessment of different polymers and drug loads for fused deposition modeling of drug loaded implants. *European Journal of Pharmaceutics and Biopharmaceutics*. 2017;115:84-93.
 16. Goyanes A, Fina F, Martorana A, Sedough D, Gaisford S, Basit AW. Development of modified release 3D printed tablets (printlets) with pharmaceutical excipients using additive manufacturing. *International Journal of Pharmaceutics*. 2017;527(1):21-30.
 17. Zhang J, Feng X, Patil H, Tiwari RV, Repka MA. Coupling 3D printing with hot-melt extrusion to produce controlled-release tablets. *International Journal of Pharmaceutics*. 2017;519(1):186-97.
 18. Dai L, Cheng T, Duan C, Zhao W, Zhang W, Zou X. 3D printing using plant-derived cellulose and its derivatives: a review. *Carbohydrate Polymer*. 2018;203:71-86.
 19. Solanki NG, Tahsin M, Shah AV, Serajuddin ATM. Formulation of 3D printed tablet for rapid drug release by fused deposition modeling: screening polymers for drug release, drug-polymer miscibility and printability. *Journal of Pharmaceutical Sciences*. 2018;107(1):390-401.
 20. Gioumouxouzis CI, Baklavaridis A, Katsamenis OL, Markopoulou CK, Bouropoulos N, Tzetzis D. A 3D printed bilayer oral solid dosage form combining metformin for prolonged and glimepiride for immediate drug delivery. *European Journal of Pharmaceutical Sciences*. 2018;120:40-52.
 21. Godwin A, Bolina K, Clochard M, Dinand E, Rankin S, Simic S. New strategies for polymer development in pharmaceutical science--a short review. *Journal of Pharmacy and Pharmacology*. 2001;53(9):1175-84.
 22. Zhang J, Xu P, Vo A, Bandari S, Yang F, Durig T. Development and evaluation of pharmaceutical 3D printability for hot melt extruded cellulose-based filaments. *Journal of Drug Delivery Science and Technology*. 2019;52.
 23. Kempin W, Domsta V, Grathoff G, Brecht I, Semmling B, Tillmann S. immediate release 3D-printed tablets produced via fused deposition modeling of a thermo-sensitive drug. *Pharmaceutical Research*. 2018;35(6):124.
 24. Ilyés K, Kovács NK, Balogh A, Borbás E, Farkas B, Casian T. The applicability of pharmaceutical polymeric blends for the fused deposition modelling (FDM) 3D technique: Material considerations-printability-process modulation, with consecutive effects on in vitro release, stability and degradation. *European Journal of Pharmaceutical Sciences*. 2019;129:110-23.
 25. Miranda MIG, Samios D, Freitas LdL, Bica CID. Influence of hydroxypropyl cellulose on molecular relaxations of epoxy-amine networks. *Polímeros*. 2013;23:1-6.
 26. Öblom H, Zhang J, Pimparade M, Speer I, Preis M, Repka M. 3D-Printed isoniazid tablets for the treatment and prevention of tuberculosis-personalized dosing and drug release. *American Association of Pharmaceutical Scientists: Pharmaceutical Science and Technology*. 2019;20(2):52.
 27. Alhijaj M, Belton P, Qi S. An investigation into the use of polymer blends to improve the printability of and regulate drug release from pharmaceutical solid

- dispersions prepared via fused deposition modeling (FDM) 3D printing. *European Journal of Pharmaceutics and Biopharmaceutics*. 2016;108:111-25.
28. Kollamaram G, Croker DM, Walker GM, Goyanes A, Basit AW, Gaisford SJI. Low temperature fused deposition modeling (FDM) 3D printing of thermolabile drugs. *International Journal of Pharmaceutics*. 2018;545(1-2):144-52.
 29. Gupta SS, Parikh T, Meena AK, Mahajan N, Vitez I, Serajuddin ATM. Effect of carbamazepine on viscoelastic properties and hot melt extrudability of Soluplus[®]. *International Journal of Pharmaceutics*. 2015;478(1):232-9.
 30. Isreb A, Baj K, Wojsz M, Isreb M, Peak M, Alhnan MA. 3D printed oral theophylline doses with innovative 'radiator-like' design: Impact of polyethylene oxide (PEO) molecular weight. *International Journal of Pharmaceutics*. 2019;564:98-105.
 31. Liu H, Wang P, Zhang X, Shen F, Gogos CG. Effects of extrusion process parameters on the dissolution behavior of indomethacin in Eudragit[®] E PO solid dispersions. *International Journal of Pharmaceutics*. 2010;383(1):161-9.
 32. Liu J, Cao F, Zhang C, Ping Q. Use of polymer combinations in the preparation of solid dispersions of a thermally unstable drug by hot-melt extrusion. *Acta Pharmaceutica Sinica B*. 2013;3(4):263-72.
 33. Djuris J, Nikolakakis I, Ibric S, Djuric Z, Kachrimanis K. Preparation of carbamazepine-Soluplus[®] solid dispersions by hot-melt extrusion, and prediction of drug-polymer miscibility by thermodynamic model fitting. *European Journal of Pharmaceutics and Biopharmaceutics*. 2013;84(1):228-37.
 34. Gupta SS, Solanki N, Serajuddin ATM. Investigation of thermal and viscoelastic properties of polymers relevant to hot melt extrusion, IV: Affinisol[™] HPMC HME polymers. *American Association of Pharmaceutical Scientists: Pharmaceutical Science and Technology*. 2016;17(1):148-57.
 35. Fu Q, Lu H-D, Xie Y-F, Liu J-Y, Han Y, Gong N-B. Salt formation of two BCS II drugs (indomethacin and naproxen) with (1R, 2R)-1,2-diphenylethylenediamine: Crystal structures, solubility and thermodynamics analysis. *Journal of Molecular Structure*. 2019;1185:281-9.
 36. Tanabe S, Higashi K, Umino M, Limwikrant W, Yamamoto K, Moribe K. Yellow coloration phenomena of incorporated indomethacin into folded sheet mesoporous materials. *International Journal of Pharmaceutics*. 2012;429(1):38-45.
 37. Nollenberger Ka, Albers JJHMEPA. Applications of poly (meth) acrylate polymers in melt extrusion. *International Journal of Pharmaceutics*. 2012:113-44.
 38. Kadry H, Al-Hilal TA, Keshavarz A, Alam F, Xu C, Joy A. Multi-purposable filaments of HPMC for 3D printing of medications with tailored drug release and timed-absorption. *International Journal of Pharmaceutics*. 2018;544(1):285-96.
 39. Korte C, Quodbach J. Formulation development and process analysis of drug-loaded filaments manufactured via hot-melt extrusion for 3D-printing of medicines. *Pharmaceutical Development and Technology*. 2018;23(10):1117-27.

40. Sadia M, Arafat B, Ahmed W, Forbes RT, Alhnan MA. Channelled tablets: An innovative approach to accelerating drug release from 3D printed tablets. *Journal of Controlled Release*. 2018;269:355-63.



CHAPTER IV

(Submitted manuscript to the International Journal of Pharmaceutics Research paper on 20th November 2020)

Tailoring immediate release FDM 3D printed tablets using a Quality by Design (QbD) approach

Yee Mon Than¹, Varin Titapiwatanakun^{1,*}

¹ Department of Pharmaceutics and Industrial Pharmacy, Faculty of Pharmaceutical Sciences, Chulalongkorn University

254 Phayathai road, Pathumwan, Bangkok, 10330, Thailand

*Corresponding author: Varin Titapiwatanakun

Department of Pharmaceutics and Industrial Pharmacy, Faculty of Pharmaceutical Sciences, Chulalongkorn University

254 Phayathai road, Pathumwan, Bangkok, 10330, Thailand

E-mail address: varin.t@pharm.chula.ac.th

4.1. Abstract

The aims of this work were to produce immediate release printed tablets using FDM technique and to systematically explore the effects of different compositions on drug release by Quality by Design approach. Screening study of various drug loadings and excipients were conducted by hot melt extrusion and FDM printing to set up the appropriate limit of each independent factor (critical material attribute, CMA) in DoE. This study demonstrated that the use of polymeric mixture containing different theophylline loadings (10, 30 and 60% w/w) in combination with multiple pharmaceutical polymers (hydroxy propyl cellulose (HPC), Eudragit[®] EPO, Kollidon[®] VA 64) and disintegrant (sodium starch glycolate) were successfully hot melt-extruded and FDM printed with no plasticizer. Rheological measurement was performed to understand the critical process parameters (CPP) while the mechanical property of extrudable and printable filaments was investigated by 3-point test for the formulation development. Surprisingly, HPC were found to be superior as a flexibility modifier in all printable filaments. A range of pharmaceutical characterizations were examined to ensure the critical quality attributes (CQA). Characteristic dissolution profiles were obtained. D-optimal mixture design of 17 formulations suggested that theophylline release was considerably affected by the combined action of different excipients and could predict the optimum formulation with the required quality target product profile (QTPP) in pharmacopoeia (85% release at 30 min). Therefore, this can be a useful platform to develop immediate release products for a specific group of patients commercially.

Keywords: immediate release tablets, hot melt extrusion, FDM 3D printing, dissolution study, QbD

4.2. Introduction

The continuous manufacturing offers a novel and versatile prototype in the field of pharmaceutical manufacturing (1, 2). For example, the combination of two novel technologies as hot-melt extrusion (HME) and fused deposition modelling (FDM) 3D printing has popularly applied to produce innovative dosage forms. The process involves pre-made extruded filaments via hot melt where the drug is molecularly dispersed in the molten polymer matrix, followed by 3D printing. While FDM 3D printing, the most extensively applied low-cost technique across many sectors (3-5), is based on the extrusion of a molten polymeric filament through a heated nozzle followed by solidification onto a moving platform into the desired 3D objects. One of the most important parameters in FDM is the qualities of the filament (6, 7) such as mechanical stability, a consistent diameter, and a homogeneous API distribution. Therefore, there is an emerging interest in developing the HME-FDM printing process technology for continuous manufacturing of 3D printed dosage forms.

Recent publications on the FDM 3D printing, however, indicate several limitations of the system that require vigorous investigation for extensive scale application of the technology for drug delivery (8). The extruded filaments of pharmaceutical grade polymers are either brittle that break in the motor gear (plunger assembly) or soft that cannot be pushed by the drive gear due to pliability of filaments (9-11). To develop proper filaments with mechanical stability (12, 13), the potential of the HME-FDM 3D printing process has been less studied. Even though most of studies has used the plasticizers in order to possibly decrease melt viscosity and thus reduce processing temperature for hot melt extrusion, the added plasticizer may not be miscible with the polymer and its existence may cause crystallization of drug from the system (14, 15).

One major constraint of FDM 3D printing is that most of prepared tablets appear to be more prominent in controlled release system and some efforts also exploited the infill function of FDM (16-18) to tailor drug release. However, the majority of the oral products currently obtainable in the market are immediate release tablets, which would account for 79% of new drug entity (NDE) (16). In particular,

immediate release dosage forms are needed for drugs necessitating rapid onset of action after oral administration (9, 19). There have been only few attempts on FDM 3D printing as the fabrication of immediate release tablets has been still challenged to gain (20). In addition, it is of great attention to adapt the 3D printing method which grant the possibility of different pharmaceutical devices with a variety of modification in dissolution profiles from one feedstock filament (6, 7, 10). To develop immediate release FDM 3D printed tablets, Okwuosa (21) developed formulations containing large amounts of talc as the crystalline filler with the limit of 50% active ingredients, where the drugs remained in the crystalline form. However, the feeding filaments have been restrictedly revealed with the major use of polymer (including polyvinyl alcohol (22), hydroxypropyl cellulose (23), Eudragit[®] EPO (20), Kollidon[®] VA 64 and Kollidon[®] 12PF (21), Soluplus[®] (24), PVP K12 and Kollicoat[®] IR (25)) and plasticizer (23).

An approach to accelerate drug release can be achieved through the integration of disintegrants (e.g, sodium starch glycolate, croscarmellose sodium and crospovidone), yet no one has reported in 3D printing area. With their porous structure, disintegrants increase water uptake into the tablet and elevate the internal pressure through swelling (16, 26). Moreover, the pharmaceutical disintegrants (e.g starch derivatives) have thermoplastic property and are known as a dissolution adjuvant for the development of solid dosage forms (27).

The next important issue stems from the limitation in dosing amount and dose flexibility which is a key element in the case of polypills dosage forms (12). It is requisite to use source materials with high API loads so as to confine the dosage form size. Pietrzak (23) made use of a high melting drug, theophylline (m.p. 270°C), at 50:50 ratios (the maximum drug loading, previously reported) with Eudragit[®] RL, RS, or E to prepare filaments with the aids of different plasticizers to enhance the flexibility of filaments, flowability of melt, and lower printing temperature (24, 27-29). In addition, dosage amount could be managed rapidly and easily by physically altering the tablet dimensions or infill percentage. However, altering printlets geometry could affect drug release, which would need to be accounted for in this study design. An approach to overcoming this could be by adjusting the 'feedstock' concentration while sustaining printlets geometry, that allow immediate release (30).

Recently, Design of experiment (DoE) is a statistical tool applied in the advanced formulation development and optimization approaches. It has been grown a great attention with the introduction of Quality by Design (QbD) by FDA in the formulation development of dosage forms (31). Some designs of DoE have been applied to fully understand both the main and interaction effects of individual component in formulation and manufacturing process factors (32, 33). Although the prior research focused on the development of different 3D printed dosage forms for evaluating processing variability and its impact on drug product performance, there has been no investigation into understanding how much variability in excipients such as API loadings, polymer and disintegrant ratios (critical material attributes, CMA) that impacts immediate release 3D printed oral dosage forms. In this work, mixture design was selected as DoE, because it minimizes the variance related with the coefficient evaluations in a model and can handle the best-possible subset by understanding the criteria for better information of matrix determinants. Moreover, this design represents the total system of formulation as 100% (34).

The main objectives were to develop immediate release tablets and to systematically investigate the influence of different compositions and their potential interactions on drug release patterns. Thus, screening study was performed with various pharmaceutical polymers, disintegrant as well as different drug loadings to specify the critical process parameters (CPP) and critical material attributes (CMA) into the appropriate limit of each factor in DoE. Meanwhile, the obtained filaments and produced dosage forms were methodically characterized the parameters such as physicochemical, mechanical properties, rheological assessment and drug release pattern to understand the critical quality attributes (CQA) before applying DoE to optimize the formulation as the required Quality Target Product Profile (QTPP) in pharmacopoeia. To maintain the formulations relatively simple, no plasticizer was used in this work.

4.3. Materials and Methods

4.3.1. Materials

Hydroxy propyl cellulose (HPC), Eudragit[®] EPO (MW. 45,000 g/mol; EPO), semi-crystalline Kollidon[®] VA 64 (MW. 67,000 g/mol; PVP/VA), sodium starch glycolate (SSG) (as a superdisintegrant) were applied as matrix formers. Theophylline (THY), a model drug, was obtained from Sigma-Aldrich. All solvents used were of analytical grade.

4.3.2. Screening study for setting up the level of components in DoE

The API, polymers and disintegrant levels (critical material attributes, CMA) were determined prior to developing the study design. Firstly, filaments using single polymers were extruded (data not shown). Then, different excipients blending was screened based on the behavior of single polymers (brittleness) to examine the extrudability and printability of filaments and printed tablets (critical process parameters, CPP) (Table 6). The obtained filaments and tablets were then used for pharmaceutical characterizations to understand the critical quality attributes (CQA) before the independent variable levels for each component were assigned in DoE.

4.3.3. Preparation of theophylline loaded filaments

Pre-mixed physical mixtures were prepared using a mortar and pestle for 15 min and fed with a gravimetric feeder. Extruded filaments were fabricated applying a single screw extruder (Noztek[®], England) with specific rotating screw speed (35-45 rpm) and extrusion temperature (135-160 °C) adjusted to formulations to control the filament diameter. The compositions of the mixtures of drug, polymer blend and disintegrants were prepared as shown in Table 7 and Table 8.

4.3.4. Rheological measurements

A rotary rheometer (MARS, Germany) equipped with a 25 mm parallel plate was utilized to investigate the melt viscosity and critical processing parameters (CPP) as a function of temperature for both HME and 3D printing. Samples were compressed into disc about 25 mm in diameter and 1mm thickness. Temperature

sweep test was conducted after melting the sample on the plate with the gap of 0.9 mm at an amplitude strain of 0.5% (within the LVR region) and frequency of 1 Hz.

4.3.5. Fused deposition modelling (FDM) 3D printing of tablets

A MakerBot Replicator 2x desktop 3D printer (Brooklyn, NY) with a dual nozzle of 0.4 mm diameter and the MakerBot MakerWare™ software were used for the production of 3D printed tablets. The temperature of printing was applied at 200°C and platform temperature is 90°C for all formulations. Tablets were printed with 100% infill density to produce solid dosage forms of high density and hexagonal infill pattern. The selected geometry was a round-face tablets with the dimensions of X=10 mm, Y=10 mm and Z=4 mm.

4.3.6. Characterization studies of filaments and 3D printed tablets

4.3.6.1. Macro and microscopic studies

The appearance including color and transparency of filaments and tablets were visually examined and the diameter of filaments were controlled within 1.6-1.7 mm to match with the nozzle of the 3D printer. The microscopic characters were observed using a Scanning Electron Microscope and Energy Dispersive X-ray Spectrometer (SEM-EDS, IT 300) at 3.0 nm resolution (1.5 KV) after being coated with a gold coater under a vacuum.

4.3.6.2. Mechanical properties of filaments

The flexibility, brittleness, and stiffness were determined to understand the appropriate mechanical properties of the printable filaments, as referred to Repka-Zhang [18]. TA-XT2 analyzer (Texture Technologies Corp, New York, NY, USA) and the TA-95N probe set with a 25 mm supporting gap were used. The extruded filaments were cut into 50 mm rods, then placed on the sample holder. The blades moved with a speed of 10 mm/s until reaching a maximum distance of 15 mm below the supported sample. The breaking distance and load force/stress data were recorded in triplicate.

4.3.6.3. Attenuated total reflectance Fourier-transform infrared spectroscopy (ATR-FTIR)

The extruded samples and pure drug were measured using a Varian 600 series FTIR spectrophotometer (ThermoFisher, Nicolet iS10, U.S.A) equipped with an ATR unit to examine the interactions between theophylline and polymer blend. Data was collected using 64 scans over a 650–4000 cm^{-1} range at a resolution of 4 cm^{-1} .

4.3.6.4. Thermal analysis

Thermal stability of theophylline and the matrix polymers was studied by thermogravimetric analysis using a TG-DTA analyzer (Rigaku Thermo plus EVO2, Japan) and performed from 30 to 300°C with a heating rate of 10°C/min. Phases transformation and thermal behavior of the drug-polymer matrix in the extruded and printed samples were analyzed by DSC (Mettler Toledo, DSC822 STAR System, Germany). 5 mg of sample was put in an aluminium pan covered with a punched lid over a heating/cooling system from 30 to 300°C with a heating rate of 10°C/min and nitrogen flow rate of 10 ml/min.

4.3.6.5. Powder X-ray diffraction (PXRD)

The powder X-ray diffractometer (Rigaku model MiniFlex II, Japan) was applied to identify the crystallinity of raw materials, filaments and printed dosage forms. The diffractometer (Rigaku model MiniFlex II, Japan) was operated with a copper anode tube at the generator voltage and the current of 30 kV and 30 mA, respectively. The samples were scanned with the diffraction angle increasing from $2\theta=5^\circ$ to 50° at a step of 0.02° and a scan speed of 2 s/step.

4.3.6.6. Drug content analysis in filaments and 3D printlets

The theophylline dispersion in filaments was verified by taking samples of 100 mg at the three different spots of filaments. The samples were dissolved in 0.1N HCl and the drug content was determined by UV/Vis Spectrometry (Shimadzu, Japan) at the wavelength of 270 nm. Polymers and other additives did not affect the measurements. The content uniformity of 3D printlets was conducted with this method.

4.3.6.7. In-vitro dissolution study

In order to study the theophylline release of 3D printed tablets, USP I (Basket) dissolution test apparatus (Vankel, Germany) was used in a dissolution medium of 900 mL 0.1 N HCl at $37 \pm 0.5^\circ\text{C}$ with a rotation speed of 100 rpm. Each experiment was performed in triplicate. Samples were collected at the intervals of 5, 10, 15, 20, 30 and 45 min and examined using a UV/Vis spectrophotometer (Shimadzu, Japan) at the wavelength of 270 nm.

4.3.7. Experimental design

Four independent variables (30-60% THY, 30-35% EPO, 5-20% HPC and 5-15% SSG set by the screening and characterization studies) were selected as the CMA with minimum and maximum levels. The measured responses (two dependent variables), the percent drug release at 30 min (Y_1) and at 45 min (Y_2) set as the CQA, were targeted to understand the influence of material factors on different phases of dissolution testing and to investigate the optimized formulation with the required quality target product profile (QTPP). The timepoint was selected as referred to the monograph of the immediate release tablets in the pharmacopoeia. All filaments and tablets were produced under the same optimized CPP in the previous sections. Minitab software was used for creating the design space, fitting the experimental results with the selected design and calculating the important statistical coefficients of the factors such as linear regression (R^2), predicted R^2 and adjusted R^2 . A total number of 17 experimental runs were prepared as per design shown in Table 7.

Table 7. D-optimal mixture design of FDM 3D printed tablet formulations.

Formulations	X ₁ :THY (%w/w)	X ₂ :EPO (%w/w)	X ₃ :HPC (%w/w)	X ₄ :SSG (%w/w)
1	45.00	35.00	5.00	15.00
2	50.00	30.00	5.00	15.00
3	42.5	33.75	16.25	7.50
4	35.00	30.00	20.00	15.00
5	45.00	31.25	16.25	7.50
6	45.00	32.50	12.50	10.00
7	37.5	33.75	16.25	12.5
8	55.00	35.00	5.00	5.00
9	40.00	31.25	16.25	12.5
10	52.50	31.25	8.75	7.50
11	45.00	30.00	20.00	5.00
12	60.00	30.00	5.00	5.00
13	47.50	31.25	8.75	12.5
14	30.00	35.00	20.00	15.00
15	50.00	33.75	8.75	7.50
16	40.00	35.00	20.00	5.00
17	45.00	33.75	8.75	12.50

4.4. Results and Discussion

4.4.1. Screening study for setting up the level of components in DoE

The water-soluble polymers with different functional properties as carriers for solid dispersion prepared by HME (HPC, EPO, PVP/ VA) and thermoplastic starch (SSG) with different ratios were screened. However, filaments based on the neat polymers of EPO and PVP/VA with theophylline were fragile, poor stiffness and crumpled in a driven wheels of 3D printer probably owing to the low molecular weight of the polymers that could not facilitate long range interlinking of the polymer chains, essential for the tensile strength of the filament (20, 35, 36). Polymer blending could be one of the solutions to improve the mechanical properties of the extruded filaments for FDM printing (24). Due to the fact that hydroxypropyl cellulose (HPC) polymer possesses glass transition temperatures at 0°C (originating from a beta

transition) and 120°C which make it easily extrudable since the melt viscosity substantially falls at the applied temperatures during printing. Furthermore, the beta transition around 0°C presents the improved flexibility of the polymer, which is desired for successful FDM 3D printing (37).

Therefore, as presented in Table. 7, HPC was used as a flexibility modifier to reduce the brittleness of the produced filaments which improved mechanical property of for successful printing without any plasticizers. SSG with thermoplastic property was also employed as disintegrant in these formulations to increase drug release rate. Moreover, various drug loadings were added to demonstrate the dose flexibility of printed tablets without altering in dosage form geometry.

Table 8. Optimized filament formulations and hot melt extrusion (HME) conditions.

Formulations	THY (%w/w)	Polymers (%w/w)	Flexibility modifier, HPC (%w/w)	Disintegrant, SSG (%w/w)	HME temperature (°C)/screw speed (rpm)
E10	10	EPO 55	20	15	135/35
E30	30	EPO 35	20	15	160/45
E60	60	EPO 30	5	5	160/45
P10	10	PVP/VA 35	40	15	135/45
P30	30	PVP/VA 35	20	15	160/45
P60	60	PVP/VA 30	5	5	160/45

For the formulations containing 10% drug loads (E10 and P10), EPO in the range of 30-55% were identified as printable when EPO was applied in combination with HPC and SSG while in the case of PVP/VA, more than 35% was not printable as of its brittleness, thus, the highest limit became 35% PVP/VA and a greater portion of HPC at 40% regardless of including 15% SSG. The similar brittle nature was observed for EPO over 55% irrespective of combining HPC in these formulations. Thus, the mechanism by which the printable property of EPO and PVP/VA (24) is enhanced by the addition of HPC that leads to the improved melt viscosity and plasticization of the combined property of polymers. It is noticeable that the suitable range of 5-40% HPC resulted in the printable filaments having optimal mechanical

properties. However, the greater proportion ($> 40\%$) of HPC tends to produce controlled release system.

When THY loading was increased to 30% (E30 and P30), the temperature and screw speed was raised as the higher extrusion temperature and speed of screw play a vital role in the dispersion of theophylline in the polymer matrix (12, 38, 39) although additional drug loading (30%) displayed partly plasticizing effect on the polymer matrix thus leading to easier processing (12). While the extrudable and printable filaments incorporated with 60% of drug (E60 and P60), which is the higher drug ratio than previously reported, were successfully obtained but relatively fragile. This could possibly be due to the higher content of crystalline drug than polymer matrix which may not withstand the tension, bending, and compression in the feeding system (7). Lastly, the appropriate amount of SSG in filament was found specifically in the range of 5-15%. Exceeding such limit resulted in a difficult-to-print filament and clogged nozzle.

4.4.2. Rheological measurement

Before oscillatory measurements are conducted, it is essential to ensure that the chosen constant strain is lied within the well linear viscoelastic region as polymers relax during such region (appendix). The rheological property demonstrated the effect of drug-exipient loads and the change of temperatures on melt viscosity as presented in the complex viscosity profile of all six (successfully extruded and printed) formulations (Fig. 22a and 22b). With an increase in temperature, the complex viscosity values gradually reduced whereas the measured viscosity of all the samples showed consecutively higher upon the increasing of drug loadings as function of temperature. The lowest complex viscosity in 10% drug loadings (E10 and P10) indicated the plastifying effect of the partially-dissolved theophylline in polymer matrix (40). However, the increased melt viscosity levels in 30% and 60% THY proportionally related to the high degree of solid crystallinity in matrix (41) which was then confirmed by the PXRD studies (section 4.4.3.5). Therefore, the plasticizing effect of the dissolved theophylline could not compensate the thickening effect of non-dissolved theophylline particles.

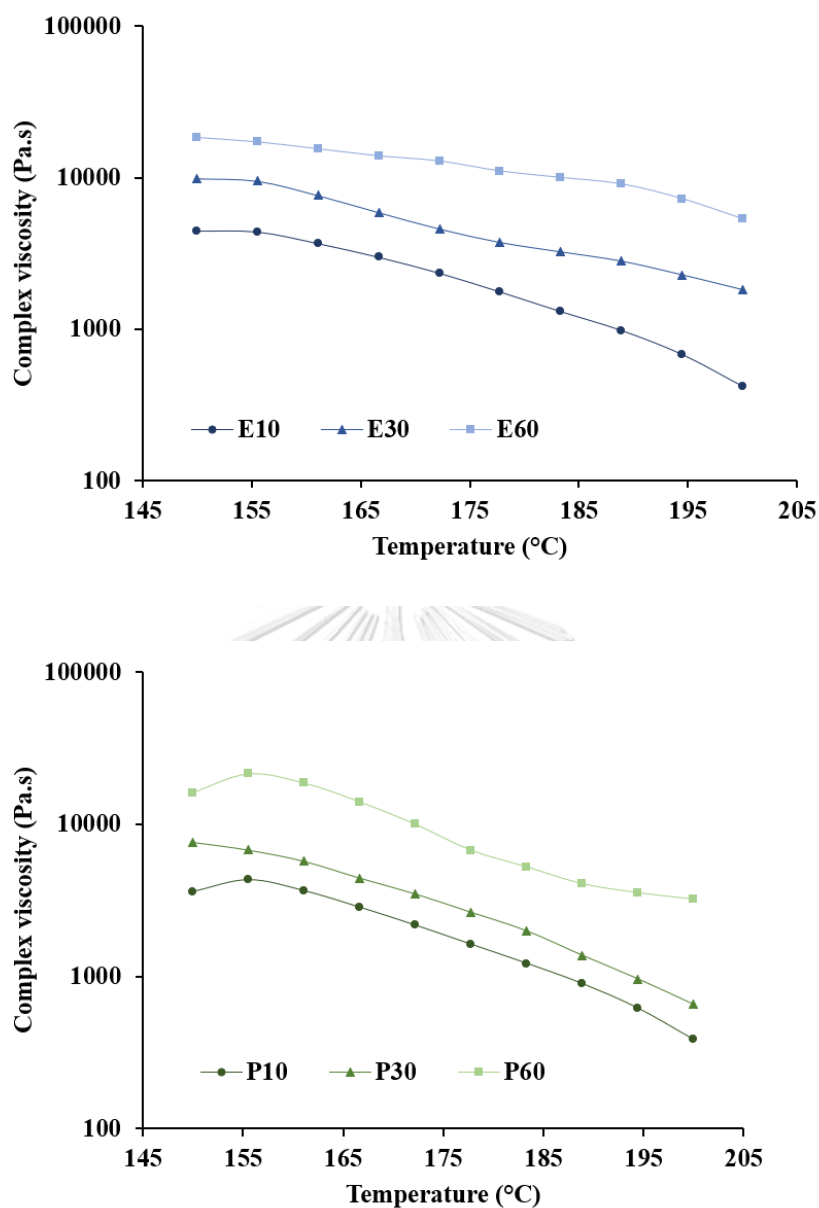


Figure 22. Temperature sweep analysis of different drug load mixtures (a) EPO-based mixtures (b) PVP/VA-based mixtures.

Optimal extrusion was reported to be in the viscosity range of 1,000 to 10,000 Pa.s (14) which is in good agreement with that of 10 and 30% drug loaded-mixtures. Interestingly, the complex viscosity of 60% drug loads mixtures was out of the reported range (14,000 Pa.s at 160°C), but both E60 and P60 could be successfully extruded at 160°C in this work. While E30 and P30 (30% drug loading) were extruded at 160°C with the viscosity range of 5,711 - 7,619 Pa.s. It is worth noting

that, although the viscosity of 10% drug loading systems was in the reported range, E10 and P10 required less temperature (at 135°C) because the lower viscosity at 160°C led to the free-flowing powder blend which then produced too thin filaments, not fit to the printing nozzles. Hence, consideration of viscosity along with its diameter must be taken in parallel. The new viscosity range of 5,000-14,000 Pa.s can be proposed for the fabrication of filaments, specifically to the FDM 3D printing.

As for the optimization of the 3D printing temperature, attempts were made to print tablets at higher temperatures (up to 200°C), and it was observed that 200°C was the most suitable printing temperature to obtain a tablet for all formulations. Noticeably, there was a drop in viscosity from 18,411 Pa.s at 150°C to 5,333 Pa.s at 200°C in EPO-based formulations with high drug loads (E60) while from 16,184 Pa.s at 150°C to 3,212 Pa.s at 200°C in the mixture prepared with PVP/VA (P60), corresponding to the previous work with the complex viscosity of less than 8000 Pa.s, required to gain sufficient material flow in the heated nozzle for FDM printing (42). The printing temperature was fixed at 200°C (rather than the lower temperature) to achieve good adhesion between the layers of printed strips and neat printed objects in all formulations. It can be summarized that more specific range of the viscosity within 5,000 Pa.s (lower than the HME process) should be optimized for FDM printing.

4.4.3. Characterization studies of filaments and 3D printed tablets

4.4.3.1. Macro and microscopic studies

The extruded formulations were successfully printed into the tablets with desired geometries and appearance (white until yellowish upon the increasing drug concentration). The uniformity in physical dimensions, with a mean thickness of 4.00 ± 0.05 mm, diameter of 10.00 ± 0.04 mm, and weight of 294.5 ± 3 mg was observed in all the formulations. The small variations lied within the narrow ranges. Such weight differences between the printed tablets for the different formulations results most probably stem from expected due to the intrinsic property of each material, such as the rheological behavior when melt and, possibly, the volumetric changes after hot processing (29).

SEM images of 10% w/w THY filament (Fig. 23. 1a and 1b) showed compact filaments with rough surface likely due to the phase separated theophylline particles.

This may be attributed to the low temperature (135°C) of HME that was not enough to dissolve completely THY particles because of its high melting temperature. Upon the addition of increasing concentrations of THY (30% w/w), the surface of compact filaments became smoother (Fig. 23. 2a and 2b), but appeared as highest roughness and irregular voids on the surface when increased THY up to 60% (Fig. 2. 3a and 3b).

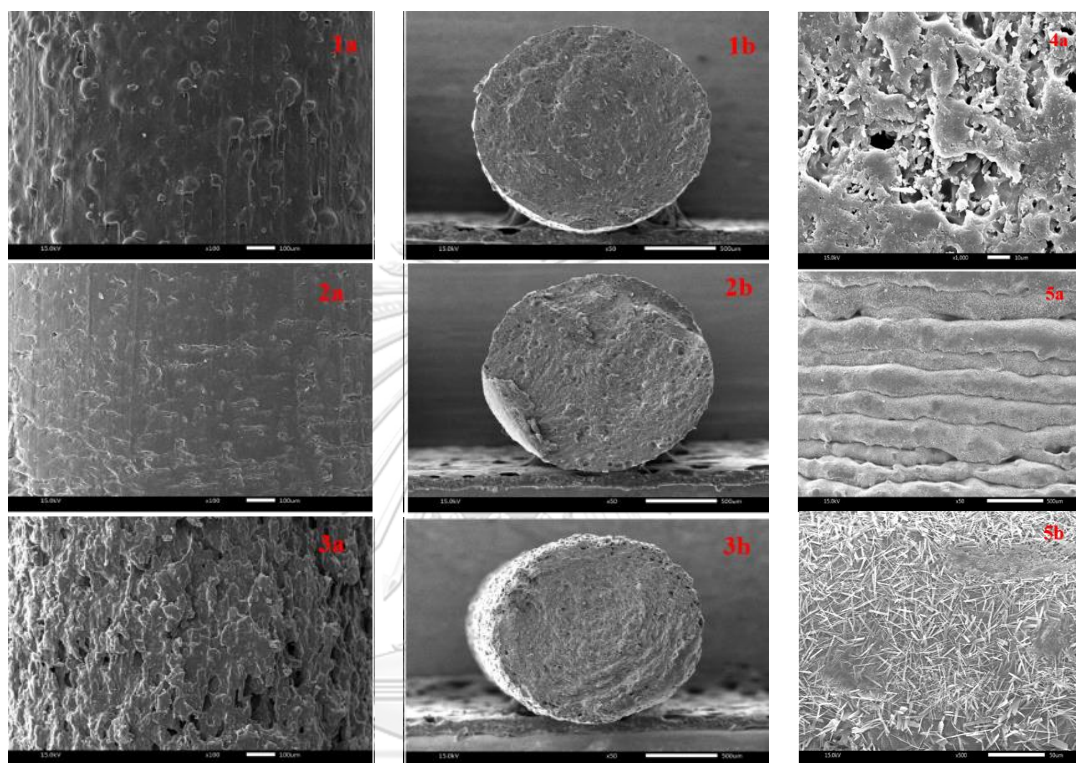


Figure 23. SEM images of HME filaments: (a) surface and (b) cross-section images of (1) E10 (2) E30 (3) E60 filaments; and FDM 3D printed tablets: (4a) cross section (x1000), (5a) side view (x50) and (5b) side view (x500) images of P30 printed tablets.

The cross section x1000 images of tablets (Fig. 23. 4a) revealed the relatively uneven surface with irregular pores and single particulate matter whereas fused multilayer of printed strips could be observed at the side view (Fig. 23. 5a). Noticeably, elongated theophylline particles were clearly seen under high magnified image (x500, Fig. 23. 5b), reflecting that the crystalline THY could hide in the polymer matrix. However, these microscopic findings did not have an effect on the physical properties as shown above. Additionally, no clear differences were found between EPO and PVP/VA formulations.

4.4.3.2. Mechanical evaluation of filaments

Apart from setting the appropriate process parameters (critical process parameters, CPP) as discussed in the previous sections, the mechanical property of the filament plays a key role during printing inside the printing nozzles (20). The very flexible or brittle filaments with poor stiffness cannot be used for printing because they tend to crumble inside the nozzles mainly affected by the transversally applied pressure of the feeding gears. In general, all the printable filaments had the breaking stress in the range of 2,298.44-3,028.76 g/mm² while the distance at break lied in the range of 0.71- 5.52 mm, which are corresponding to the previous report (43). Nonetheless, Zhang reported that filaments with a higher breaking distance had a tendency to be printable while filaments with a breaking distance below 1.00 mm were easy to be brittle to be loaded into the head of the 3D printer (10); however, in this study, 60% drug loading filaments (E60 and P60), which had less than 1 mm breaking distance, can be printed.

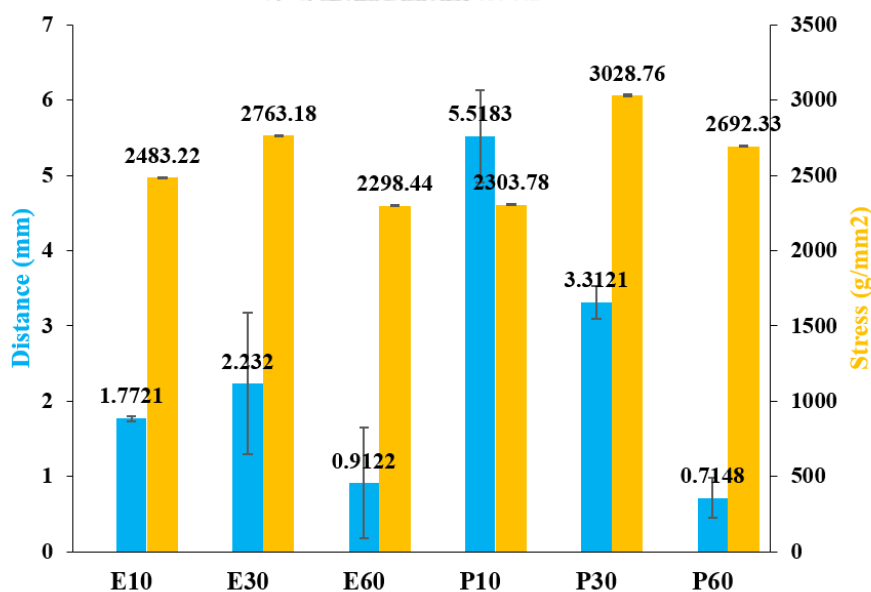


Figure 24. Breaking distance and breaking stress of all extrudable and printable filaments obtained from the 3-point bend testing.

It is apparent that the highest breaking distance, reflecting highest flexibility, was found in the formulation with the highest amount of HPC (40%), which can confirm its function as a flexibility modifier in this work. As for the polymer type, the results demonstrated that the EPO-based filaments (E30, E60) have lower stress value than those made of PVP/VA (P30, P60) as shown in Fig. 24, indicating less elastic property. Regarding drug loading, an increase in stress values was experienced when increasing in theophylline from 10 to 30% in both EPO and PVP/VA, implying that the stiffness and toughness of filaments was possibly improved to more elastic (10, 43) by the partial dissolving of drug in the polymer mixture. Whereas high drug loading in the form of crystalline at 60% (both E60 and P60, with less excipients) gave the lowest breaking distance and stress values, leading to weak filament and rigid character (less bendable) (12).

4.4.3.3. Attenuated total reflectance-Fourier transform infrared spectroscopy (ATR-FTIR)

The band shifts and broadening peaks were found in the FT-IR spectrum of the THY-EPO (Fig. 25) and THY-PVP/VA (Appendix C, Fig. 36), indicating the intermolecular interactions in solid dispersion (SD) (44). The peaks assigned for NH stretching and bending of crystalline THY decreased significantly in the E10 and E30, owing to the formation of hydrogen bond. Moreover, the carboxyl peak of EPO (1725 cm^{-1}) in SD showed small intensity peak with a lower shift (ca. 1720 cm^{-1}) than pure polymer, likely due to the intermolecular hydrogen bonding between electronegative groups including nitrogen or oxygen in THY (hydrogen bond donor) and EPO carboxyl group (hydrogen bond receptor) (45). Also, the disappearance of hydroxyl group of HPC in SD at 3616 cm^{-1} indicated the formation of H-bond with electronegative groups presented in drug molecules which increased the solubility of the drugs (46) due to less concentration of theophylline in the formulations.

Regarding E60 formulation, the significant attenuation of the active functional groups for theophylline were prominently observed at 3120 , 1664 and 1559 cm^{-1} as strong bands (Fig. 25). This may be attributed to higher theophylline concentration than that of other components which indicated the crystalline solid dispersion of THY

in the polymer matrix. The disintegrant, SSG, did not show characteristic peaks due to its low concentration in the formulations compared to other excipients.

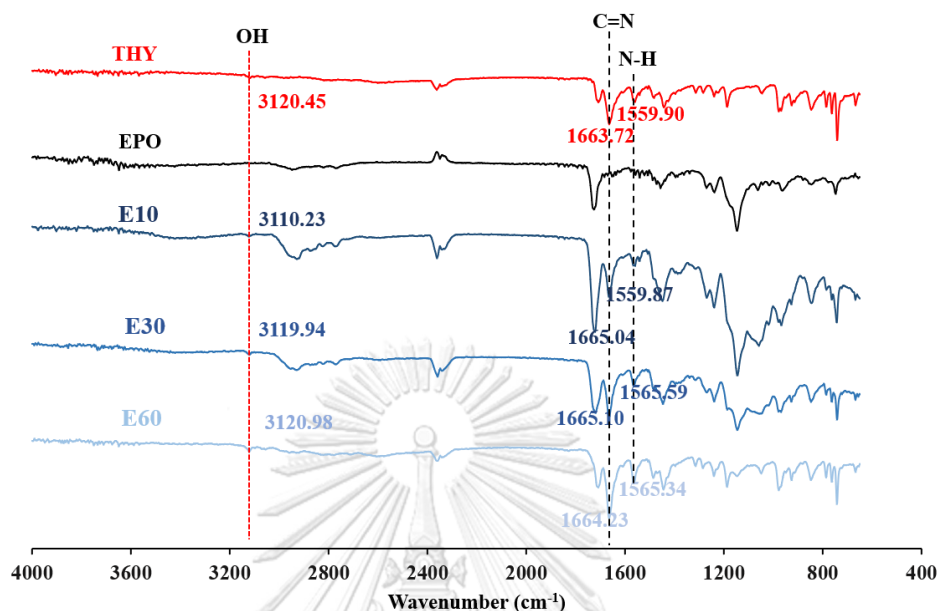


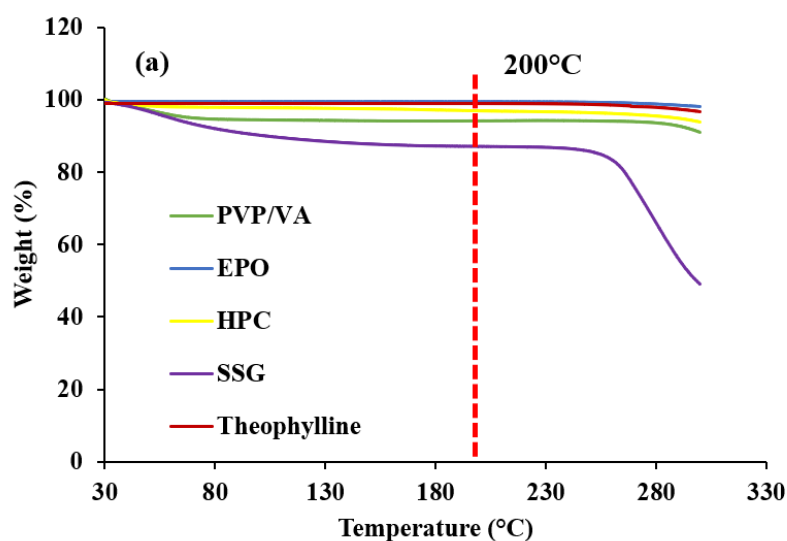
Figure 25. FTIR spectrum of EPO-based filaments compared with the pure drug.

In both P10 and P30, the OH stretching shifted from 3143 to 3122 cm^{-1} with slight red shift pointed out that a hydrogen bond has experienced between THY and PVP/VA. In addition, this carbonyl peak in PVP/VA is still visible but has considerably shifted down from 1654 cm^{-1} to 1566 cm^{-1} (88 cm^{-1}) which again indicates stronger hydrogen bonding between this functional group in the polymer PVP/VA and theophylline (44) (Appendix C, Fig. 36). Because PVP/VA includes two hydrogen acceptors, which are derived from the C=O groups of the pyrrolidone ring and the acetate structure. It would be superior that the hydrogen bond of NH group forms with the C=O group of the pyrrolidone group because this group is a stronger hydrogen bond acceptor than the acetate group (44).

4.4.3.4. Thermal analysis

Fig. 26a showed that most substances are not heat-sensitive except for SSG upon processing temperature. SSG has slight weight drop between 45 and 263°C corresponding to the gradual loss of water molecules and followed by decomposition that is in accordance with the previous finding (47). Nevertheless, the small amount of

SSG was used in the formulation, thus the filaments did not show a major step change over the HME (135-160°C) and printing temperature used in the study (< 200°C, Fig. 26b), suggesting no thermal degradation occurred. EPO was stable up to 216°C with little weight loss of 0.84% (48) while PVP/VA was thermally stable up to 230°C although 1.85% of free water molecules was lost at the temperature below 150°C.



The TGA curve of HPC showed the minimal weight loss of 2.89% probably due to the removal of residual moisture removed from the structure since HPC has the ability of moisture absorption (49), indicating no further change in weight until 300°C.

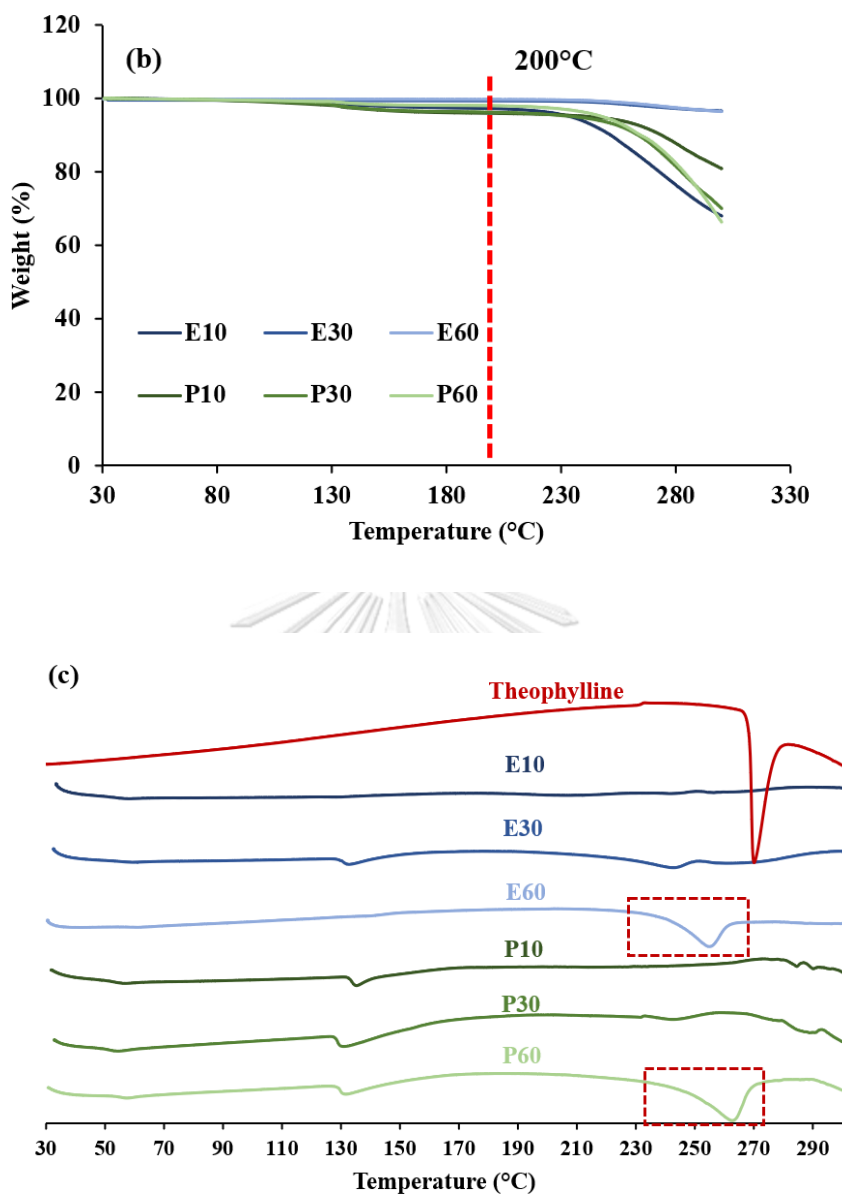


Figure 26. Thermogravimetric analysis of (a) API and excipients, (b) extruded filaments, and (c) DSC thermogram of extruded filaments.

In DSC analysis (Fig. 26c), the melting peak of THY appeared at approximately 273 °C (50) and the absent of melting enthalpy reflected the partial amorphization of drug in E10, E30, P10 and P30 which was later confirmed by the XRD. E60 and P60 had the melting point depression of THY, suggesting that a large proportion of theophylline remained in a crystalline form following HME. In the meantime, printed tablets had similar results (data not shown).

4.4.3.5. Powder X-ray powder diffraction (PXRD)

The PXRD data (Fig. 27) showed a small number of crystalline THY peaks with low intensity in both E10 and P10 filaments, which indicated partial amorphous solid dispersion. Whereas other filaments (filaments containing 30 and 60% w/w drug) had more number of diffraction peaks with higher intensity (at 7, 12, 14 and 24° 2 θ) that match with the diffraction pattern of THY (23, 51), suggesting the larger proportion of THY remained crystalline. It is likely due to the use of HME temperatures (160°C) under the melting point of theophylline (273°C), resulted in incomplete melting of the high amount drug and yielded a crystalline filament matrix. The crystallinity presented in printed tablets remained the same as the filament (Appendix D, Fig. 37). The PXRD results were consistent with the DSC profiles, confirming the crystallinity of the drug-polymer systems (52).

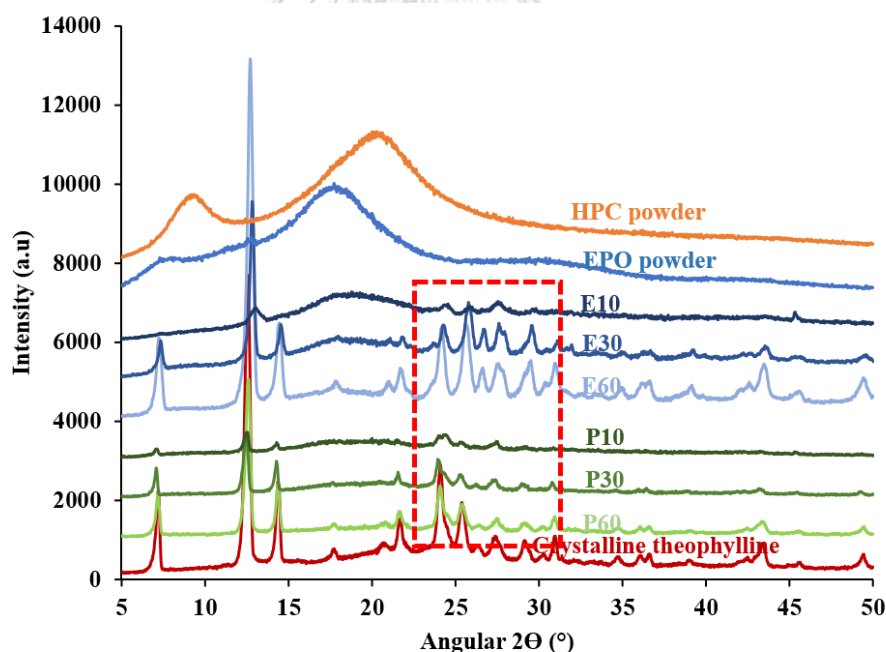


Figure 27. X-ray powder diffractograms of pure API, excipients and extruded filaments.

4.4.3.6. Drug content analysis in filaments and 3D printed tablets

The uniformity of theophylline distribution along the whole filament spool is essential as a systematic understanding of the production process of the filament is

needed to produce dosage forms with homogeneous theophylline content (12). Moreover, in order to examine the temperature effect of hot melt extrusion and 3D printing on the APIs, we assessed the percentage of different drug loading in the filaments and each tablet after fabrication. As elucidated in Table 8, the percentage of theophylline content was found to be in the range of $99.94 \pm 1.212\%$ to $101.65 \pm 1.567\%$ in filaments and $99.96 \pm 1.246\%$ to $100.69 \pm 2.146\%$ in tablets, suggesting that the drug content was neither affected by the temperature during the hot extrusion nor printing processes. It was, therefore, concluded that there was good thermal stability of API during extrusion and printing.

Table 9. Drug content analysis of filaments and printed tablets ($n=3$).

Formulations	Drug content (%)	Drug content in filament (%)	Drug content in printed tablet (%)
E10	10	100.81 ± 1.356	100.69 ± 2.146
E30	30	100.41 ± 0.689	99.96 ± 1.246
E60	60	101.65 ± 1.567	100.40 ± 1.209
P10	10	99.94 ± 1.212	100.53 ± 1.895
P30	30	101.06 ± 0.908	100.42 ± 1.419
P60	60	100.62 ± 0.765	100.36 ± 1.403

The drug content was not exactly 100%, because of subtle lot-to lot variations and irregular pores as seen in the x1000 resolution images of SEM. However, this type of under-content or overage is common in pharmaceutical products and acceptable across the regulatory agencies (52). Furthermore, the range of drug loading in the filaments was 10-60% w/w, which allowed for dose flexibility in printing of tablets without altering the tablet size.

4.4.3.7. In-vitro dissolution study

The drug release mechanism is a complicated integration of drug and polymer crystallinity, drug loading which take into account for the matrix porosity and extrusion temperature which affected the relative amount of amorphous and crystalline drug (53). It was observed that EPO-based tablets (E10, E30 and E60, blue lines, Fig. 28) showed faster drug release rate than PVP/VA-based tablets due to the dissolution rate of the polymer (24), polymer type and polymer permeability (53). The higher pH threshold of EPO than PVP/VA achieves the rapid ionizing of side chains in polymer in pH 1.2 (24). At this pH, the dimethyl aminoethyl side chains in EPO ionizes, leading to electrostatic repulsion between the cationic polymeric chains. Consequently, this improves the polymeric chain spaces thus allowing the dissolution of the polymer and drug release (20). Of these EPO-based tablets, the tablets with 30% drug loading showed a slightly faster drug release rate than the other two drug loadings with $T_{85\%} = 30$ min. This is likely due to the partially amorphous solid dispersion, which was caused by the synergistic effect of rising the extrusion temperature and high shear condition produced by the faster screw speed (12).

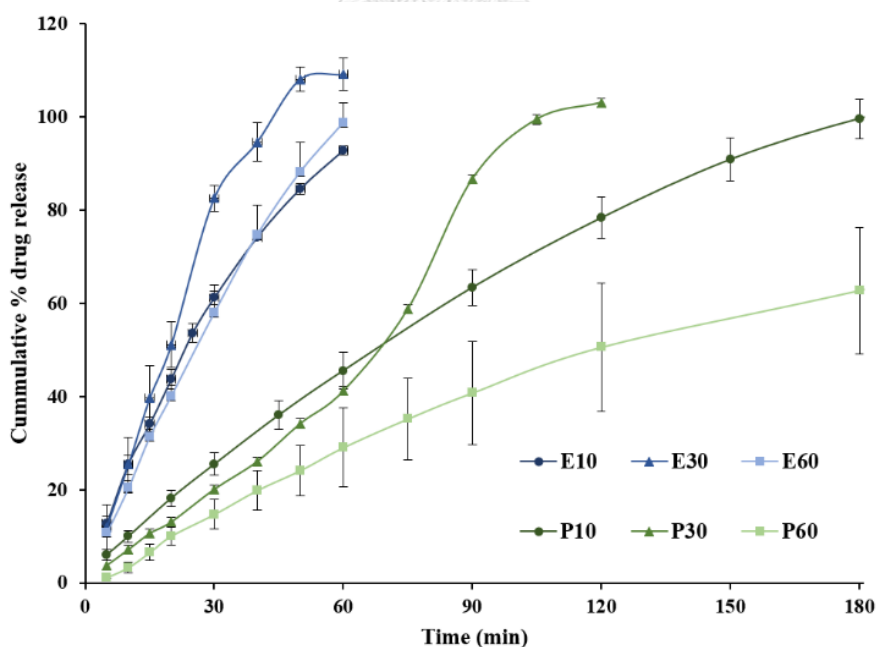


Figure 28. In-vitro drug release profiles of FDM 3D printed tablets from EPO (blue lines) and PVP/VA (green lines)-based filaments.

However, tablets with 10% and 60% drug loads exhibited a rapid drug release of $T_{85\%} = 50$ and 48 min, respectively. On the other hand, printed tablets with the PVP/VA polymeric matrix demonstrated a considerably slower drug release because PVP/VA caused some extent of swelling and formation of gel layer in acid stage (54). 30% drug loads tablets displayed faster THY release ($T_{85\%} = 90$ min.) compared to that of the 10% drug loaded tablets which showed $T_{85\%} = 130$ min. There may be due to the fact that the use of large polymer ratio (40%) of HPC with high molecular weight in such 10% drug load sample engenders high density of polymeric network with limited porosity, thus resulting in long drug release patterns (13, 17, 20, 55-57). The slowest drug release pattern was observed in 60% drug loads PVP/VA formulation over 180 min.

According to the six formulations, it is difficult to conclude which material factors have the main impact on drug release. The previous report stated that low concentration of drug (10%) possessed faster dissolution rate than high drug loads (50%) (58). There may also be the fact that the impact of drug loading is directly correlated to the quantity of drug exposed on the surface of the printed tablets, seen by SEM image (section - 4.4.3.1), the dissolution of which is not controlled by diffusion mechanism. Moreover, when drug crystals may dissolve and form pores for water to infiltrate into the tablet, and for the drug to diffuse out of it. However, its effect (drug loading) gradually drops on drug release rate over time, probably due to the presence of exhausted THY particles externally exposed the medium, leading to diffusion-controlled release (60).

Here, the 10% THY systems, which are partially amorphous solid dispersion, did not show the fastest drug release, possibly caused by the polymer blending. Moreover, 10 and 30% THY systems with a higher amount of disintegrant did not always show a significant impact on dissolution rate, indicating that both polymer and disintegrant type could significantly modulate tablet dissolution (54). Overall, EPO-based tablets tend to have an immediate theophylline release. Therefore, EPO system was chosen for further investigation with specific experimental design.

4.4.4. Design of Experiment

The previous sections showed that drug, polymers and disintegrant concentrations have a relatively complicated effect on the drug release behavior. Thus, D-optimal mixture design was carried out to identify the possible interactions between such factors on drug release at specific timepoints. The results obtained after fitting and calculation of the statistical parameters R^2 values were shown in Table 9.

Table 10. ANOVA results of the 17-formulations design.

Responses	Model	F-value	p-value	R^2	R^2 (predicted)	R^2 (adjusted)
Y ₁	Full quartic	15.26	0.010	90.77%	0.00%	75.39%
Y ₂	Full quartic	60.91	0.019	91.03%	24.05%	76.09%

The meaningfulness of responses was well fitted and predicted by the different models as R^2 had high values ($R^2 > 0.9$) for Y₁ (% drug release at 30 min) and Y₂ (% drug release at 45 min), suggesting that they could predict the responses validly. In addition, the impact of each factor yielded different theophylline release rates at 30 min., ranging from 50.93% in F4 (minimum) to 101.86% in F8 (maximum). The observed values of all the 17 formulations were shown in Table 10. The polynomial equations were obtained as the followings:

$$Y_1 = -330X_1 + 1345X_2 + 8734X_3 - 34448X_4 - 67340X_1 * X_2 * X_3 + 227759X_1 * X_2 * X_4 - 30026X_1 * X_3 * X_4 + 190822X_2 * X_3 * X_4$$

$$Y_2 = -325X_1 + 1016X_2 + 703X_3 - 29244X_4 - 57934X_1 * X_2 * X_3 + 190405X_1 * X_2 * X_4 + 149634X_2 * X_3 * X_4$$

These equations represent the quantitative effect of variables (X₁, X₂, X₃ and X₄) and their interactions on the responses (Y₁ and Y₂). The magnitude of each predicted regression coefficient specified the relative contribution of the independent factors corresponding to the responses. Coefficients with more than one factor term and those with higher order terms represent interaction terms and quadratic relationships. A positive sign represents a synergistic effect, while a negative sign indicates an antagonistic effect (59). It can be interpreted from both equations of Y₁ and Y₂ that X₂ (EPO) and X₃ (HPC) affected the release effectively, whereas X₁

(THY) and X_4 (SSG) had an insignificant effect on drug release in this design space. Nonetheless, the significant interaction was observed in combinations of X_1 , X_2 and X_4 because a stronger interaction appeared between these factors.

Table 11. Observed values of responses obtained from the D-optimal mixture design.

Formulations	Y₁	Y₂
1	59.92	80.22
2	59.42	73.84
3	61.13	83.33
4	50.93	72.22
5	55.42	75.06
6	60.67	83.21
7	70.53	98.37
8	101.86	109.67
9	57.54	75.17
10	81.53	99.78
11	59.57	80.73
12	58.29	86.04
13	90.87	106.39
14	82.61	95.13
15	75.37	96.12
16	86.05	112.88
17	93.39	107.72

Furthermore, the main effect of each parameter on the drug release properties of 3D printed tablets is shown in Fig. 29. This plot showed that the drug release rate was highly affected by EPO (X_2) and HPC (X_3) which agree well with the two equations above. Nonetheless, the relevant concentrations of SSG at 5% and 12.5% potentially increase the drug release. While there was no clear trend of different concentrations (30-60%) of THY (X_1), implying no main effect on the drug release.

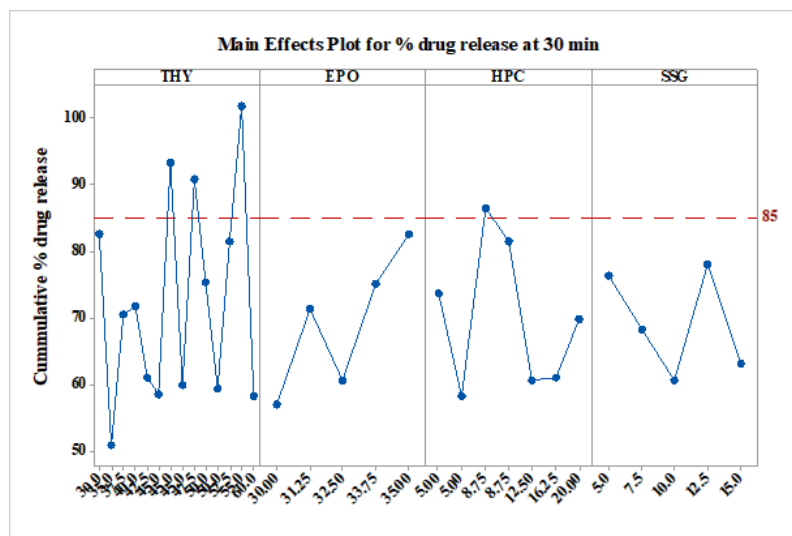


Figure 29. Main effect plot of all four independent variables (THY, EPO, HPC and SSG).

Generally, darker green regions indicate the higher dissolution rate of theophylline (Fig. 30). Fig. 30a shows that the high dissolution rate was obtained with the condition of low concentrations range (7.5-10%) of HPC (X_3) and almost all range (30-35%) of EPO (X_2), suggesting the strong influence of EPO on dissolution time. Fig. 30b shows the combined effect of HPC and SSG at the lower part of the contour plot where the increasing drug release rate can be achieved with the low amount (7.5-10%) of HPC and 12.5% of SSG. In contrast, the maximum drug release can be seen at the left corner of Fig. 30c through a significant effect of high percentage (ca. 35%) of EPO and low content (ca. 5-6%) of SSG. It is noteworthy that the highest drug release (more than 90% within 30 min, superior than the target) was found in F 8, 13 and 17 using a high level of THY, EPO and SSG which can be beneficial for dose adjustment (up to 55% THY). Thus, the QbD approach suggested that an optimum balance among drug, polymers and disintegrant levels is necessary to obtain the desired drug release. The result of drug release at 45 min (Y_2) had a similar trend as Y_1 response (Appendix E, Fig. 40).

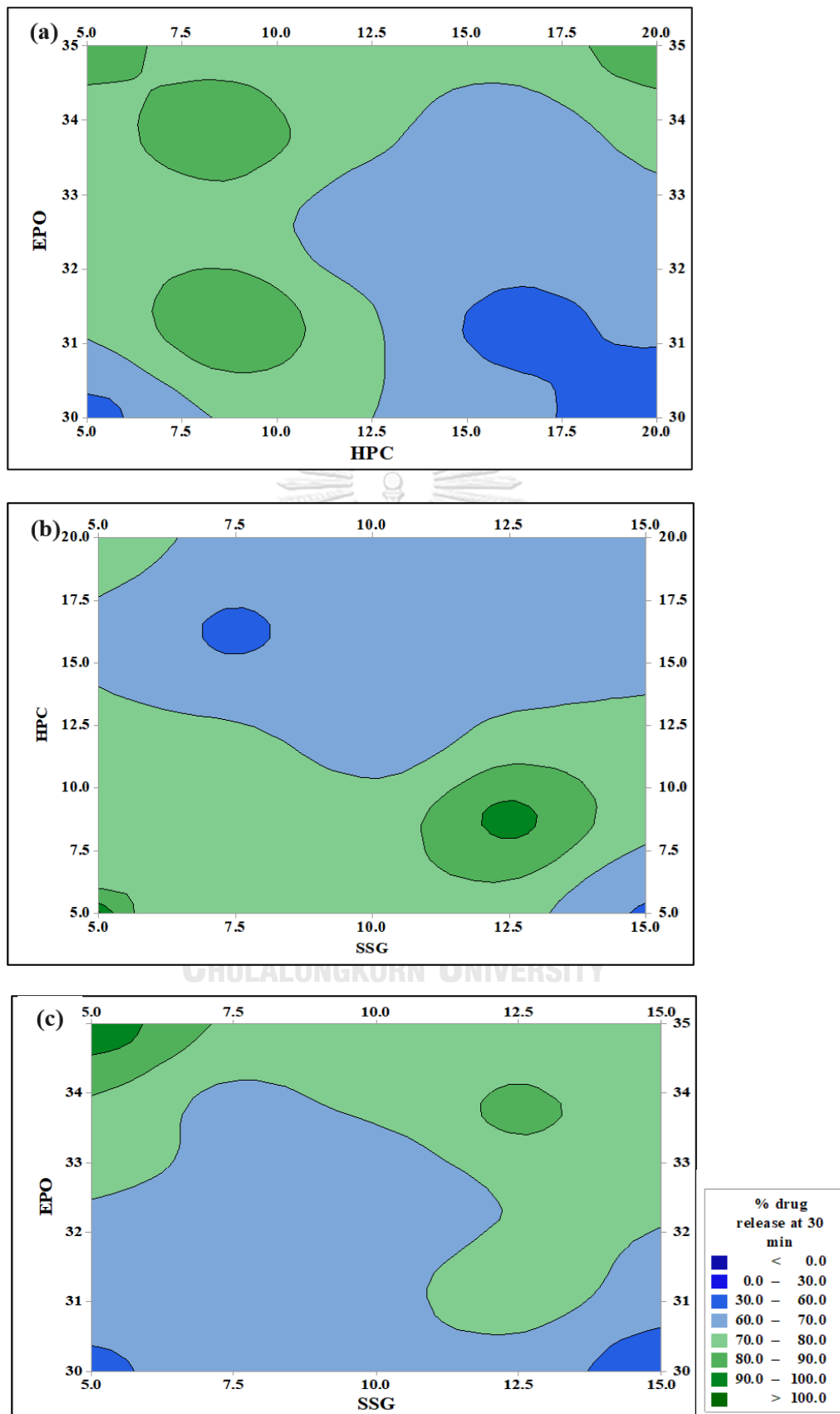


Figure 30. Contour plot depicting effect of variables on % drug release at 30 min.

Finally, in the response optimization analysis, the optimized formulation ratios of 3D printed tablets of X_1 , X_2 , X_3 and X_4 were 30% THY, 35% EPO, 20% HPC and 15% SSG, respectively which coincidentally agree with the screening study. These values were verified by a desirability function values of 0.99966 for Y_1 and 0.97988 for Y_2 . The experimental results were in good agreement with the predicted values for the two responses Y_1 (% drug release at 30 min) and Y_2 (% drug release at 45 min) through the optimization study which had low % error (Table 12).

Table 12. Comparison of predicted and observed value of responses for the optimal formulation.

Responses	Predicted value (%)	Observed value (%)	Desirability	% error (%)
Y_1	83.01	86.64	0.99966	4.372
Y_2	96.65	96.83	0.97988	0.186

4.5. Conclusion

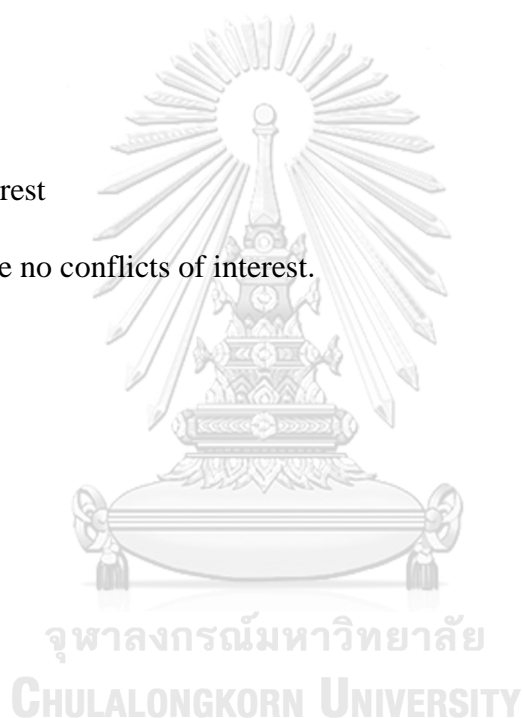
The fabrication of immediate release printed tablets using three different types of polymers, (hydroxy propyl cellulose (HPC), Eudragit[®] EPO, Kollidon[®] VA 64), disintegrant (sodium starch glycolate) and THY drug loadings up to 60% were successfully conducted, characterized and optimized by using QbD. The more specific range of viscosity of solid dispersion, appropriate for HME and FDM printing, were revealed and compared with the previous reports. Surprisingly, the mechanical property of the filaments prepared by polymer blending was distinctively improved by adding HPC as a flexibility modifier. All extrudable filaments and printable tablets after screening study showed reasonable characterizations but characteristic dissolution profiles. The D-optimal mixture design was able to explain the effects of different compositions on drug release and develop the highly predicted models from small number of runs together with the optimum formulation for immediate release tablets as referred to a certain amount of drug release in the pharmacopoeia. Accordingly, this work will be a useful platform for the formulation development of immediate release FDM 3D printed tablets and could step towards an alternative scenario for pharmaceutical field of oral products.

Acknowledgements

This work was financially supported by Chulalongkorn University-ASEAN (CU-ASEAN), Thailand; Graduate School Thesis Grant, Chulalongkorn University; a research fund (Grant number Phar2561-RGI-04 and Phar2562-RGI-01) to V.T.; and T.F., Department of Molecular Pharmaceutics, Meiji Pharmaceutical University. We also thank Pharmaceutical Research Instrument Center, Faculty of Pharmaceutical Sciences, Chulalongkorn University and to Chulalongkorn University Centenary Academic Development Project for supporting powder X-ray diffractometer within CU.D.HIP.

Declaration of interest

The authors declare no conflicts of interest.



REFERENCES

1. Puri V, Brancazio D, Desai PM, Jensen KD, Chun J-H, Myerson AS. development of maltodextrin-based immediate-release tablets using an integrated twin-screw hot-melt extrusion and injection-molding continuous manufacturing process. *Journal of Pharmaceutical Sciences*. 2017;106(11):3328-36.
2. Yu LJV. Continuous manufacturing has a strong impact on drug quality. *The Journal of the American Pharmacists Association*. 2016;2016.
3. Vithani K, Goyanes A, Jannin V, Basit AW, Gaisford S, Boyd BJ. An overview of 3D printing technologies for soft materials and potential opportunities for lipid-based drug delivery systems. *Pharmaceutical Research*. 2018;36(1):4.
4. Pham DT, Gault RS. A comparison of rapid prototyping technologies. *International Journal of Machine Tools and Manufacture*. 1998;38(10):1257-87.
5. Waldbaur A, Rapp H, Länge K, Rapp BE. Let there be chip-towards rapid prototyping of microfluidic devices: one-step manufacturing processes. *Analytical Methods*. 2011;3(12):2681-716.
6. Jamróz W, Kurek M, Szafraniec-Szczęsny J, Czech A, Gawlak K, Knapik-Kowalczyk J. Speed it up, slow it down. An issue of bicalutamide release from 3D printed tablets. *European Journal of Pharmaceutical Sciences*. 2020;143:105169.
7. Aho J, Bøtker JP, Genina N, Edinger M, Arnfast L, Rantanen J. Roadmap to 3D-Printed Oral Pharmaceutical Dosage Forms: Feedstock Filament Properties and Characterization for Fused Deposition Modeling. *Journal of Pharmaceutical Sciences*. 2019;108(1):26-35.
8. Perissutti B, Newton JM, Podczeczek F, Rubessa F. Preparation of extruded carbamazepine and PEG 4000 as a potential rapid release dosage form. *European Journal of Pharmaceutics and Biopharmaceutics*. 2002;53(1):125-32.
9. Solanki NG, Tahsin M, Shah AV, Serajuddin ATM. Formulation of 3D printed tablet for rapid drug release by fused deposition modeling: screening polymers for drug release, drug-polymer miscibility and printability. *Journal of Pharmaceutical Sciences*. 2018;107(1):390-401.
10. Zhang J, Feng X, Patil H, Tiwari RV, Repka MA. Coupling 3D printing with hot-melt extrusion to produce controlled-release tablets. *International Journal of Pharmaceutics*. 2017;519(1):186-97.
11. Hwang S, Reyes EI, Moon K-s, Rumpf RC, Kim NS. Thermo-mechanical characterization of metal/polymer composite filaments and printing parameter study for fused deposition modeling in the 3d printing process. *Journal of Electronic Materials*. 2015;44(3):771-7.
12. Tidau M, Kwade A, Finke HJ. Influence of high, disperse API load on properties along the fused-layer modeling process chain of solid dosage forms. *Pharmaceutics*. 2019;11(4).
13. Goyanes A, Chang H, Sedough D, Hatton GB, Wang J, Buanz A. Fabrication of controlled-release budesonide tablets via desktop (FDM) 3D printing. *International Journal of Pharmaceutics*. 2015;496(2):414-20.

14. Solanki N, Gupta SS, Serajuddin ATM. Rheological analysis of itraconazole-polymer mixtures to determine optimal melt extrusion temperature for development of amorphous solid dispersion. *European Journal of Pharmaceutical Sciences*. 2018;111:482-91.
15. Gumaste SG, Gupta SS, Serajuddin ATM. Investigation of polymer-surfactant and polymer-drug-surfactant miscibility for solid dispersion. *The American Association of Pharmaceutical Scientists: Pharmaceutical Science and Technology*. 2016;18(5):1131-43.
16. Sadia M, Arafat B, Ahmed W, Forbes RT, Alhnan MA. Channelled tablets: An innovative approach to accelerating drug release from 3D printed tablets. *Journal of Controlled Release*. 2018;269:355-63.
17. Goyanes A, et al. Fused-filament 3D printing (3DP) for fabrication of tablets. *International Journal of pharmaceutics*. 2014;476(1):88-92.
18. Tagami T, Fukushige K, Ogawa E, Hayashi N, Ozeki T. 3D Printing Factors Important for the Fabrication of polyvinylalcohol filament-based tablets. *Biological and Pharmaceutical Bulletin*. 2017;40(3):357-64.
19. Selen A, Dickinson PA, Müllertz A, Crison JR, Mistry HB, Cruaños MT. The Biopharmaceutics Risk Assessment Roadmap for Optimizing Clinical Drug Product Performance. *Journal of Pharmaceutical Sciences*. 2014;103(11):3377-97.
20. Sadia M, Sośnicka A, Arafat B, Isreb A, Ahmed W, Kellarakis A. Adaptation of pharmaceutical excipients to FDM 3D printing for the fabrication of patient-tailored immediate release tablets. *International Journal of Pharmaceutics*. 2016;513(1):659-68.
21. Okwuosa TC, Stefaniak D, Arafat B, Isreb A, Wan K-W, Alhnan MA. A Lower Temperature FDM 3D Printing for the Manufacture of Patient-Specific Immediate Release Tablets. *Pharmaceutical Research*. 2016;33(11):2704-12.
22. Palekar S, Nukala PK, Mishra SM, Kipping T, Patel K. Application of 3D printing technology and quality by design approach for development of age-appropriate pediatric formulation of baclofen. *International Journal of Pharmaceutics*. 2019;556:106-16.
23. Pietrzak K, Isreb A, Alhnan MA. A flexible-dose dispenser for immediate and extended release 3D printed tablets. *European Journal of Pharmaceutics and Biopharmaceutics*. 2015;96:380-7.
24. Alhijaj M, Belton P, Qi S. An investigation into the use of polymer blends to improve the printability of and regulate drug release from pharmaceutical solid dispersions prepared via fused deposition modeling (FDM) 3D printing. *European Journal of Pharmaceutics and Biopharmaceutics*. 2016;108:111-25.
25. Kempin W, Domsta V, Grathoff G, Brecht I, Semmling B, Tillmann S, et al. Immediate release 3D-printed tablets produced via fused deposition modeling of a thermo-sensitive drug. *Pharmaceutical Research*. 2018;35(6):124.
26. Shah U, Augsburger L. Multiple sources of sodium starch glycolate, NF: Evaluation of functional equivalence and development of standard performance tests. *Pharmaceutical Development and Technology*. 2002;7(3):345-59.
27. Melocchi A, Parietti F, Loreti G, Maroni A, Gazzaniga A, Zema L. 3D printing by fused deposition modeling (FDM) of a swellable/erodible capsular

- device for oral pulsatile release of drugs. *Journal of Drug Delivery Science and Technology*. 2015;30:360-7.
28. Kempin W, Franz C, Koster L-C, Schneider F, Bogdahn M, Weitschies W. Assessment of different polymers and drug loads for fused deposition modeling of drug loaded implants. *European Journal of Pharmaceutics and Biopharmaceutics*. 2017;115:84-93.
 29. Melocchi A, Parietti F, Maroni A, Foppoli A, Gazzaniga A, Zema L. Hot-melt extruded filaments based on pharmaceutical grade polymers for 3D printing by fused deposition modeling. *International Journal of Pharmaceutics*. 2016;509(1):255-63.
 30. Trenfield SJ, Awad A, Goyanes A, Gaisford S, Basit AW. 3D printing pharmaceuticals: Drug Development to Frontline Care. *Trends in Pharmacological Sciences*. 2018;39(5):440-51.
 31. Mishra SM. An integrated, quality by design (QbD) approach for design, development and optimization of orally disintegrating tablet formulation of carbamazepine. *Rohera BDJPD, Technology* 2017;22:889 - 903.
 32. Tung N-T, Tran C-S, Pham T-M-H, Nguyen H-A, Nguyen T-L, Chi S-C. Development of solidified self-microemulsifying drug delivery systems containing 1-tetrahydropalmatine: Design of experiment approach and bioavailability comparison. *International Journal of Pharmaceutics*. 2018;537(1):9-21.
 33. Kushner J, Langdon BA, Hicks I, Song D, Li F, Kathiria L. A Quality-by-Design study for an immediate-release tablet platform: examining the relative impact of active pharmaceutical ingredient properties, processing methods, and excipient variability on drug product quality attributes. *Journal of Pharmaceutical Sciences*. 2014;103(2):527-38.
 34. Son H, Chae B, Choi J, Shin D, Goo Y, Lee E. Optimization of self-microemulsifying drug delivery system for phospholipid complex of telmisartan using D-optimal mixture design. *Publish Library of Science One*. 2018;13:e0208339.
 35. Gupta SS, Solanki N, Serajuddin ATM. Investigation of thermal and viscoelastic properties of polymers relevant to hot melt extrusion, IV: Affinisol™ HPMC HME polymers. *The American Association of Pharmaceutical Scientists: Pharmaceutical Science and Technology*. 2016;17(1):148-57.
 36. Kollamaram G, Croker DM, Walker GM, Goyanes A, Basit AW, Gaisford S. Low temperature fused deposition modeling (FDM) 3D printing of thermolabile drugs. *International Journal of Pharmaceutics*. 2018;545(1):144-52.
 37. Öblom H, Zhang J, Pimparade M, Speer I, Preis M, Repka M. 3D-Printed Isoniazid Tablets for the Treatment and Prevention of Tuberculosis- Personalized Dosing and Drug Release. *The American Association of Pharmaceutical Scientists: Pharmaceutical Science and Technology*. 2019;20(2):52.
 38. Hsiao W-K, Lorber B, Reitsamer H, Khinast J. 3D printing of oral drugs: a new reality or hype? *Expert Opinion on Drug Delivery*. 2018;15(1):1-4.

39. Norman J, Madurawe RD, Moore CMV, Khan MA, Khairuzzaman A. A new chapter in pharmaceutical manufacturing: 3D-printed drug products. *Advanced Drug Delivery Reviews*. 2017;108:39-50.
40. Tidau M, Kwade A, Finke JH. Influence of high, disperse API load on properties along the fused-layer modeling process chain of solid dosage forms. *Pharmaceutics*. 2019;11(4):194.
41. Aho J, Edinger M, Botker J, Baldursdottir S, Rantanen J. Oscillatory shear rheology in examining the drug-polymer interactions relevant in hot melt extrusion. *Journal of Pharmaceutical Sciences*. 2016;105(1):160-7.
42. Isreb A, Baj K, Wojsz M, Isreb M, Peak M, Alhnan MA. 3D printed oral theophylline doses with innovative 'radiator-like' design: Impact of polyethylene oxide (PEO) molecular weight. *International Journal of Pharmaceutics*. 2019;564:98-105.
43. Zhang J, Xu P, Vo A, Bandari S, Yang F, Durig T. Development and evaluation of pharmaceutical 3D printability for hot melt extruded cellulose-based filaments. *Journal of Drug Delivery Science and Technology*. 2019;52.
44. Song Y, Wang L, Yang P, Wenslow RM, Tan B, Zhang H. Physicochemical characterization of Felodipine-Kollidon VA64 amorphous solid dispersions prepared by hot-melt extrusion. *Journal of Pharmaceutical Sciences*. 2013;102(6):1915-23.
45. Meng F, Trivino A, Prasad D, Chauhan H. Investigation and correlation of drug polymer miscibility and molecular interactions by various approaches for the preparation of amorphous solid dispersions. *European Journal of Pharmaceutical Sciences*. 2015;71:12-24.
46. Yu M, Ocando JE, Trombetta L, Chatterjee P. Molecular interaction studies of amorphous solid dispersions of the antimelanoma agent betulinic acid. *The American Association of Pharmaceutical Scientists: Pharmaceutical Science and Technology*. 2015;16(2):384-97.
47. Ali F, Kumar R, Sahu PL, Singh GN. Physicochemical characterization and compatibility study of roflumilast with various pharmaceutical excipients. *Journal of Thermal Analysis and Calorimetry*. 2017;130(3):1627-41.
48. Liu J, Cao F, Zhang C, Ping Q. Use of polymer combinations in the preparation of solid dispersions of a thermally unstable drug by hot-melt extrusion. *Acta Pharmaceutica Sinica B*. 2013;3(4):263-72.
49. Chen W, Weng W, Fu M. Hydroxypropyl cellulose-based esters for thermal energy storage by grafting with palmitic-stearic binary acids. *Journal of Applied Polymer*. 2017;134(24).
50. Pietrzak K, Isreb A, Alhnan MAJE, Biopharmaceutics. A flexible-dose dispenser for immediate and extended release 3D printed tablets. *European Journal of Pharmaceutics and Biopharmaceutics*. 2015;96:380-7.
51. Räsänen E, Rantanen J, Jørgensen A, Karjalainen M, Paakkari T, Yliruusi J. Novel identification of pseudopolymorphic changes of theophylline during wet granulation using near infrared spectroscopy. *Journal of Pharmaceutical Sciences*. 2001;90(3):389-96.
52. Kadry H, Al-Hilal TA, Keshavarz A, Alam F, Xu C, Joy A. Multi-purposable filaments of HPMC for 3D printing of medications with tailored drug release

- and timed-absorption. *International Journal of Pharmaceutics*. 2018;544(1):285-96.
53. Apichatwatana N. Hot melt extrusion for the production of controlled drug delivery systems 2011.
 54. Agrawal A, Dudhedia M, Deng W, Shepard K, Zhong L, Povilaitis E. Development of Tablet Formulation of amorphous solid dispersions prepared by hot melt extrusion using quality by design approach. *The American Association of Pharmaceutical Scientists: Pharmaceutical Science and Technology*. 2016;17(1):214-32.
 55. Goyanes A, Buanz ABM, Hatton GB, Gaisford S, Basit AW. 3D printing of modified-release aminosalicylate (4-ASA and 5-ASA) tablets. *European Journal of Pharmaceutics and Biopharmaceutics*. 2015;89:157-62.
 56. Sandler N, Salmela I, Fallarero A, Rosling A, Khajeheian M, Kolakovic R. Towards fabrication of 3D printed medical devices to prevent biofilm formation. *International Journal of Pharmaceutics*. 2014;459(1):62-4.
 57. Skowrya J, Pietrzak K, Alhnan MA. Fabrication of extended-release patient-tailored prednisolone tablets via fused deposition modelling (FDM) 3D printing. *European Journal of Pharmaceutical Sciences*. 2015;68:11-7.
 58. Prasad E, Islam MT, Goodwin DJ, Megarry AJ, Halbert GW, Florence AJ. Development of a hot-melt extrusion (HME) process to produce drug loaded Affinisol™ 15LV filaments for fused filament fabrication (FFF) 3D printing. *Additive Manufacturing*. 2019;29:100776.
 59. Zaghoul A, Vaithiyalingam S, Faltinek J, Reddy I, Khan M. Response surface methodology to obtain naproxen controlled release tablets from its microspheres with Eudragit L100-55. *Journal of Microencapsulation*. 2001;18:651-62.
 60. Vo AQ, Feng X, Morott JT, Pimparade MB, Tiwari RV, Zhang F, and Repka MA. A novel floating controlled release drug delivery system prepared by hot-melt extrusion. *International Journal of Pharmaceutics and Biopharmaceutics*. 2016; 98: 108–121

CHAPTER V

CONCLUSION

5.1. Conclusion

In this research, the extended and immediate release FDM printed tablets were successfully fabricated using QbD design. The production of controlled release formulation using the blending of HPC with SLP, PVP/VA Eudragit® RS, Eudragit® RL polymers or disintegrant (SSG, MCC, Cros PVP, CCM and L-HPC) were successfully achieved and characterized. It was found that in case of single polymer extrusion, HPC filaments showed too soft filament to be loaded into the printer while the other polymers (PVP/VA, SLP, Eu RL and Eu RS) filaments displayed brittleness character which hinder the printing process. Interestingly, the mechanical resilience of all polymer-polymer and polymer-disintegrant blending filaments was considerably enhanced by incorporating of HPC as a flexible modifier with 3:1 and 1:1 in polymer blending and 3:1 ratio in polymer and disintegrant mixture. HPC is a suitable polymer for printing applications in the range of 45-67.5% (w/w). Furthermore, all five disintegrants was found to be polymer processability of filaments in both technique (HME and FDM printing), thus pointing out a potential application in FDM printing for the manufacturing of dosage forms. The defined viscosity range (5,000-11,000 Pa.s) of polymeric solid dispersions, appropriate for HME and FDM printing was described and compared with the previous studies (1,000-10,000 for HME and less than 8,000 Pa.s for FDM printing). In this study, the specified temperature, screw speed and viscosity range were screened as critical processing parameters for additive HME-FDM manufacturing for both controlled and immediate systems by considering the critical quality attributes of the products.

All printable filaments and tablets after screening experiment show the satisfactory characterizations including physical properties, molecular interaction in FT-IR, thermal property and drug contents. The advanced findings of HPC-disintegrant blends could propose that the stiff but rather brittle filaments are possible for successful FDM printing. The miscibility and intermolecular interactions between

IMC and polymeric blends were also confirmed by alterations in the wavenumber and peak shape. In TGA analysis, all the excipients and extruded filaments were shown to be stable up to 250 °C while the printing process converted all systems to be completely amorphous solid dispersions with smooth the halo pattern confirmed by PXRD. The results of drug contents showed uniform distribution of the drug throughout the filament as well as in the tablets with little variation. In the dissolution study, it was found that the 3D-printed tablets made of polymer-disintegrant mixtures showed more sustained drug release than those of polymer-polymer blend tablets while the tablets made of HPC-Eu RS and Eu RL combinations displayed incomplete drug release (approximately 22%) over 24 h which are less suitable for oral dosage forms.

In addition, the D-optimal mixture design enabled to elucidate the effects of different polymers on drug release and generated the estimated models from small number of tests. The factors such as X_1 , HPC and X_2 , PVP/VA positively affected the drug release, while X_3 , SLP had negatively effect on drug release. The optimum formulation (X_1 , HPC, X_2 , PVA/VA and X_3 , SLP) were 49.97%, 19.09% and 20.94%, respectively that showed good extended-release tablets as reported to a predetermined amount of drug release in the pharmacopoeia.

In terms of the immediate release tablets, THY drug loadings up to 60% and 15% SSG using two polymers, EPO and PVP/VA, were successfully conducted and characterized as critical quality attributes of produced dosage forms. The more specified viscosity range (5,000-14,000 Pa.s) of solid dispersions, appropriate for HME and FDM printing was described and compared with the previous studies (1,000-10,000 for HME and less than 8,000 Pa.s for FDM printing). Moreover, the robust filaments could be perfectly produced when HPC polymer with different ratios is adjusted by mixing with water soluble polymers either EPO or PVP/VA polymers and different amounts (5-15%) of thermoplastic SSG disintegrant based on the mechanical property of the filaments. Moreover, although the amount of SSG used in 3D printed tablets was a slightly higher (up to 15%) compared to the conventional tablet formulations using in the range of 2-8%, it was illustrated to be processable as a

thermoplastic starch with an intrinsic property in 3D printing. However, it also seems that more than 15% SSG could affect the printing process by blocking at the nozzles.

All extrudable filaments and printable tablets obtained from screening study showed reasonable characterizations to ensure critical quality attributes of the products such as physicochemical property, content uniformity and dissolutions profile. The improved filaments properties regarding brittleness and stiffness were reflected by the polymer blending when 3-point bend test was used to measure the extruded filaments as a preliminary monitoring method. Noticeably, high drug loading in the form of crystalline at 60% (both E60 and P60, with less excipients) described the lowest breaking distance (<1 mm) and stress values such as 2298 g/mm² in E60 and 2692 g/mm² which lead to less bendable character. The intermolecular interactions between THY and polymeric blends in both 10% and 30% drug loads filaments were also found by changing in the wavenumber and peak intensity, on the other hand, 60% drug loads filaments showed the strong bands of THY due to the higher amount of THY than the other components, confirmed by DSC.

In TGA analysis, all the polymers, SSG and extruded filaments did not depict a significant weight loss. Further, the two systems containing low drug loads (10% and 30%) showed partially amorphous solid dispersions with tiny peaks with low intensity while 60% drug loads demonstrated more number of diffraction peaks confirmed by PXRD. The drug contents showed proper distribution of the drug throughout the filament and the tablets with small variation. As dissolution profiles, EPO-based tablets showed faster drug release rate than PVP/VA-based tablets due to the higher pH threshold of EPO than PVP/VA achieved the rapid ionizing of side chains in polymer in acidic medium.

The D-optimal mixture design was shown to be very advantageous because the responses were well fitted and predicted by the different models and R^2 had high values for both Y_1 and Y_2 . The independent variables such as X_2 (EPO) and X_3 (HPC) affected the release effectively, whereas X_1 (THY) and X_4 (SSG) had an insignificant effect on drug release in this design space. Nonetheless, the significant interaction was observed in combinations of X_1 , X_2 and X_4 because a stronger interaction appeared between these factors. It is noteworthy that the highest drug release (more than 90%

within 30 min, superior than the target) was found in F 8, 13 and 17 using a high level of THY, EPO and SSG which can be beneficial for dose adjustment (up to 55% THY). The optimized formulation ratios of 3D printed tablets of X_1 , X_2 , X_3 and X_4 were 30% THY, 35% EPO, 20% HPC and 15% SSG, respectively and the experimental results were in good agreement with the predicted values for the two responses Y_1 (% drug release at 30 min) and Y_2 (% drug release at 45 min) through the optimization study with low % error. The QbD approach suggested that an optimum balance among drug, polymers and disintegrant levels is necessary to obtain the desired drug release.

Conclusively, the systematic study of printed tablets was conducted to clarify the influence of excipients ratios in terms of the various drug release profiles instead of changing FDM processing parameters using Quality by design approach. The tablet platform is robust to a wide range of excipients variability for the manufacturing of individualized dosage forms using FDM printing.

5.2. Limitations

The limitations of this study are as follow:

Methods of testing printable filaments

Generally, there are two methods to test the mechanical properties of filaments such as tensile strength and 3-point bend test. The filaments produced in this research cannot be performed tensile strength test because the filaments are slipped and dropped during testing with high variations when the filaments were vertically fixed to the clamps and stretched gradually during the test. Therefore, 3-point bend test is suitable for filaments in this study.

Effect of plasticizer and SSG on printability

In this study, the plasticizers and high amount of SSG (more than 15%) cannot be applied possibly due to the incompatibility with the printed nozzles.

5.3. Suggestion and future work

Drug release kinetic

Korsmeyer-Peppas model should be used to identify the release transport by considering Fickian diffusion, polymer relaxation/erosion as 3D printed tablets have inherently tight structure, where the polymer relaxation/erosion-based release kinetics could be more influenced from the compact structures. The *Korsmeyer-Peppas* model was depicted in the following equation (1), is a reliable approach for showing the controlled drug release behavior from matrix.

$$F = k*t^n \quad (1)$$

F is the percentage of the drug released at time t , k is the kinetic constant for structural and geometric characteristics of the tablet, and n is the release exponent of mechanism.

Furthermore, several mechanisms such as water up-take including water diffusion, polymer swelling, drug diffusion, and polymer erosion may influence in of solid dispersion filaments made of swellable/erodible polymers. Therefore, the *zero-order* model: equation (2) can also be described the constant drug release rate with time, where k_0 is the release constant. This model can be mostly applied for the matrix systems with poorly soluble drugs.

$$F = k_0*t \quad (2)$$

Moreover, the tablets should be weighed before and after the dissolution studies or measured the swelling index for the comparison of the change in mass. And another way is that hot stage microscopy (HSM) can also be utilized for identifying the dissolution of drug and polymer species during testing and helped pre-formulation input for the subsequent experimental design. The mechanism of disintegrant comprise of swelling, interruption of particle-particle bonds, wicking (capillary action), and heat of interaction that cause the tablet-matrix break up in aqueous medium and start drug release (3).

The pharmacokinetic and bioequivalent studies of printed dosage forms will be conducted as future study.

REFERENCES

1. Buyukgoz G G, Soffer D, Defendre J, Pizzano G M, Dav'e R N. Exploring tablet design options for tailoring drug release and dose via fused deposition modeling (FDM) 3D printing. *International Journal of Pharmaceutics* 2020;591:119987
2. Huanbutta K, Sangnim T. Design and development of zero-order drug release gastroretentive floating tablets fabricated by 3D printing technology. *Journal of Drug Delivery Science and Technology*. 2019;52:831-837.
3. Desai PM, Liew CL, Heng PWS, Review of disintegrants and the disintegration phenomena, *Journal of Pharmaceutical Sciences*. 2016;105 2545-2555.





จุฬาลงกรณ์มหาวิทยาลัย
CHULALONGKORN UNIVERSITY

REFERENCES



จุฬาลงกรณ์มหาวิทยาลัย
CHULALONGKORN UNIVERSITY

APPENDIX A
RHEOLOGICAL STRAIN GRAPHS



จุฬาลงกรณ์มหาวิทยาลัย
CHULALONGKORN UNIVERSITY

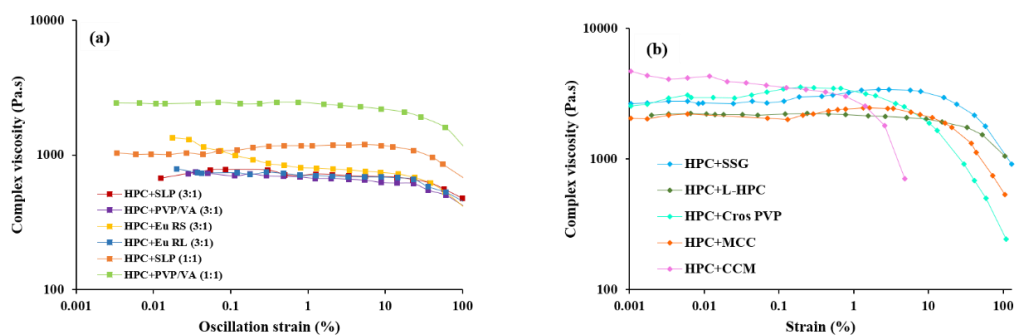


Figure 31. Strain curves (a) polymeric blends and (b) polymer-disintegrants formulations.

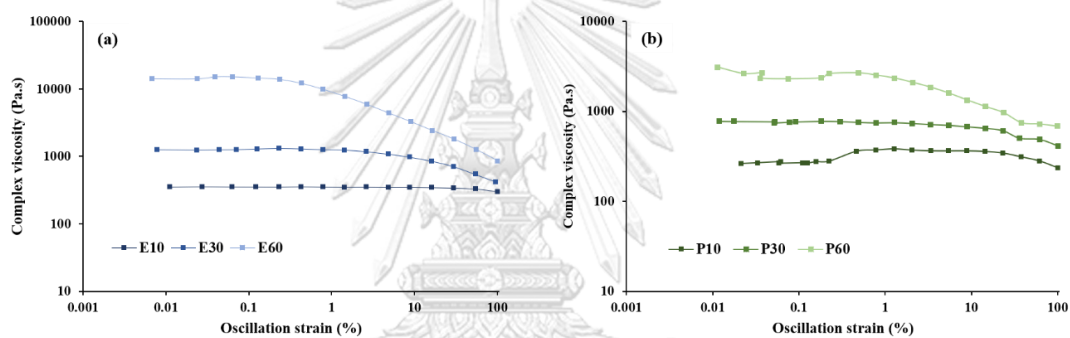


Figure 32. Strain curves (a) EPO-based formulations and (b) PVP/VA-based formulations.

APPENDIX B**IMAGES OF EXTRUDED FILAMENTS AND 3D PRINTED TABLETS**

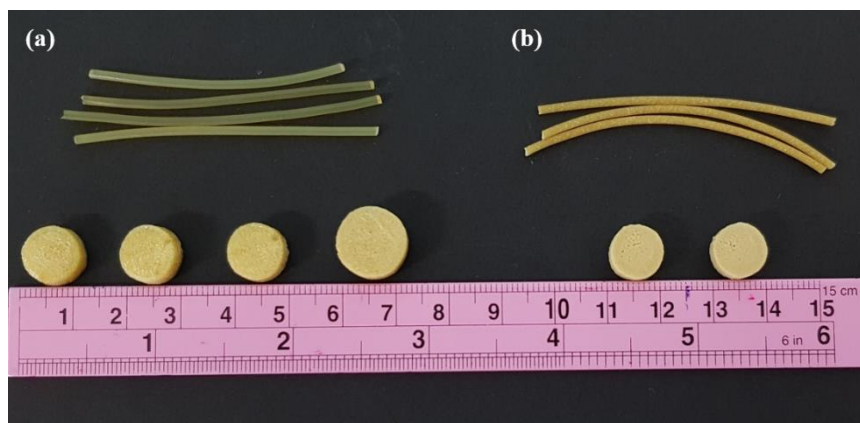


Figure 33. Image of (a) different polymeric-blend (b) polymer-disintegrants filaments and printed tablets.

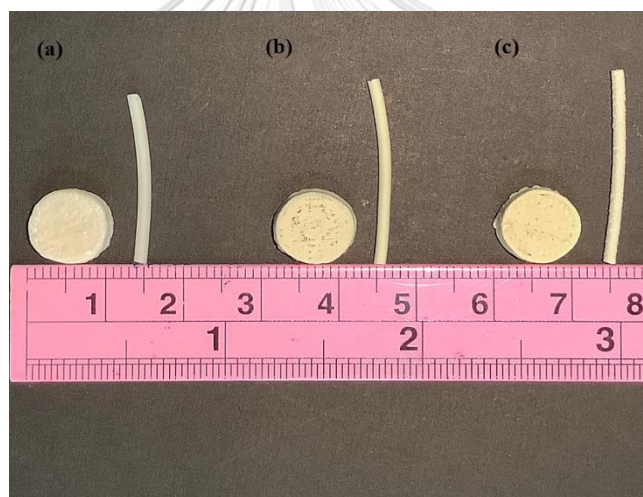


Figure 34. Image of different drug loads filaments and printed tablets (a) 10%, (b) 30% and (c) 60%.

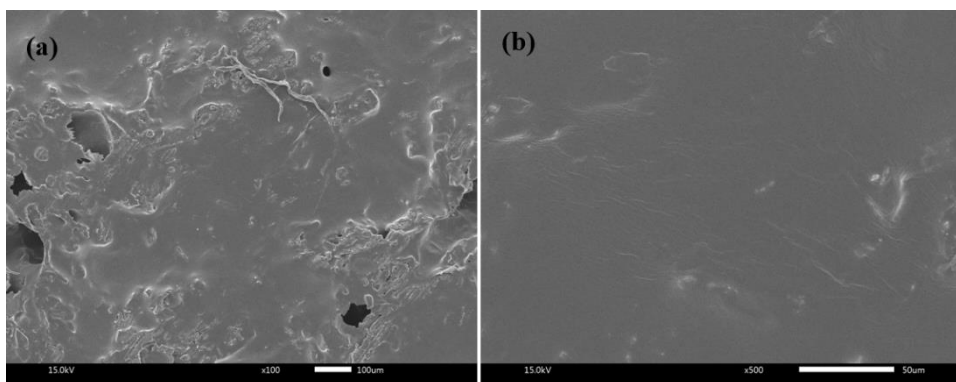


Figure 35. SEM image of HPC-disintegrant filaments (a) cross-section (b) cross-section (x1000)



APPENDIX C
FT-IR SPECTRUM



จุฬาลงกรณ์มหาวิทยาลัย
CHULALONGKORN UNIVERSITY

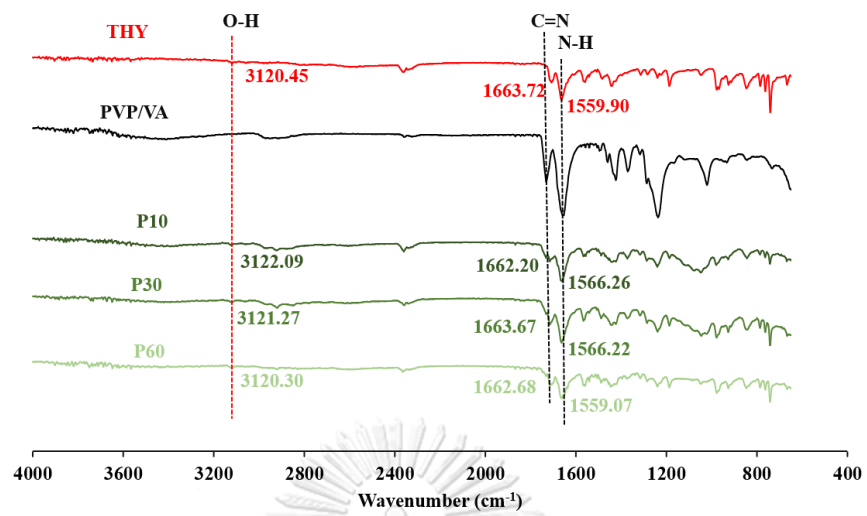


Figure 36. 15. FT-IR spectrum of PVP-based extruded filaments

APPENDIX D
POWDER X-RAY DIFFRACTOGRAM



จุฬาลงกรณ์มหาวิทยาลัย
CHULALONGKORN UNIVERSITY

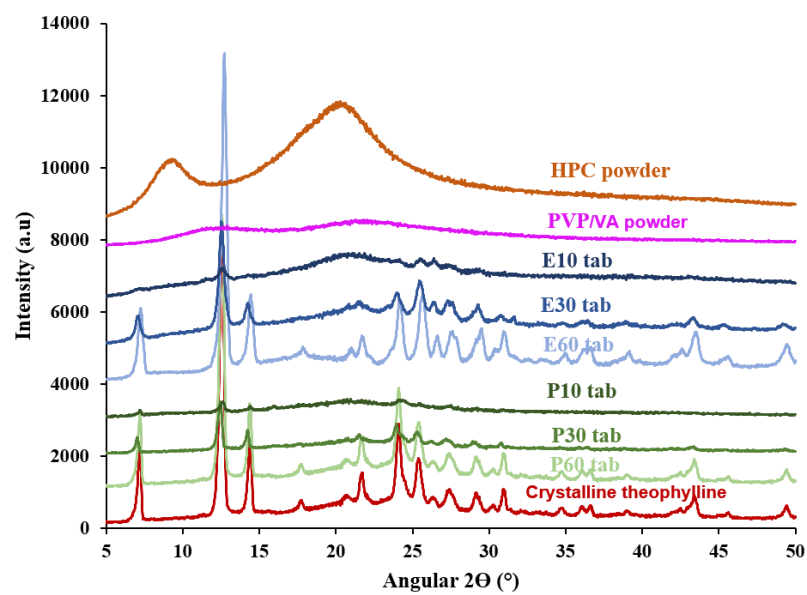


Figure 37. X-ray powder diffractograms of pure API, excipients and printed tablets.



APPENDIX E
RESULTS FROM DESIGN OF EXPERIMENT



จุฬาลงกรณ์มหาวิทยาลัย
CHULALONGKORN UNIVERSITY

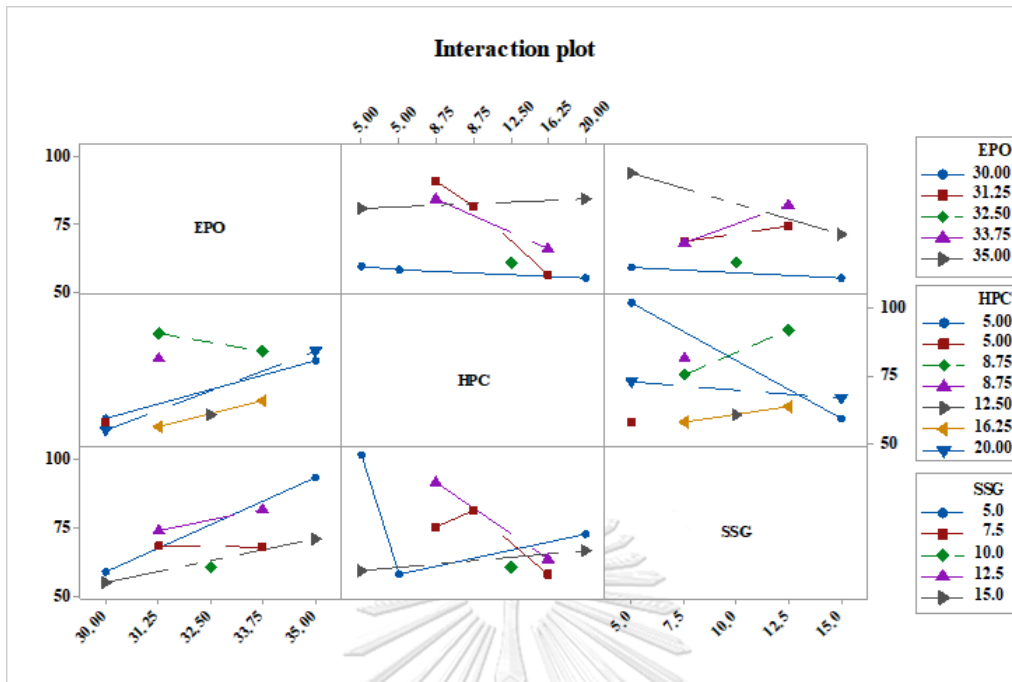


Figure 38. Interaction plot for different formulation factors (EPO, HPC and SSG)

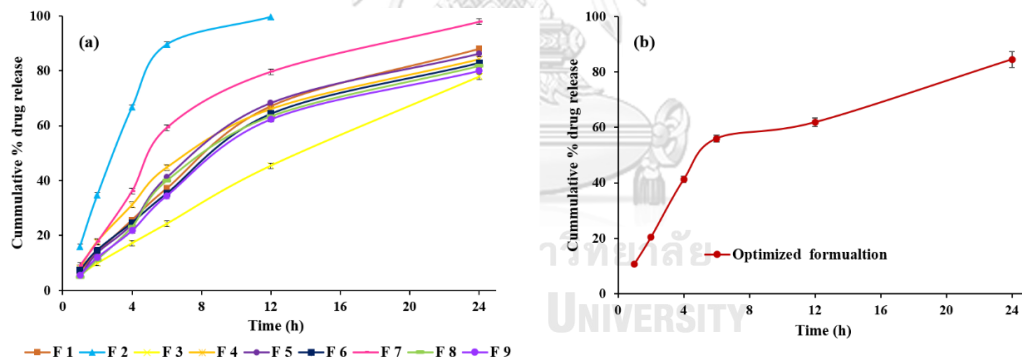


Figure 39. (a) In-vitro drug release studies of controlled release printed tablets obtained from DoE runs (b) Optimized formulation.

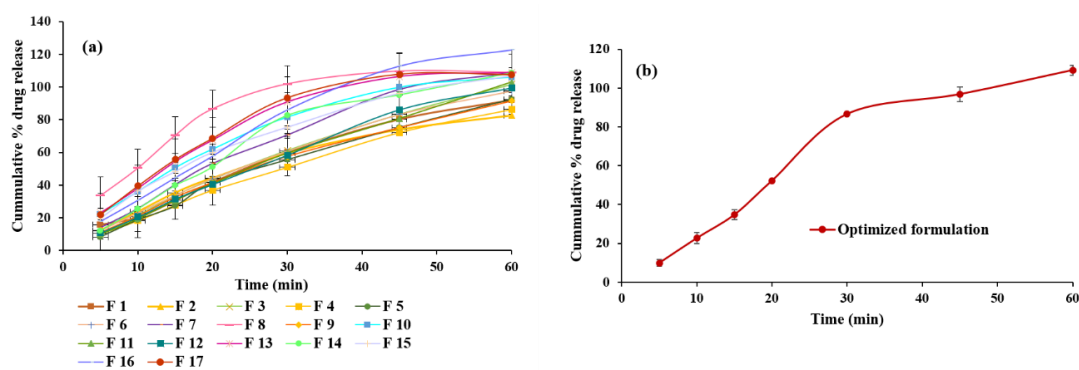


Figure 40. (a) In-vitro drug release studies of immediate release printed tablets obtained from DoE runs (b) Optimized formulation.

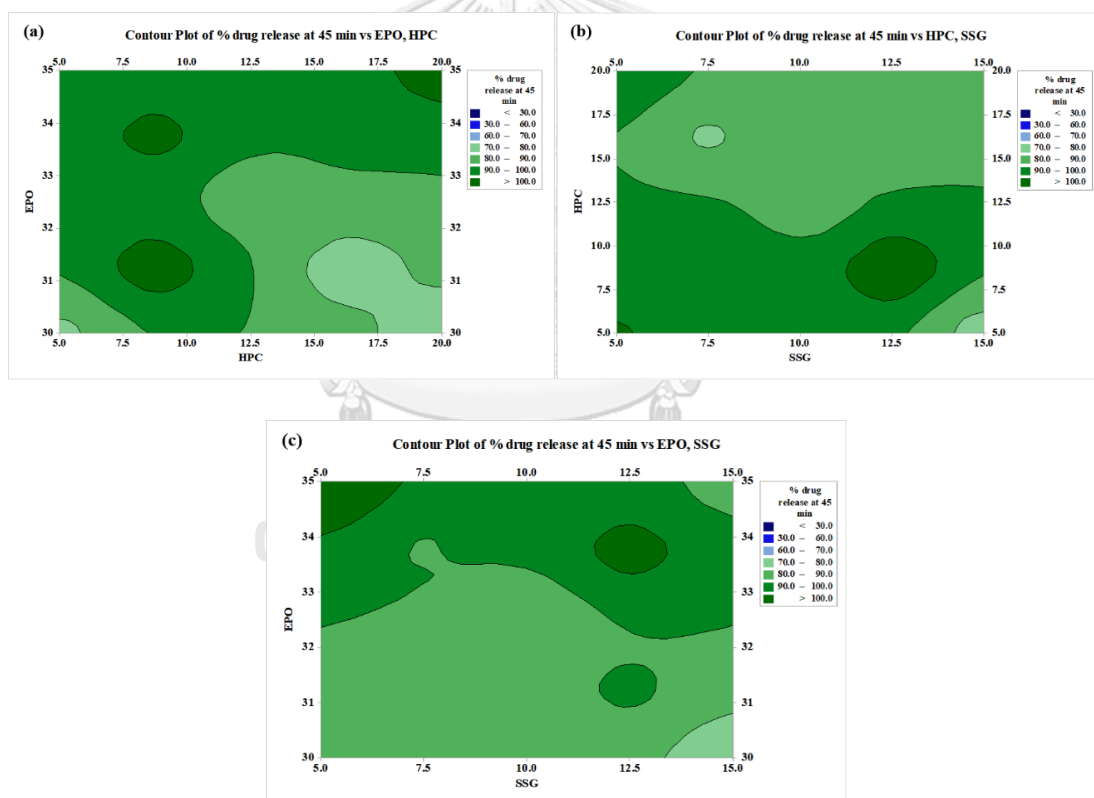


Figure 41. Contour plot depicting effect of variables on % drug release at 45 min.



จุฬาลงกรณ์มหาวิทยาลัย
CHULALONGKORN UNIVERSITY

VITA

NAME Yee Mon Than

DATE OF BIRTH 23.3.1983

PLACE OF BIRTH Meikhtila, Myanmar

**INSTITUTIONS
ATTENDED** University of Pharmacy, Mandalay

HOME ADDRESS (3) street, Pauk Chaung (2), Meikhtila, Myanmar



จุฬาลงกรณ์มหาวิทยาลัย
CHULALONGKORN UNIVERSITY